A Thesis Entitled

An investigation into the properties of Nuclear Research Emulsions in their Application to Electronographic Image Devices.

by

Stanley Jeffers, B.Sc., A.R.C.S.

submitted for the degree of Doctor of Philosophy.

Applied Physics Dept.
Imperial College,
London, S.W.7.

February 1968

ABSTRACT

The scientific applications of nuclear research emulsions are reviewed with special reference to their application for recording electron images generated in electronographic image tubes.

The effect of electron irradiation of these emulsions is considered from a theoretical point of view. Apparatus is described which has been developed to investigate this effect quantitatively and results are presented for G5, L4 and XM emulsions exposed to electrons in the energy range up to 35kV. The agreement of these results with the theoretical considerations is discussed.

The question of the granularity of nuclear research emulsions exposed to electrons is considered from a theoretical point of view. Experiments are described to evaluate the granularity of nuclear research emulsions and the agreement of the experimental results with theory is discussed.

From the results obtained in this investigation, a figure is derived for the equivalent quantum efficiency of a single-stage electronographic device employing direct recording of 25kV electrons on G5 emulsion.

Some aspects of the comparative performance of electronographic tubes employing direct and indirect recording of electron images are discussed.

The benefits of operating electronographic image tube systems at higher accelerating potentials are indicated.

CONTENTS

		Page
Chapter I:	GENERAL INTRODUCTION	
	1. Introduction.	8
	2. Composition of nuclear research emulsions.	9
	3. Other applications of nuclear research emulsions.	11
	4. Requirements of nuclear research emulsions for recording electron images.	12
Chapter II:	IMAGE INTENSIFIER SYSTEMS	
	1. Introduction - Photon detection.	15
	2. Image intensifiers with internal multiplication.	17
	3. Electronographic image intensifiers.	19
Chapter III:	THEORETICAL CONSIDERATION OF THE EFFECT OF THE EXPOSURE OF NUCLEAR RESEARCH EMULSIONS TO ELECTRONS.	
	1. Introduction.	31
	2. Fog level of nuclear research emulsions.	32
	3. Production of developable silver grains in nuclear research emulsions exposed to electrons.	33
	4. Optical density theoretically related to exposure.	35
	5. Contrast of nuclear research emulsions.	39

		Page
	6. Conclusions.	40
Chapter IV:	EXPERIMENTAL APPARATUS FOR THE INVESTIGATION OF NUCLEAR RESEARCH EMULSIONS.	
	1. Design considerations.	42
	2. Initial experiments:-	43
	(i) Choice of electron gun.	
	(ii) Value and measurement of electron beam current.	
	3. Construction of experimental tube.	47
	4. Use of indirectly-heated oxide-coated cathode as gun.	50
	5. Cathode processing procedure.	51
	6. Shutter mechanism for sub-second exposures.	53
	7. Background of tube.	61
	8. Procedure for exposing emulsion.	66
	9. Conclusions.	68
Chapter V:	RESULTS OBTAINED WITH NUCLEAR RESEARCH EMULSIONS L4, G5 and XM.	
	1. Procedure for processing emulsion.	72
	2. Reproducibility of results.	76
	3. Results of speed of emulsions.	76
	4. Validity of the Single-hit law - results of contrast.	85

		Page
5.	Effect of beam energy on the density produced.	89
6.	Degree of linearity of emulsion characteristic.	93
7.	Conclusions.	99
Chapter VI:	GRANULARITY OF NUCLEAR RESEARCH EMULSIONS	
1.	Graininess and granularity.	101
2.	Definition of granularity used in the present investigation.	104
3.	Theoretical treatment of the granularity of nuclear research emulsions exposed to electrons.	104
4.	Method of measurement of granularity.	106
5.	Results:-	109
(a)	Check on theory.	
(b)	Comparative granularity of XM and G5 emulsions.	
(c)	Least detectable density variation.	
(d)	Comparison with photographic emulsions.	
6.	Degradation in Signal-to-noise ratio due to electronographic recording.	118
7.	Overall reduction of Signal-to-noise ratio in a single-stage electronographic image tube.	120
8.	Variation of equivalent quantum efficiency with exposure.	123

			Page
	9.	Use of grain counting techniques for image evaluation.	124
	10.	Conclusions.	126
Chapter VII:		COMPARATIVE SPEED AND GRANULARITY OF THE SPECTRACON AND LALLEMAND'S ELECTRONIC CAMERA.	
	1.	Introduction.	127
	2.	Calculation of Comparative Speeds.	129
	3.	Experimental procedure.	134
	4.	Comparative speeds of Spectracon and Lallemand's electronic camera.	138
	5.	Comparative granularity of the Spectracon and Lallemand's electronic camera.	138
	6.	Calculation of the spread in the number of developed grains produced per electron by the Spectracon.	139
	7.	Experimental results.	145
	8.	Comparative equivalent quantum efficiencies.	146
	9.	Conclusions.	147
Chapter VIII:		CONCLUSIONS.	148
ACKNOWLEDGEMENTS			151
REFERENCES.			152
APPENDIX I			157
APPENDIX II			161

Chapter 1.

1.1. Introduction.

Photographic emulsions have been used to detect nuclear particles since the beginning of the science of radioactivity. Becquerel discovered radioactivity by noticing the blackening of photographic plates caused by radiation emitted by uranium salts. The first investigation of this effect was made by Kinoshita (1) working under Rutherford, in 1910. Using a microscope and counting silver grains he was able to show that a single α - particle is capable of rendering a halide grain developable. It was soon realised that the photographic emulsion could be a very useful instrument for the detection and measurement of the properties of nuclear particles. The systematic investigations of Powell (2-3) proved that under proper experimental conditions the energy of a particle can be measured accurately from the length of its track in the emulsion and that this applies not only to protons and α - particles but that even the energy of neutrons can be determined with a high degree of accuracy. The work of Powell established the emulsion technique as a quantitative and versatile method capable of giving results of high precision and reproducibility. Since this time a whole range of 'Nuclear Research Emulsions' has been developed, particularly by Ilford Ltd, having a wide range of sensitivities to meet the needs of particular applications. Emulsions are now

available which will detect any charged particle having an energy greater than a few kV. As their name implies Nuclear Research Emulsions have been most widely used in applications where it is required to detect single particles i.e. in nuclear physics and cosmic ray physics. Thus the development of these emulsions has been aimed at satisfying the requirements of workers in these fields. Whereas there is much information in the literature [4] concerning the properties of emulsions of interest to nuclear physicists, only quite recently, with the development of electron microscopes and electronographic image tubes, has interest been shown in the qualities of emulsions required for these particular applications. Nuclear research emulsions have been developed to meet certain applications in nuclear physics, thus the physical characteristics of currently available emulsions have been matched to the specific requirements of single particle detection. Thus consideration is given to these requirements and their effect on emulsion composition.

1.2. Composition of Nuclear Research Emulsions.

The main requirements of an emulsion for use in nuclear physics or cosmic ray work are :-

(I) All charged particles should produce tracks in the emulsion.

(II) The tracks should be well defined and be clearly visible above fog background.

(III) Particles of different charges and masses should produce tracks of different appearances.

(IV) Fog background should be minimal.

Nuclear research emulsions consist of about equal parts by volume of silver halide crystals, of the order of a micron in diameter, and a matrix element which is mainly gelatine. The parameters of the emulsion which may be adjusted to meet the requirements listed above are the concentration of silver halide, the mean grain size and the mean grain spacing. The development of emulsion manufacturing technique has not resulted in a single emulsion with all the required properties but in a range of emulsions designed for specific applications in particle detection. The emulsions which are of particular interest in this investigation are the Ilford emulsions G5, L4 and XM. These emulsions have found widespread use as electron image recorders in electronographic image tube systems. The emulsions G5 and L4 were developed specifically for use in nuclear physics. In the original nomendature emulsion types were designated by a letter and a number, the letter indicating the grain size (decreasing in alphabetical order) and the number indicating sensitivity (increasing with the number). The emulsion XM was primarily developed for autoradiographic purposes. The emulsions G5 and L4 are sensitive to all charged particles of energy greater than a few kV. These emulsions differ mainly in the diameter of the silver halide crystals. These are 0.14 micron for L4, 0.27 micron for G5 and 2.0 micron for XM. Emulsions of the G and L series have the following

composition [5] These figures give the mean composition of 40 batches of G5 emulsion in gm/cc in equilibrium with air at 58% R.H. at room temperature :-

Element	Composition, gm/cc
Silver	1.817 ± 0.029
Bromine	1.338 ± 0.020
Iodine	0.0120 ± 0.0002
Carbon	0.277 ± 0.006
Hydrogen	0.0534 ± 0.0012
Oxygen	0.249 ± 0.005
Nitrogen	0.074 ± 0.002
Sulphur	0.0072 ± 0.0002

Information on the composition of XM emulsion is not available from the manufacturers. The composition of emulsion is liable to variation from batch to batch and with the prevailing humidity. The mean density of emulsion is 3.8278 ± 0.0354 gm/cc.

1.3. Other Applications of Nuclear Research Emulsions

The application of emulsions in nuclear physics has already been noted and in this field at least eight sub-atomic particles were discovered using emulsion techniques. Other applications [4] of emulsions have been made in the medical sciences for tracer work and

autoradiography. There are also applications in analytical chemistry, metallurgy, plant physiology and mineral prospecting.

This thesis is mainly concerned with the application of nuclear research emulsions for recording electron images generated from photocathodes in image intensifier systems and thus the main interest is in the 'photographic' qualities of these emulsions i.e. the shape of the optical density - exposure characteristic, speed, contrast and granularity. Image intensifier systems employing nuclear research emulsions will be considered in detail in a later Chapter.

1.4. Requirements of Nuclear Research Emulsions for Recording Electron Images.

The requirements of nuclear research emulsions for the recording of electron images are essentially the same as the requirements of ordinary photographic emulsions for the recording of light images. Thus, for this application, nuclear research emulsions must possess a high speed (i.e. a high rate of production of developable grains for a low incident electron flux), good contrast, low granularity and low fog level. The requirements of high speed and low granularity are contradictory since high emulsion speeds are generally obtained by increasing the grain size of the emulsion and this leads to an increase in the granularity. In addition the optical density produced on the emulsion expressed as a function of exposure should be linear. It is well known [6] that the response of photocathodes to light is linear over a very wide range of light intensities. Thus by combining a

photocathode as a photon detector and using a nuclear research emulsion to record the resulting electron image, a linear image detecting device can be made. The degree of linearity of such a system will depend on the response of the emulsion. The technique for recording electron images using nuclear research emulsions is termed electronography and devices employing this principle are called electronographic image intensifier systems. Such electronographic intensifier systems that have been developed operate with electron energies up to 40 kV. This is the energy range of interest in the present investigation.

Some of the required properties of emulsions outlined above have been assessed for some emulsions for some electron energies. Most of the work described in the literature refers to essentially photographic emulsions. Thus Cranberg and Halpern[7] have investigated Ilford B-2 plates in the electron energy range 4.4 to 45kV. Premsela et al [8] have investigated some Kodak and Gevaert photographic plates for an electron energy of 42.5 kV. The only comprehensive set of quantitative data on the electronographic effect are that reported by Digby, Firth and Hercock [9] These authors investigated the Ilford photographic emulsions Contact Lantern, N.60 Photomechanical, N.50 Thin Film Half Tone and Rapid Process Experimental for a number of electron energies up to 70 kV. Very little quantitative information is available for the Nuclear research emulsions. Of these Valentine and Wrigley [10] have published some information on G5, L4 and XM but only for an electron energy of 60 kV.

The work described in this thesis is aimed at providing some quantitative information on those aspects of nuclear research emulsions of interest to users of electronographic image intensifier systems employing the emulsions G5, L4 and XM. Before describing the experiments that have been made, image intensifier systems are considered in more detail.

Chapter 2

Image Intensifier Systems

The purpose of this Chapter is to review the methods that have been developed in order to intensify weak optical images using photoelectronic methods.

2.1. Introduction - Photon Detection.

The process of photon detection can be characterised by a quantity, known as equivalent quantum efficiency. This concept was introduced by Rose (11) and further developed by Fellgett (12) and Jones (13) It is a measure of the effectiveness of a detector for producing registrable output events i.e. developable silver halide grains in the case of photographic emulsions or photoelectrons in the case of photoemissive surfaces, when exposed to a given incident photon flux. This quantity has been measured (12) in the case of some photographic emulsions. Kodak Royal X Pan has given some of the best results and in this case peak monochromatic quantum efficiencies of 0.9% at a wavelength of 4300A° and 0.6% at 6070A° were found to occur at optical densities of only 0.1 - 0.2 above fog. At the more useful densities around 0.6, in the linear region of the optical density - log exposure characteristic, the equivalent quantum efficiency falls to only 0.1%. Also, with the long integration times

necessary to record faint low-contrast optical images, the effect of reciprocity failure will result in even lower quantum efficiencies than the values quoted above. Clearly the photographic emulsion is a very poor photon detector.

Other photon detectors include photoemissive surfaces. Of these, Sommer and Spicer (14-17) have reported quantum efficiencies of tri-alkali photocathodes of 40% for incident radiation of wavelength 4000A°. Bi-alkali cathodes have been reported (18) as having quantum efficiencies of 30% at this wavelength. In fact, at any point, throughout the wavelength range 1000 - 14000A° photocathodes can be obtained with much higher quantum efficiencies than any photographic emulsion. The quantum efficiencies of photocathodes are independent of the intensity of illumination over a wide range of light intensities. The high quantum efficiency over a wide spectral range, the linearity of response, low dark current and absence of reciprocity failure of photocathodes offer great advantages over the photographic emulsion in photon detection.

In astronomy and spectroscopy it is required to produce permanent records of observations on star fields or spectra. Photocathodes cannot store information and to exploit their increased

quantum efficiencies to the maximum the photoelectrons liberated by an optical image must be recorded with certainty. Two main methods have been developed to achieve this :-

2.2. Image Intensifiers with Internal Multiplication

The simplest conceivable image intensifier is a parallel photocathode - phosphor arrangement in the same vacuum envelope. The electron image liberated by the photocathode is accelerated and focussed by a suitable electron-optical arrangement on to the phosphor screen. Theoretically [19,20] such a tube should have a blue light gain in speed over direct photography of the order of 100. It has not been possible to realise this in practice due to extensive losses in the transfer optics between phosphor and recording photographic emulsion. In order to record single photoelectrons with such a system, devices employing internal electron multiplication have been developed. Two types of multiplying dynode have been used :-

(a) Transmission Secondary Emission (T.S.E.) Image Intensifier.

Secondary electron emission is employed in this device to produce electron multiplication. The primary photoelectrons emitted from the photocathode are accelerated and focussed on to a thin film of secondary emitting material. Secondary electrons are produced and emitted from the other side of the film and can then be accelerated and focussed on to another secondary emitting film. The multiplying dynode comprises a composite film of a 500A° layer of potassium

chloride with a conducting film of aluminium 150-200A° thickness. Tubes of this type have been developed by Wilcock et al [21], 20th Century Electronics, English Electric Valve Co. Ltd. and by Westinghouse Research Laboratories. This type of multiplying dynode has a low electron gain and thus the deviation from the average number of secondary electrons is large resulting in a low signal-to-noise ratio. Also there is a high probability that a photoelectron will not produce any secondary electrons thus reducing the quantum efficiency of the system. Blue light gains of 10^6 and a resolution of 30 line pairs per mm have been obtained [22, 23] This type of tube has not yet been developed to the stage where it can record single photoelectrons with a high degree of certainty.

(b) Cascade Image Intensifiers

These tubes employ cascade phosphor-photocathode screens for electron multiplication. Tubes of this type having several stages of multiplication have been reported [24-29] A three gain stage tube, having two cascade multiplying screens, has been developed by McGee et al. For this kind of multiplying dynode current gains of the order of 100 have been measured and consequently the signal-to-noise characteristics of this tube should be improved over the T.S.E. tube. Blue light gains of the order of 10^6 have been measured and a resolution of 50-55 line pairs per mm has been achieved. Single photoelectrons can be detected with this tube and the photoelectron

recording efficiency is of the order of 73% [29]

2.3. Electronographic Image Intensifiers

An alternative approach to the problem of recording single photoelectrons with certainty is the direct method of recording photoelectrons on electron sensitive emulsions. This approach was originally suggested by Lallemand [30] in 1936 and since then many methods of electronographic recording have been developed.

(a) Lallemand's Electronic Camera

Of the image intensifiers employing electronographic recording yet developed, the Lallemand electronic camera [31-35] is the simplest in conception but the most complex in operation. The basic principle is to accelerate the photoelectrons released from the photocathode by the incident optical image and to focus them electrostatically onto an electron sensitive emulsion which is contained in the same vacuum enclosure. Unfortunately these emulsions outgas in vacuum and the gases produced have a detrimental effect on the photocathode sensitivity. Initially photocathodes had a useful lifetime of only 15 mins. but with the use of getters, titanium ion pumps and refrigeration of the photocathode and emulsion, this has now been extended to several days and very long exposures are now possible. Using a specially constructed plate holder a total of 24 exposures can be made. The photocathodes are prefabricated and are contained in protective glass envelopes until actually required for

use. The glass envelope is broken with a magnetically activated hammer and the photocathode is then moved into position. When all the plates have been used or when the photocathode sensitivity has dropped to a very low level, air is admitted to the system and the plates are recovered for development. Then new cathode and emulsion plates are loaded and the system is repumped for subsequent use.

Antimony - caesium photocathodes have been most widely used with this system with peak quantum efficiencies of 12-15% at a wavelength of 4000A°. More recently (36) infra-red sensitive cathodes have been successfully used in the tube. An electron accelerating potential of 25 kV is typically used in this tube. At this potential each electron will cause several grains in the emulsion to become developable. Thus, almost the full quantum efficiency of the photocathode is used and speed gains of the order of the relative quantum efficiencies of photocathodes to photographic emulsions may be expected i.e. of the order of 100. Lallemand (31) has reported a blue light gain in speed over Kodak 103a - O photographic emulsion of 50-100 times. Walker, (37) using the Lallemand technique, has reported speed gains of 20 times at short exposure times to 120 times at long exposures of 100 minutes. The variation in speed gain with exposure time is due to the effect of reciprocity failure of photographic emulsions. In the infra-red (10,000A°) speed gains of several hundred times are reported (36) over the best infra-red sensitive

photographic emulsions, Eastman-Kodak I.Z plates. The speed of the Lallemand system may be enhanced by electron optical demagnification and typically the electron image is demagnified by a factor of 0.7, although a demagnification of 1/7 has also been used.(33) The resolution obtained by this tube is limited by the optical and electron-optical systems and by the type of emulsion used. A resolution of 70 line pairs per mm has been obtained on Ilford G5 emulsion. Resolution falls off at the edge of the exposed area due to optical abberrations. By using curved cathode plates and increasing the field gradient at the cathode, good resolution has been obtained over three-quarters of the working area.

This tube has been used for making astronomical observations and has given excellent results. Its complex design and mode of operation and the difficulties associated with focussing the tube are its main disadvantages. The fact that the photocathode and emulsion plates have to be periodically replaced can result in a waste of telescope time. To overcome these difficulties other types of tube based on the same principle have been developed.

(b) Kron's Electronic Camera.

The essential feature of this type of camera is the introduction of a metal gate type of valve between the photocathode and the emulsion (38) After each set of exposures this valve can be closed in order to preserve the photocathode for repeated use. The

photocathodes used have been antimony-caesium cathodes of quantum efficiency 8-12% at 4200A°. (39) More recently rubidium-caesium-antimony cathodes have been used with quantum efficiencies of 10-15% at 4200A° (40) The cathodes used are not prefabricated but are formed inside the tube. The flooding of the tube with caesium vapour during this process results in a lowering of the work function of the metal parts in the tube and consequently the background of the tube is high. This use of a valve has resulted in photocathode lifetimes of up to seven months. As with the Lallemand system, Kron's electronic camera uses electrostatic focussing and the electron image is demagnified in the ratio 1.55 : 1. A resolution of up to 65 line pairs per mm has been obtained. Until recently exposure times of less than one hour on G5 emulsion have only been possible due to the problem of background and this limited the use of the tube to lunar photography. Improved technique now makes possible exposures of several hours. In the present design of tube it is only possible to expose five or six plates at any one time.

(c) Hiltner's Electronic Camera.

In this modification of the Lallemand technique, (41,42) the photocathode is preserved by containing it in a special compartment which is sealed by a thin aluminium oxide film, 0.14 microns thick. The photocathode chamber is highly evacuated and the recording emulsions are exposed in another chamber behind the

aluminium oxide film which is moderately evacuated. During exposure the emulsion is held to within 50 microns of the aluminium oxide film. Arrangements are made for a phosphor to be mounted in this position for adjusting the tube focus. The emulsions are introduced through a vacuum lock, thus preserving the aluminium oxide film which can only withstand a pressure differential of the order of 500 μmHg. The electron image from the photocathode is accelerated to 20 kV and is electrostatically focussed. It penetrates the aluminium oxide film and strikes the emulsion. Resolution of 40 line pairs per mm have been achieved and it is anticipated that this can be improved to 65 line pairs per mm. Long exposures with little background are possible with this tube and the photocathode can be preserved for more than one month. A big disadvantage of this tube is the fact that it has to be continually pumped and it is hoped to incorporate a cryogenic pumping system.

(d) The Spectracon.

The electronographic image tubes described above all suffer from the problem of exposing and subsequently recovering the electron-sensitive emulsion without affecting the photocathode sensitivity. The tubes described have to be continually pumped and the optical and electron-optical systems have to be carefully re-adjusted after the emulsion plates have been replaced. The gradual loss in sensitivity exhibited by the photocathodes in these devices makes it unlikely that

reproducible results can be obtained.

There are obviously many attractive features in a completely sealed-off electronographic device. Such a device has been developed by McGee et al (43-46) and is known as the Spectracon. The Spectracon is a development of work carried out on a specially designed single-stage image intensifier described by Wheeler (47) and Zacharov.(48) The problem of the inefficiency of the transfer optics of this type of tube has already been referred to. The loss of speed was considerably reduced using a mica window 12-15 microns thick sealed to the end of the tube. A phosphor screen was deposited on the internal side of the mica, which was robust enough to withstand atmospheric pressure. To record the image from the phosphor screen, a flexible photographic emulsion was pressed against the window and a contact print was made. This represented a considerable advance over the original tube design and it was realised that even better results could be achieved if very thin mica windows, transparent to electrons, could be used. Then the phosphor could be eliminated and the photographic emulsion replaced by an electron sensitive emulsion. Of the electronographic image tubes yet developed, the Spectracon is one of the most promising both from a practical and performance point of view and so it will be considered in detail :-

The initial design of the tube, known as type - A,

consisted of a lime soda envelope 5 cm in diameter and 28 cm long. One end of the tube is sealed with a flat lime-soda glass disc. The other end of the tube is sealed with a chrome iron disc which has a central slot milled in it. The slot dimensions are typically (5-10) x 30 mm. The mica window which is between 3.5 to 4.0 microns thick is sealed across this slot using solder glass. Stainless-steel annuli are mounted at 1 cm intervals inside the tube using Pyrex spacers. Type - A Spectracons are characterised by having their photocathodes formed inside the tube using a special processing compartment to minimise the effect of caesium contamination of the tube parts. In type - B Spectracons, the photocathode is formed on a cathode plate in a separate processing cell. Cathodes of high sensitivity can then be selected for transfer into a tube. The tube and cathode cell are both sealed to a pumping system. The cathode cell has a sidearm extension which has a thin glass bulb attached to it. When the tube side of the system has been pumped and baked, this bulb is broken with a magnetically-activated hammer and the cathode plate with its holder can be transferred to the tube using external magnets. The cathode plate is held on the holder using spring catches. The cathode plate is deposited inside the tube by releasing these catches using external magnets and the cathode holder is then retracted. The tube can then be sealed-off. Initially, difficulties were encountered with this technique since the gases evolved from the glass during

seal-off poisoned the photocathode. Barium getters are now employed to absorb these gases and the cathode plate is allowed to rest, photocathode downwards, on a barium-coated glass plate mounted inside the tube. The cathode remains in this position for up to two days after seal-off. It is then manipulated down the tube and mounted in its working position. The barium-coated glass plate is clipped into position behind one of the annuli. This technique has been successfully developed for S.9., S.11. and S.1. photocathodes. Its advantages are (i) Penetration of caesium vapour into the tube is substantially reduced. Thus the tube background should be considerably improved. (ii) One can select only those photocathodes with the highest sensitivity for insertion into a tube. (iii) Unlike type - A tubes the photocathode is mounted in good contact with the end-window of the tube resulting in a much more satisfactory optical arrangement.

Difficulties have been encountered in the transfer of the very sensitive S.20. photocathodes. These cathodes lose their sensitivity very quickly after transfer into a tube. This is thought to be due to diffusion of caesium from the cathode surface and also to small amounts of gas liberated by minute discharges when the tube is operated. More research is being conducted into the problem of transferring S.20. photocathodes into the Spectracon.

Mode of Operation of the Spectracon.

The electron image from the photocathode is focussed at the mica window using a system of parallel electric and magnetic fields. A total accelerating potential of 40 kV is applied across the tube - this has been found to give the best compromise between electron transmission through the mica window and tube background. At this potential an axial magnetic field of 160G is required to produce two-loop imaging of the electrons. The electron image is recorded by pressing the electron sensitive emulsion firmly against the mica window. The mica windows currently used are between 3.5 - 4.0 microns thick and cover a useful working area of 5 x 30 mm. The electron sensitive emulsions used are specially prepared by Ilford Ltd. They are 10 microns thick and are coated on to a flexible Melinex supporting layer 50 microns thick. A strip of film is cut to size and mounted on a rubber roller. When exposing the film the rubber roller is gently but firmly held against the mica window. A special camera attachment has been designed which is mounted on to the mica window end of the tube. Successive exposures can be made without removing the camera from the tube and a total of eight exposures can be made on one strip of film.

Performance of the Spectracon

1. Speed Gain over Direct Photography.

This factor will depend on the type of photocathode used,

its quantum efficiency and spectral response, the accelerating potential used, the thickness of the mica window and the type of recording emulsion used. For a tube having a mica window of 4.5 microns thickness, an antimony-caesium photocathode of 10% quantum efficiency in the blue and operated at 40 kV using G5 emulsion, a speed (rate of emulsion blackening) gain of about 25 times over Kodak baked II a-O is predicted.[49] For the more efficient tri-alkali photocathode this may rise to 75 times. For the S.1. infra-red sensitive cathodes, the speed gain will be much greater due to the poor performance of photographic plates at these wavelengths. A speed gain of the order of 1,000 for an S.1. Spectracon has been measured [50] at 10,000A°. These measurements were made at a density of 0.6 on G5 emulsion and the comparison was made with I-Z photographic emulsions. Further consideration is given in a later chapter to the speed gain of the Spectracon and in particular to the relative speed gains of Lallemand's Electronic camera and the Spectracon.

Resolution of the Spectracon.

The limiting resolution of the Spectracon will be set by the distribution in energy of the photoelectrons leaving the cathode, the electron-optical arrangement and electron scattering in the mica window and emulsion. Khogali [49] has considered the contribution of these effects and a limiting resolution of 95 ± 20 line pairs per mm is predicted for a tube of mica window thickness 4.5 microns operated

at 40 kV and recording with G5 emulsion. A limiting resolution of 80 line pairs per mm is regularly obtained with recent tubes on G5 emulsion and a resolution of 95 line pairs per mm has been recorded on the finer grained L4 emulsion.

Background of the Spectracon.

The background of the tube will set a limit on the length of exposure that may be made with this tube. Exposures of several hours are typically required in astronomical observations. Background will arise inside the tube from such effects as thermionic and field emission. In the case of the Spectracon, which is normally operated with the mica window end at earth potential and the photocathode end at - 40 kV, background can arise from corona discharge at the photocathode. By careful design of the photocathode end of the tube and the internal tube parts, exposures of up to one hour can be made on the fast emulsion XM. This is equivalent to an exposure of approximately 5 hours on G5 emulsion.

It is clear that this tube has been developed to the stage where it can make a valuable contribution to the detection of faint, low-contrast optical images in astronomy and spectroscopy.

(e) Electronographic Cathode Ray Tube.

The electronographic devices described above have been developed in order to fully exploit the greater efficiency of the photocathode as a photon detector. Another device employing the

electronographic principle has been described in the literature (51) This is the electronographic cathode ray tube. The design of the tube is similar to the conventional cathode ray tube in so far as it contains an electron gun and deflecting electron-optics but instead of the conventional phosphor screen output, a mica window of the type used with the Spectracon is used. The deflections of the electron beam are recorded on electron-sensitive emulsion pressed against the mica window. The electronographic process is far more efficient at recording information than the conventional phosphor screen-transfer optics system and in this particular application should result in higher writing speeds and higher resolution. The problem of moving the film past the mica window has yet to be solved and this has limited the use of this tube to static recordings.

Other devices employing the electronographic technique exist, in particular electron microscopes. This thesis is mainly concerned with the application of emulsions to recording electron images and the requirements of emulsions for use with electronographic image intensifiers and electron microscopes are essentially the same. Of the requirements outlined in 1.4 above speed, degree of liniarity and contrast will be considered from a theoretical point of view in the next chapter.

Chapter 3.

Theoretical Consideration of the Effect of the Exposure of Nuclear Research Emulsions to Electrons.

3.1. Introduction :-

For recording electron images, nuclear research emulsions ideally should posses high speed and contrast and low granularity and chemical fog. It is also desirable that the response of the emulsion be linear i.e. the optical density produced should be strictly proportional to the incident electron flux. For the detection of very low contrasts, one needs to make the maximum use of the available storage capacity of the emulsion i.e. ideally one would like one output event (a developed silver grain) for each incident electron. Fellgett [52] has shown that if q is the quantum efficiency of the photocathode and m is the average number of output events produced by a primary photoelectron then the equivalent quantum efficiency of the system, q_e is given by :-

$$q_e = \frac{q}{1 + \frac{1}{m}}$$

This assumes that the output events are statistically independent and are spatially distributed according to Poisson's Law. The value of m for electron sensitive emulsions is a function of electron energy which can be varied to any desired value. It can be seen from the equation above that to make m unity results in a system

where only half the photocathode quantum efficiency is used. High values of m improves the equivalent quantum efficiency of the system but results in a waste of available storage capacity. A compromise value of around eight is typically used.

The choice of electron sensitive emulsion to be used with an electronographic image intensifier depends on the actual observation to be made. For the detection of low contrasts, fine grained emulsions are required but there are some applications where a high speed is essential and for these much coarser grained emulsions will be required. The emulsions which have come to be favoured by users of electronographic tubes are L4, G5 and XM and these give a useful range of speed and granularity.

3.2. Fog Level of Nuclear Research Emulsions.

When a developer acts upon an emulsion, some grains which have not been exposed are reduced to metallic silver. The density obtained in the unexposed portions of the image is known as fog. As Mees (53) points out the origins of fog are complex and the production of developable grains of silver halide without exposure may be ascribed to the emulsion or to the developer. Some developers have a greater tendency to produce fog than others. Nuclear research emulsions are manufactured primarily to meet the requirements of nuclear physicists. Here it is required to discriminate single tracks and thus the requirements of the emulsion regarding fog are

much more stringent than for ordinary photographic emulsions. For this reason the manufacturers take special care to reduce the fog of nuclear research emulsions. The fog density of L4 emulsion is around 0.03, that of G5 is also around 0.03 and the fog density produced in the faster emulsion XM is around .08. This compares with fog density of typical photographic emulsions of between 0.1 - 0.15. The low fog level of these emulsions is, of course, advantageous in their application to electronographic image tubes because a low fog level means greater available storage capacity and thus a greater ability to detect low contrasts.

3.3. Production of Developable Silver Grains in Nuclear Research Emulsions exposed to Electrons

Photographic and nuclear research emulsions consist of a suspension of crystals of silver halide (mainly silver bromide) in gelatine. The effect of exposure to light or moving charged particles on the crystal is to form specks of silver atoms at points on the surface of the crystal. The actual process which takes place within the crystal as a result of exposure to light or electrons is thought to be fundamentally the same i.e. the energy absorbed by the crystal from the incident photons or electrons raises electrons in the crystal to the conduction bands. These electrons move freely until they encounter a local potential energy minimum where they can be trapped. After capturing electrons the traps, being then negatively charged

attract interstitial silver ions to the trap sites and thus particles of silver are formed. These minute specks of silver constitute the latent image. The developer, which is a solution containing a chemical reducing agent, acts selectively to convert those crystals containing a latent image to metallic silver. The silver halide crystal is converted in this process to a silver grain. Whereas the silver crystal is nearly spherical in shape, the silver grain is a fibrous mass of silver, larger than the silver crystal. When development is complete the emulsion is fixed, the action of the fixer is to dissolve all the unexposed crystals of silver halide. Although the physical effect produced by the exposure of silver halide to light and moving charged particles is the same, Valentine (54) has drawn attention to an important fundamental distinction between these two processes. This involves the amount of energy the silver crystal has to absorb in order that electrons be raised to the conduction band and the crystal become developable. For exposure to light of wavelength 4,500A°, the energy required for this process to occur is about 30eV i.e. of the order of 10 photons are required. For exposure to moving charged particles, electrons of energy of around 500 eV are required in order to transfer sufficient energy to the crystal to render it developable. Thus for the energy range used in electronographic image tubes and electron microscopy i.e. 25 - 100 kV, if an electron with energy in this range, strikes a crystal of silver

halide it will transfer more than sufficient energy to produce a latent image. Thus for electrons of sufficient energy, the exposure of electron-sensitive emulsions is a single-hit process. For photographic emulsions, the cumulative effect of the absorption of several photons is required to produce a latent image and this has complicated the mathematical treatment of the photographic effect. Assuming a single-hit process (the experimental evidence for this is considered later), the mathematical treatment of electron-sensitive emulsions is relatively easy. Certain simplifying assumptions concerning the structure of emulsions have to be made. It is assumed that each halide crystal has a cross-sectional area equal to A. In fact, there is a wide distribution of the areas of halide crystals. After development each silver grain has a cross-sectional area A^1 for stopping light, which will be greater than A. The following analysis relating optical density to exposure has been given by Valentine. (54)

3.4. Optical Density Theoretically Related to Exposure.

E, the exposure, is defined as the incident number of electrons per unit area. Then the average number of electrons striking a crystal is E.A. From the Poissonian distribution law, the fraction F of all the crystals in the emulsion that are hit at least once is given by :-

$$F = 1 - e^{-EA} \quad \ldots\ldots\ldots\ldots\ldots\ldots\ldots\ldots\ldots\ldots\ldots\ldots (1)$$

After development, each silver grain has a cross-sectional area A^1 for stopping light. Considering a unit area of a thin layer of emulsion (in which there is no overlap of silver grains) initially containing δN halide crystals, the fraction of the incident light $-\delta L/L$ stopped by this elementary layer after development will be equal to $A^1.F.\delta N$. Integrating through the full thickness of emulsion gives :-

$$\ln \left(L_o/L_1 \right) = \ln \left(1/T \right) = A^1.F.N. \quad \ldots\ldots (2)$$

where T is the fraction of light transmitted through the emulsion ($T = L_1/L_o$) and N is the total number of halide crystals per unit area of unexposed emulsion. Combining (1) and (2) gives :-

$$D = \log_{10} \left(1/T \right) = \left(\frac{A^1 N}{2.3} \right) \left(1 - e^{-EA} \right) \quad \ldots\ldots\ldots\ldots\ldots (3)$$

where D is the optical density

The factor $\frac{A^1 N}{2.3}$ is the saturation density Ds and is reached when every crystal of silver halide is developed

Thus ;-

$$D = Ds \ (1 - e^{-EA}) \quad \ldots\ldots\ldots\ldots\ldots\ldots\ldots\ldots\ldots\ldots\ldots\ldots (4)$$

For values of D $< Ds/4$ this equation can be approximated with less than 5% error to :-

$$D = Ds.A.E. \quad \ldots\ldots\ldots\ldots\ldots\ldots\ldots\ldots\ldots\ldots\ldots\ldots\ldots\ldots (5)$$

Thus, for densities up to $Ds/4$ density should be linearly related to exposure. Normal photographic emulsions are designed by

the manufacturers to have a saturation density of the order of 6. Since nuclear research emulsions are more heavily loaded with silver halide than ordinary photographic emulsions a saturation density of at least 6 may be expected. Thus, these emulsions should be linear up to densities of at least 1.5. It should be pointed out that equation (5) is more likely to hold for specular rather than diffuse density measurements. In specular density measurements, the light that is scattered by the grains is largely excluded. In the above analysis, the optical transmission of the emulsion is taken to be the ratio of the light intensity directly transmitted by the emulsion to the original light intensity of the beam.

This theory may be re-worked on the basis that several hits, are required to render a silver halide crystal developable Equation (4) then becomes :-

$$D = D_s\left[1 - e^{-EA}\sum_{0}^{r-1}(EA)^r/r!\right] \quad \ldots\ldots\ldots\ldots\ldots\ldots (6)$$

The general form of equation (6) is shown in Fig.1 where optical density is plotted against $\log_{10}$ (exposure) for values of r in the range 1 - 32. As we have seen, emulsions exposed to electrons should follow the single-hit, $r = 1$, curve.

For the linear part of the optical density - exposure characteristic, we see from equation (5) that the speed of the emulsion is given by Ds.A. A, the area of the silver halide crystals,

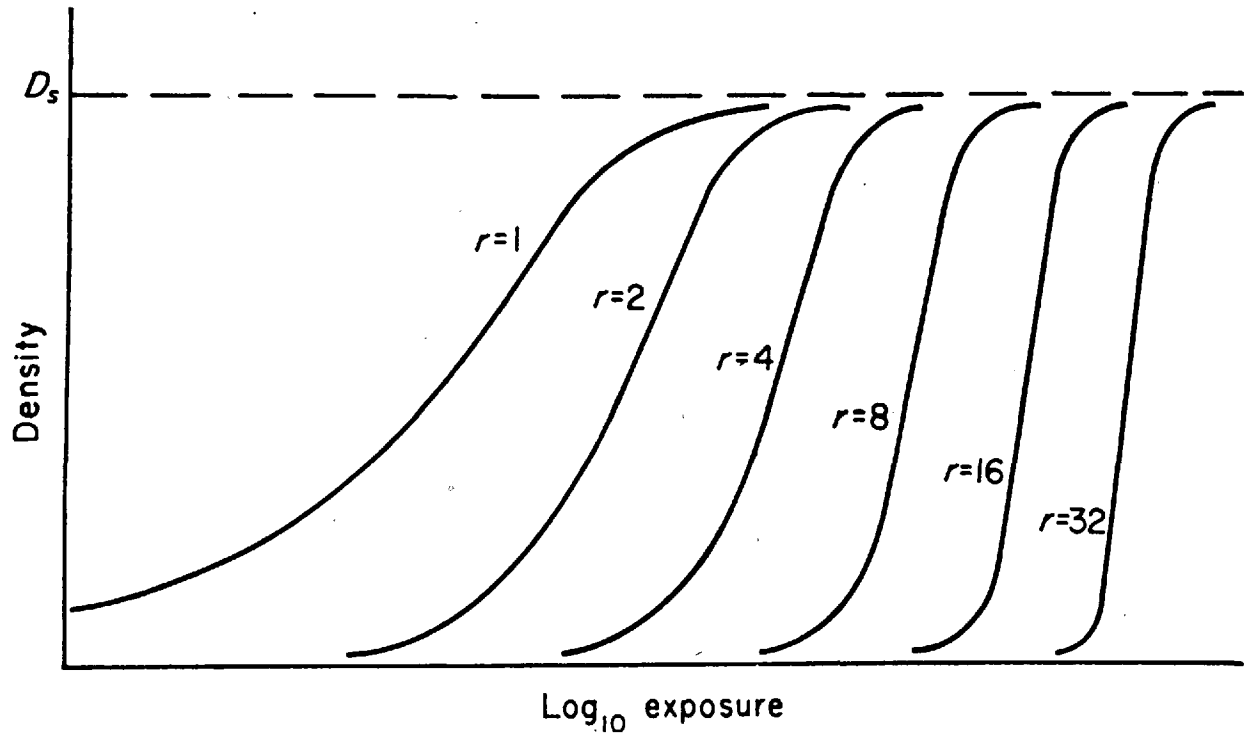


FIG. 1. Theoretical curves of density against log exposure for various values of r, the number of hits required to produce a developed silver grain from a silver halide crystal. The single-hit curve $r = 1$ should be followed by emulsions exposed to electrons.

is a constant of the emulsion and Ds, the saturation density, is a function of the number of silver halide crystals per unit volume in the emulsion and also of the emulsion thickness. For electron ranges less than emulsion thickness, the saturation density will be a function of electron range and consequently electron energy. Thus, Ds will rise with electron energy and since the degree of linearity is related to Ds, this should also increase with electron energy. Thus, for electron ranges less than the emulsion thickness, both the speed and degree of linearity of the emulsion are expected to increase with the energy of the incident electrons. Barkas [5] gives information on electron range in emulsion and states that a 40 kV electron has a range in emulsion of 10 microns. The emulsions used in this investigation were 25 microns thick and the electron energies used were 40 kV and so all the electron energy will be completely absorbed by the emulsion.

3.5. Contrast of Nuclear Research Emulsions.

The contrast, γ, of photographic or electron sensitive emulsions at a density, D, is defined as the slope of the characteristic H and D curve at that density. For photographic emulsions the value of γ depends strongly on the emulsion and its processing conditions. Thus,

$$\gamma = \frac{dD}{dH} = \frac{dD}{d(\log_{10}E)} = 2.3E \frac{dD}{dE} \quad \ldots\ldots\ldots\ldots (7)$$

Equation (5) may be re-written as D = kE, where k depends on

the emulsion and the incident electron energy. Thus, $\frac{dD}{dE} = k$ and so :-

$$\gamma = 2.3\ E.k = 2.3\ D \quad \ldots\ldots\ldots\ldots\ldots\ldots\ (8)$$

The very simple result is obtained that the contrast of electron-sensitive emulsions is a function only of the density to which the emulsion has been exposed and is independent of the type of emulsion, the developer used, the energy of the incident electrons etc. Equation (7) holds for the linear region of the characteristic curve and is a direct result of the assumption that the process involved in the exposure of nuclear research emulsions to electrons is a single-hit process. As such it provides a direct check on the assumption of a single-hit law. For contrast at densities greater than $Ds/_4$ the more complete expression of equation (4) has to be used. This gives :-

$$\gamma = 2.3\ (Ds - D)\ \ln\left(\frac{Ds}{Ds - D}\right) \quad \ldots\ldots\ldots\ldots\ldots\ (9)$$

By differentiating this expression it can be shown that the maximum value of contrast is given by :-

$$\gamma_{MAX} = \frac{2.3}{e}\ Ds = 0.85\ Ds \quad \ldots\ldots\ldots\ldots\ldots\ (10)$$

occurring at a density of

$$D = \frac{e - 1}{e}\ Ds = 0.65\ Ds \quad \ldots\ldots\ldots\ldots\ldots\ (11)$$

3.6. Conclusions :-

The speed, contrast and degree of linearity of nuclear

research emulsions exposed to electrons have been considered from a theoretical point of view. The other important property of these emulsions of interest in this investigation i.e. granularity will be considered separately in a later chapter.

The analysis of this chapter may be summarised as follows :-

(I) Emulsions exposed to electrons should obey a single-hit law.

(II) It follows from the single-hit law that the response of the emulsion should be linear up to densities equal to a quarter of the saturation density.

(III) The speed and degree of linearity of the emulsion should increase with increasing electron energy.

(IV) The contrast of electron sensitive emulsions is a simple linear function of optical density, for densities within the linear region of the emulsion characteristic and is independent of the type of emulsion, incident electron energy or emulsion processing conditions.

The extent to which the electron-sensitive emulsions used with electronographic image tubes bear out these theoretical predictions has been investigated. The apparatus which was devised in order to carry out this investigation will now be described.

Chapter 4.

Experimental Apparatus for the Investigation of Nuclear Research Emulsions.

4.1. Design Considerations

It is required to be able to expose nuclear research emulsions to a known, uniform flux of electrons of a known energy. The effect to be measured (i.e. the optical density produced on the emulsion) must be that due to the electron beam alone and so care must be taken to avoid the emulsion becoming exposed to any source of fogging. Any apparatus designed for the quantitative investigation of this effect must embody the following essential features :-

(I) A source of electrons.

(II) An instrument for measuring the electron beam current.

(III) A shutter mechanism for exposing the emulsion.

(IV) A means of measuring the exposure time.

(V) A means of varying and measuring the energy of the electrons in the beam.

(VI) A phosphor screen for viewing the uniformity of the beam.

It was pointed out by McGee that an apparatus of this design could also be used to partially simulate the operational conditions of Lallemand's electronic camera and the Spectracon. The following exposures could be made on the same strip of film :-

(I) direct exposure of a beam of 25 kV energy, the typical operating potential of Lallemand's electronic camera.

(II) indirect exposure (i.e. by making the beam pass through thin mica foils before striking the emulsion) of a beam having a primary energy of 40 kV, the Spectracon's operating potential.

In this way, a comparison can be made of the relative rates of blackening of the emulsion under these conditions. Experiments of this kind have been done and will be described in a later chapter. To do this experiment requires that the electron energy can be varied from 25 - 40 kV without altering the uniformity of the beam.

Although nuclear research emulsions are primarily sensitive to moving charged particles, they also respond slowly to light and this fact was a major consideration in the design of the apparatus. The ideal type of equipment for this investigation would be a modified electron microscope and this has been used by other investigators in this field. (9) Such apparatus was not available to the author and McGee suggested a continuously pumped glass system to be described below.

4.2. Initial Experiments :- (I) Choice of Electron Gun

The fact that the emulsion had to be protected from fogging meant care had to be taken in the choice of electron gun. The most convenient source of electrons is a heated hairpin tungsten filament but unfortunately the electron emission from a tungsten filament is

also accompanied by considerable light emission which could fog the emulsion if it was directly exposed. Some initial experiments were made using a tungsten filament gun and with a 45° angle bend in the tube in order to protect the emulsion from direct filament light. In this way the emulsion was protected from fogging but the problems involved in bringing the electron beam round the bend in the tube proved to be difficult. The alternative of an indirectly-heated oxide-coated cathode was successfully used. When in operation the surface of this cathode glows a dull red colour and it was found that the emulsion could be directly exposed to this light for up to 10 mins. at a distance of 14" without any detectable fogging. Using an indirectly-heated oxide-coated cathode as source of electrons meant that a straight - through design of experimental tube as described below could be used.

II Value and Measurement of Electron Beam Current.

For a given emulsion sensitivity the factors determining the value of the electron beam current are (a) the type of beam shuttering mechanism employed (b) the fact that the appearance of the beam has to be registered on a phosphor screen in order to check its uniformity.

In the investigation of the photoelectron recording efficiency of the Spectracon, Khogali (49) made a measurement of the electron flux required to produce a certain density on G5 emulsion. It was found that for a Spectracon, with a 4.5 micron thick mica

window, a density of 0.5 is obtained on G5 emulsion with a charge of 6.7. 10^{-12} couls/cm^2 transmitted through the mica window. Thus if beam currents of the order of 10^{-12} amps/cm^2 are used it should be possible to use exposure times of several seconds to achieve reasonable densities and thus a mechanical shuttering system could be used.

A green-emitting Willemite phosphor was used to check the beam uniformity. This did not fluoresce at current levels of the order of 10^{-12} amps/cm^2 and beam energy of 25 kV. The current had to be raised by an order of magnitude before the dark-adapted eye could detect any fluorescence. This was unsatisfactory since the beam current had to be changed every time the beam uniformity had to be checked and when the beam current was changed a period of 5 - 10 mins. elapsed before the current stabilised to a steady value again. Also, there was no guarantee that the beam uniformity was maintained in changing the current from 10^{-12} amps/cm^2 to 10^{-11} amps/cm^2. It was obviously desirable to work with currents of the order of 10^{-11} amps/cm^2 and to employ a shuttering mechanism that would allow sub-second exposures to be made. Such a shuttering mechanism was developed and is described below. The phosphor screen was mounted on the nuclear emulsion plate holder (see Fig.2.) and this could be moved across the aperture for exposure to the beam. Thus care had to be taken to avoid fogging the emulsion by light from the phosphor

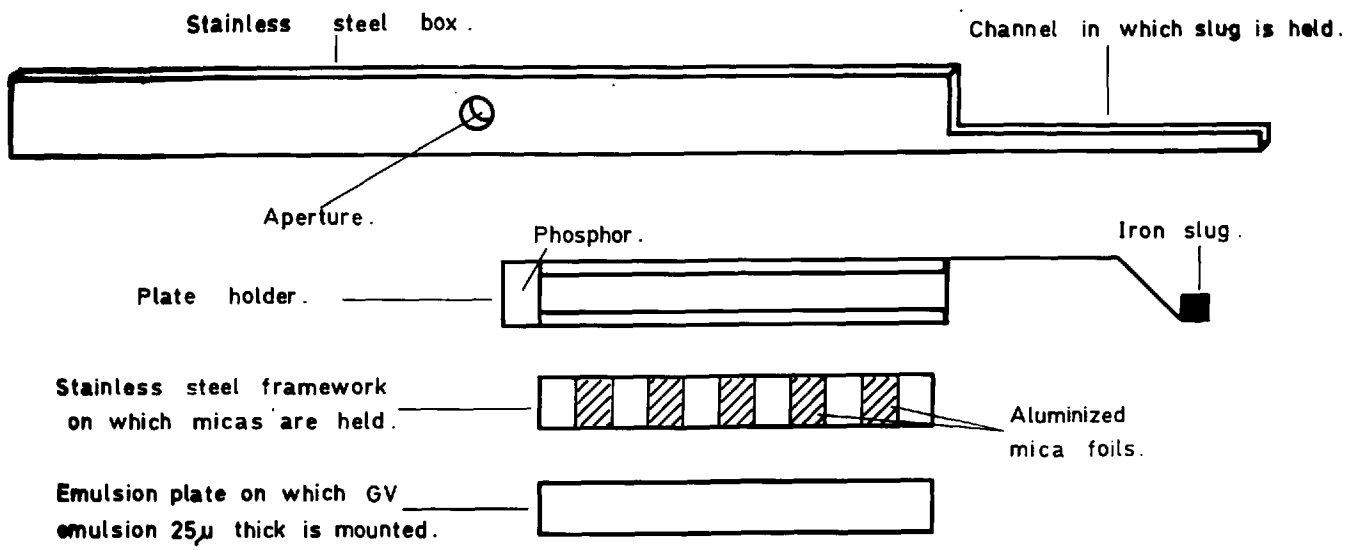


FIG 2

BOX AND PLATE HOLDER ASSEMBLY

screen. The exposure of the phosphor screen to the beam was kept to a minimum both in duration and intensity and also the back of the phosphor screen was aluminised so that most of the light was emitted in the forward direction away from the emulsion. These precautions ensured that the emulsion did not become fogged due to light emitted by the phosphor.

Measurements of beam current were made using a Faraday cage arrangement. The inside of the domed end of the tube (see Fig.3.) was coated with a conducting layer of Aquadag with the exception of a small central area about 1 cm in diameter, which was internally coated with Nesa. This completed the conducting layer and also provided a window through which the appearance of the image on the phosphor screen could be observed. Beam currents were measured on an E.I.L. vibrating reed electrometer connected to the Faraday cage. This had a measuring range from 10^{-9}A to 10^{-15}A and was accurate to 1%. To guard against the effects of any stray electric fields, the Faraday cage was screened using an earthed brass cylinder mounted around it.

4.3. Construction of the Experimental Tube.

The design of the tube is shown in Fig. 3. The tube was made from Pyrex glass, 6 cm in diameter and was constructed in two halves, which will be referred to as the gun section of the tube and the main section of the tube. The two halves were joined together by an 'O' ring seal compressed between two Dural flanges which were sealed

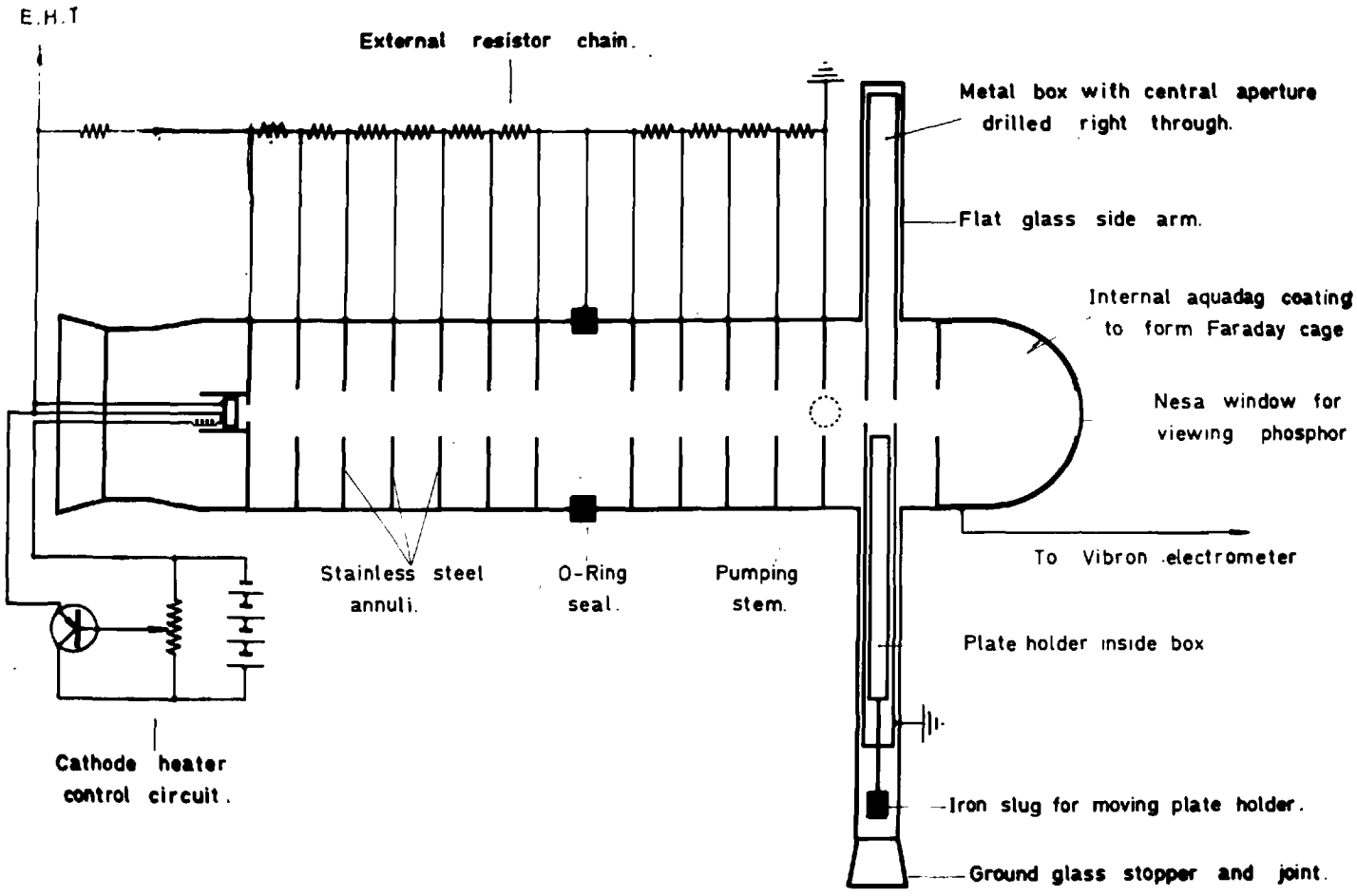


FIG 3

PLAN OF EXPERIMENTAL TUBE

to the ground and polished ends of the tube sections with Picien sealing wax. The accelerating electric field in the tube was defined by potentials applied to suitably placed stainless steel annuli mounted inside the tube. This use of annular baffles helps to reduce the background caused by electron multiplication along the walls of the tube. The annuli which had previously been electro-polished and vacuum stoved at 1000°C were mounted in each section using small inconel springs which slotted into grooves cut in the glass. Electrical connection to the electrodes was made through platinum tapes sealed through the tube walls. Fig. 2. shows diagrams of a stainless-steel box which fitted into the flat side-arms of the tube such that the aperture in the box was aligned with the tube axis. The box was held firmly in position by inconel springs pressing against the side arm walls and contact was made to it by a platinum tape sealed through the glass wall. The plate holder shown was a close fit inside the box and could be moved inside it by applying an external magnet to the magnetic slug. The electron beam was screened from the effect of this magnet using a mild steel magnetic screen mounted round the side arm, as shown in Fig. 2a. Further electrical screening was provided by an earthed aquadag coating applied to the external surface of the side arms. This provided an electrical screen for the beam and a light screen for the emulsion.

For reasons of safety the tube was operated with the gun end at high negative potential, and the other end of the tube at earth

potential. Potentials were applied to the annuli using a potential divider chain wired to the external surface of the tube. Corona discharge from this chain of resistors was suppressed by coating it with a layer of insulating rubber 'Silastomer'.

The tube was continuously pumped using a standard oil-immersed rotary backing pump, a single-stage mercury diffusion pump and vapour trap. A conventional 'hot wire' ionisation gauge was used to measure the pressure in the system.

The emulsions whichwere used in this tube were L4, G5 and XM. They were obtained from Ilford Ltd. on glass plates 5" x $\frac{3}{4}$" and 1 mm thick. The emulsion layers were 25 microns thick. The exposing aperture in the stainless steel box was 3 mm in diameter and with these dimensions of plate and aperture a total of eleven exposures could be made on each plate.

The use of an indirectly-heated oxide-coated cathode as source of electrons will now be considered in detail.

4.4. Use of Indirectly-Heated Oxide-Coated Cathode as Gun.

This type of cathode is extensively used in cathode ray tubes and television camera tubes. Suitable cathodes were obtained from E.M.I. Ltd. They consisted of a capped nickel cylinder which contained an aluminium-oxide coated tungsten spiral which served as a heater. The nickel cap was 5 mm in diameter and was coated with a mixture of barium and strontium carbonates. The cathode was mounted

on a stop cock as shown in Fig.3. and was adjusted to the centre of a 3 mm aperture of a small cylinder fitted to the first electrode in the tube. This cone-and-socket joint and also the one at the end of the flat sidearm, allowing the emulsion access to the tube, were both initially sealed with silicone grease. These joints were later sealed with black wax as the vapours from the silicone grease attack the sensitive surface of the cathode. Before the cathode could be used to supply current, it had to be processed in order to convert the mixed barium and strontium carbonate crystals into mixed crystals of the oxides of the metals, activated by small traces of metallic barium. This process is described below.

4.5. Cathode Processing Procedure.

When the gun and emulsion had been mounted into the tube the system was pumped until the pressure had fallen to 10^{-6} torr. The gun was processed using a gun processing unit which was essentially a power supply enabling the heater voltage and cathode to anode voltage to be independently varied and monitored over the ranges 0 - 12 and 0 - 100 volts respectively (anode here refers to the first electrode of the tube which was 2-3 mm from the cathode surface). Separate meters allowed the heater and emission currents to be continuously monitored. To activate the cathode the heater voltage was slowly raised by half volt stages to 10 volts, taking care that the pressure in the tube never rose above 5.10^{-6} torr. Slow heating of the cathode ensured that good vacuum conditons were

maintained in the tube and minimised the risk of the coating becoming cracked through being too rapidly heated at the processing stage. The heater was rated at 7 volts but it was over-run during processing, this being necessary to take the temperature up to 1350°A when the carbonates were completely reduced, not just to the oxides of barium and strontium but to form mixed oxide crystals (Ba.Sr).O. The process involved in cathode activation is described by Herrmann et al(55) in more detail. To further ensure complete activation, the cathode was then 'flashed' with 11 volts applied across the heater for two minutes. The heater voltage was then reduced to 7 volts when it was generally found that the pressure had fallen to 5.10^{-7} torr. When the cathode was used in the tube after completing this process, the cathode emission was usually found to slowly fluctuate by around 20% of its initial value. However, when the cathode was 'aged' by drawing an emission current of a few mAs for 2-3 hours, the emission current was then found to be stable.

It was thought, at first, that the cathode would have to be replaced after each set of exposures since the system would have to be let down to air to recover the emulsion. It is well known that water vapour, in particular, attacks the sensitive cathode surface and if exposure to water vapour is prolonged the cathode sensitivity can be completely destroyed. It was found, however, that if dry argon was admitted to the system after the exposures had been made and it was

kept passing through the system while the emulsion was removed and replaced by a fresh plate, that the cathode sensitivity after re-processing was not diminished. In this way cathodes could be used for a maximum of ten times.

During actual operation, the current for the gun heater was supplied from a transistor control circuit run by six 2 volt accumulators. This circuit was maintained at the high negative potential of the gun (-25 to -40 kV) and was housed in a Perspex box. The electron beam current was varied by changing the gun heater voltage. When used to supply a beam current of 10^{-11} amps/cm^2 at 25 kV, it was found that the heater voltage had to be reduced to about 4.5 volts. Under-running the heater further ensured against fogging of the emulsion from this source.

4.6. Shutter Mechanism for Sub-Second Exposures.

As already indicated it proved necessary to devise a shutter mechanism for the electron beam in order to use beam currents of the order of 10^{-11} amps/cm^2. The deflection of the beam produced by an applied transverse magnetic field was used as the basis of a shutter system. Two coils were mounted in a protective Perspex case, and arranged in Helmholtz configuration across the tube just in front of the electron gun. They were wired in series and the current through them was adjusted, so that the magnetic field produced by them deflected the electron beam off-axis in the horizontal plane.

Normally the current through these coils was switched on and the beam was deflected off the target. To make an exposure the current was interrupted for a measured length of time (in the 10 - 300 millisecond range) thus allowing the beam to pass axially down the tube and impinge on the emulsion. The interruption was achieved using the circuitry of Fig.4.

This is basically a flip-flop triggered relay. The period of interruption was determined by the potentiometer and condensers in the flip-flop circuit and these were chosen to give a range of interruption times from 10 - 300 milliseconds. Initially the deflecting coils circuit was wired directly in series with a pair of relay contacts which were normally closed and opened on activation of the relay coil. This proved unsatisfactory since arcing took place across the open relay points. This was overcome by wiring three E.L 34 valves in series with the coils as shown in Fig.5. Now, a pair of relay points which were normally open were wired in series with the cathode-grid circuit of the valves together with two H.T. batteries giving 250V. When the relay was activated, this circuit was made and the grids were biassed 250V negative with respect to the cathodes thus cutting off the valves. When the relay points opened again, this bias was removed and the current flowed through the coils again and the deflecting magnetic field re-applied.

It was possible using this type of circuit to measure the

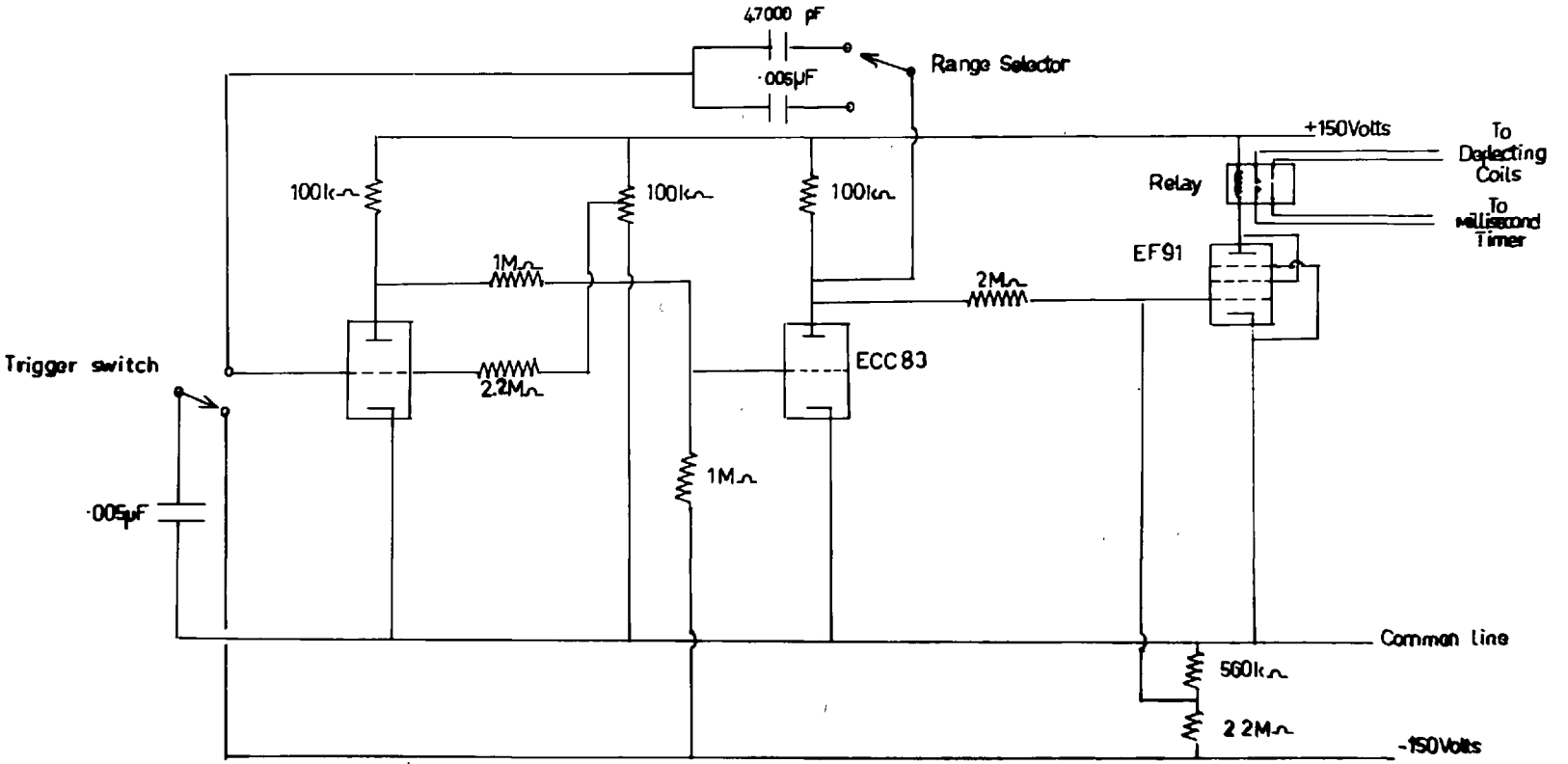


Fig 4

TIMER CIRCUIT FOR INTERUPTING THE DEFLECTING COIL CURRENT

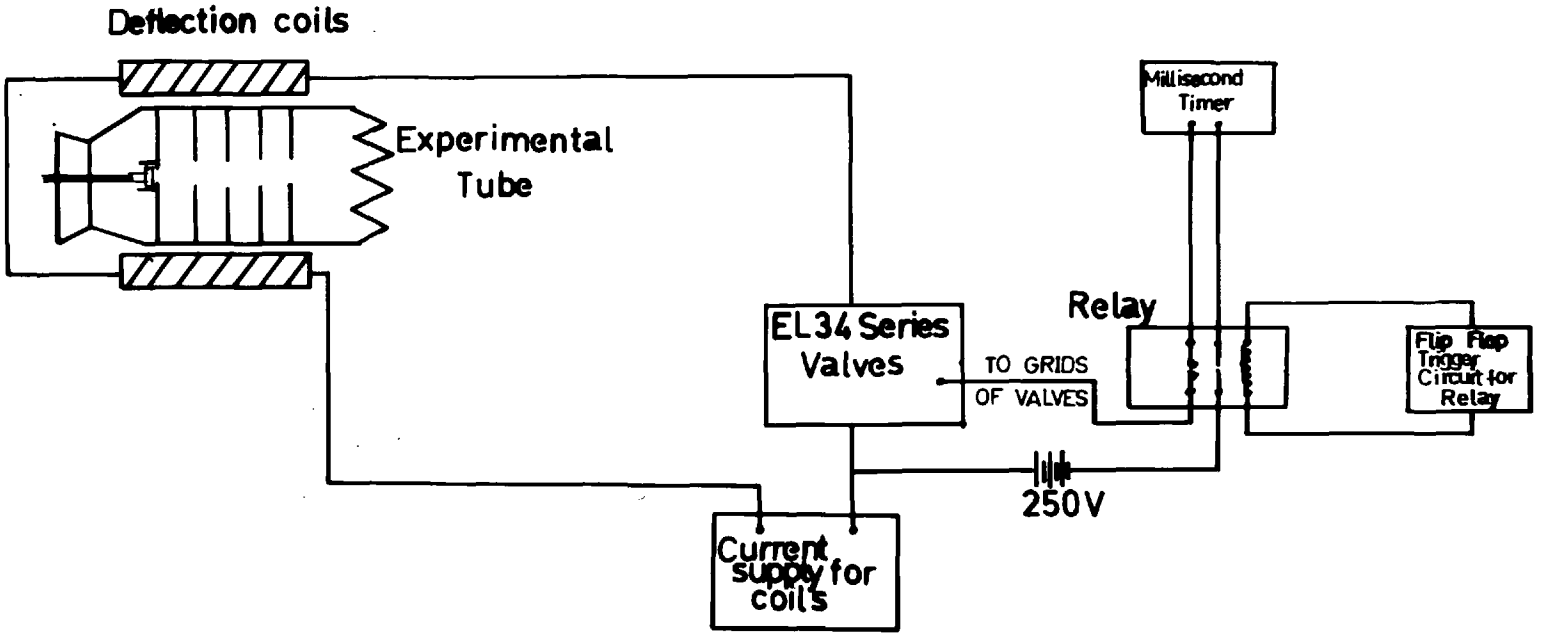


Fig 6

Deflection Coil Circuit

period of interruption directly in a very convenient way. An E.I.L. Millisecond Timer was used to measure the period of interruption. This instrument gives a direct measurement of time intervals from 1 millisec to 10 secs with an accuracy of the order of 1%. Two terminals of this instrument were connected across another pair of relay contacts which were normally open. The timer records the time interval during which the relay contacts are closed. The time interval of interest, however, is that during which the electron beam dwells at the aperture in front of the emulsion and this is not necessarily equal to the time interval during which the relay contacts remain closed. To check that no spurious delays are introduced in the circuitry the following tests were made :-

The beam was collected on the stainless steel box by applying 120V positive to it and passing the collected current through a 50 M Ω resistor to earth. The voltage changes produced across the resistor when the beam arrived at the aperture and was subsequently deflected away were observed on a Tetronix 545A oscilloscope and the traces produced were photographed using a Polaroid camera attachment. In order to see the voltage rise clearly a second flip-flop was used to trigger the first flip-flop which activated the relay. The oscilloscope was triggered using the input triggering pulse of the second flip-flop - this gave a time delay of about 10 millisecs before the first flip-flop was triggered. This gave the

oscilloscope beam time to move across the screen before displaying the voltage changes produced across the 50 M Ω resistor.

Fig.6.(a) shows the appearance of the voltage rise across the resistor. This shows considerable 'ringing' produced by stray capacitance in the coil circuit. These oscillations were damped by using a suitable resistance wired across the coils. The best value of the damping resistance was found to be 5000 Ω and the improvement produced is shown in Fig.6.(b) Complete pulses obtained during an exposure showing the beam's arrival and departure at the aperture are shown in Fig.7. This shows that whereas the beam switch-off time is very quick, the pulse rise-time is of the order of 2 millisecs. The slow pulse rise-time was further investigated and while it did not appear to depend markedly on the strength of the deflecting magnetic field or beam current, it did depend on the position of the coils with respect to the tube. If the coils were moved further down the tube away from the electron gun the pulse rise-time increased to a maximum of 1 minute. The annuli in the main section of the tube were spaced at 2 cm intervals - twice the separation of the annuli in the gun section so that moving the point of direction of the beam down the tube increases the possibility of the beam striking the glass walls and it also increases the energy of the deflected electrons. The slow pulse

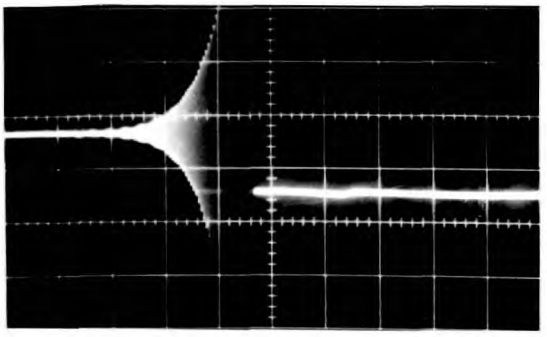


Fig.6(a).

Pulse rise showing 'ringing'.

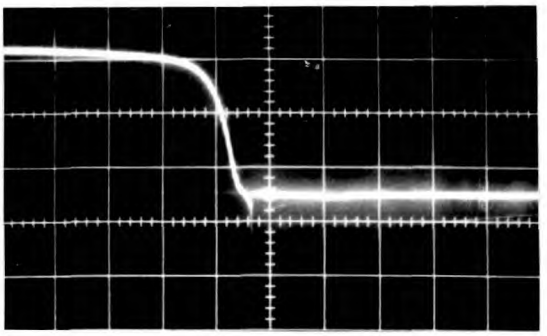


Fig.6(b).

Pulse rise-improved by using damping resistance of 5kΩ.

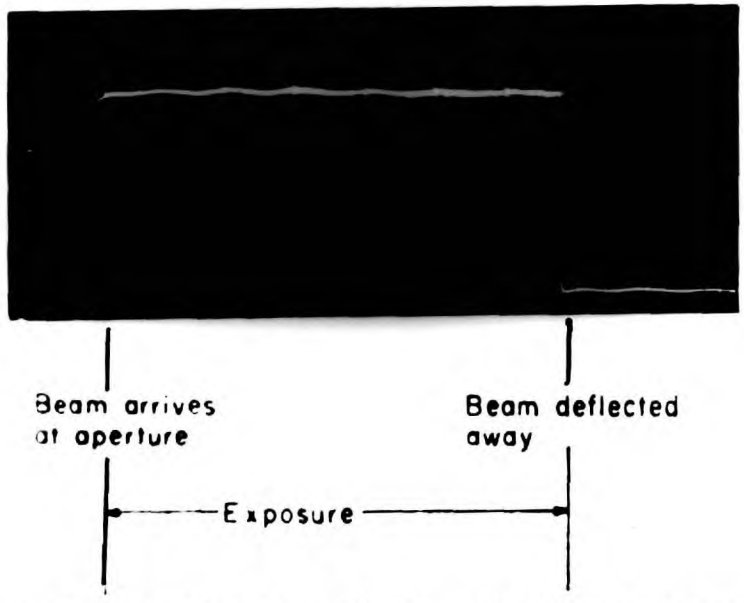


Fig. 7 Pulse obtained across 50-MΩ resistor by collecting the beam. Vertical scale is 2 V/cm. Horizontal scale is 20 msec/cm. Pulse length is 136 msec.

rise-time can then be explained if it is assumed that the glass walls charge positively under electron bombardment. If this happens the beam will tend to be held near the wall until the wall discharges by leakage from the annuli. It was found that the shortest rise-time it was possible to achieve was of the order of 2 millisecs and the error introduced by this is about 2% for exposures of 50 millisec duration.

In order to correlate the reading recorded by the Millisecond Timer with the time spent by the beam at the aperture, a series of measurements were made where the pulse produced on the oscilloscope was photographed and the corresponding Millisecond Timer reading was recorded. The exposure time of the beam was then measured by squaring-off the photographed pulse and measuring its length along the time axis. This was done over the range 10 - 300 millisecs and in this way a correction curve was obtained for the Millisecond Timer. In fact a constant difference of 2 millisecs was found between the oscilloscope measurement and the reading recorded on the timer over the whole of the measured range. This could be due to a slight difference in response of the two pairs of relay contacts.

4.7. Background of the Tube.

Some tests on the background of the tube were made by exposing some G5 emulsion in the tube with the electron beam deflected off-axis. It was found that serious background densities of the order of 0.1 were produced in exposure times of around 1 minute. Possible

sources of background are :-

(I) Secondary electrons produced by beam bombardment of the glass walls of the tube.

(II) Field emission from sharp points in the system i.e. inconel springs on the annuli.

(III) Soft X-rays produced in the tube.

Rather than attempt to reduce the background from these sources, the background was limited to a negligible amount in the following way :-

A mechanical shutter was used as a background limiter. Fig.8. shows a section through the tube at the position of the flat side-arms. This shows another side-arm mounted on top of the tube and which contains a metal shutter mounted on a silver steel slug. This could be lifted up to clear the aperture by passing current through a coil mounted around the side-arm as shown. This side-arm had a platinum tape sealed through it in order to earth the shutter. The internal surface of the side-arm was coated with platinum paste and inconel springs attached to the shutter pressed against the platinum paste so the shutter was always earthed. A stabilised D.C. power supply was constructed to supply the operating coil and the current was adjusted to the minimum value consistent with efficient operation of the shutter. This coil then produced a vertical field component of 0.9G at the position of the aperture. The measurement

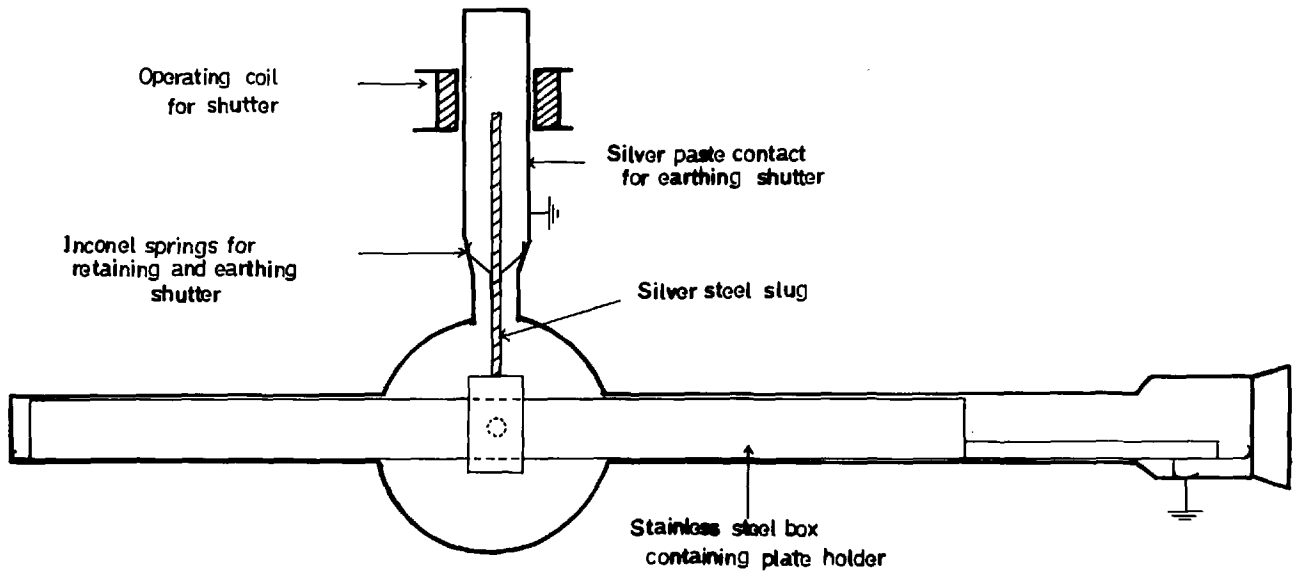


Fig8

SECTION THROUGH EXPERIMENTAL TUBE SHOWING MECHANICAL SHUTTER

of beam current and the exposure of the emulsion were both made with the shutter coil on and so this magnetic field will not affect the reliability of the results.

This mechanical shutter was used to limit the background by using the circuit shown in Fig.9. With both the dipole switch S2 and switch S1 closed, the shutter coil circuit was complete and the shutter lifted clear of the aperture. After a time determined by the resistance and capacitance in the circuit, the current in the relay coil built up sufficiently to activate the relay thus breaking the shutter coil circuit and so the shutter closed again. The time during which the shutter was lifted clear of the aperture was set to be 1.5 secs and the exposures of the emulsion to the beam were made during this time. In this way the emulsion was exposed to the background of the tube for only 1.5. secs and in general no serious background could accumulate in this time. As a check on the tube background, the first exposure on each plate was one of 1.5 secs with the emulsion exposed only to the tube background in with the beam deflected away. If any background was detected on this exposure, then suitable corrections to the densities obtained by exposure to the beam could be made.

For measuring the beam current and for observing the phosphor screen, the relay circuit was switched out and then the shutter could be raised for any length of time.

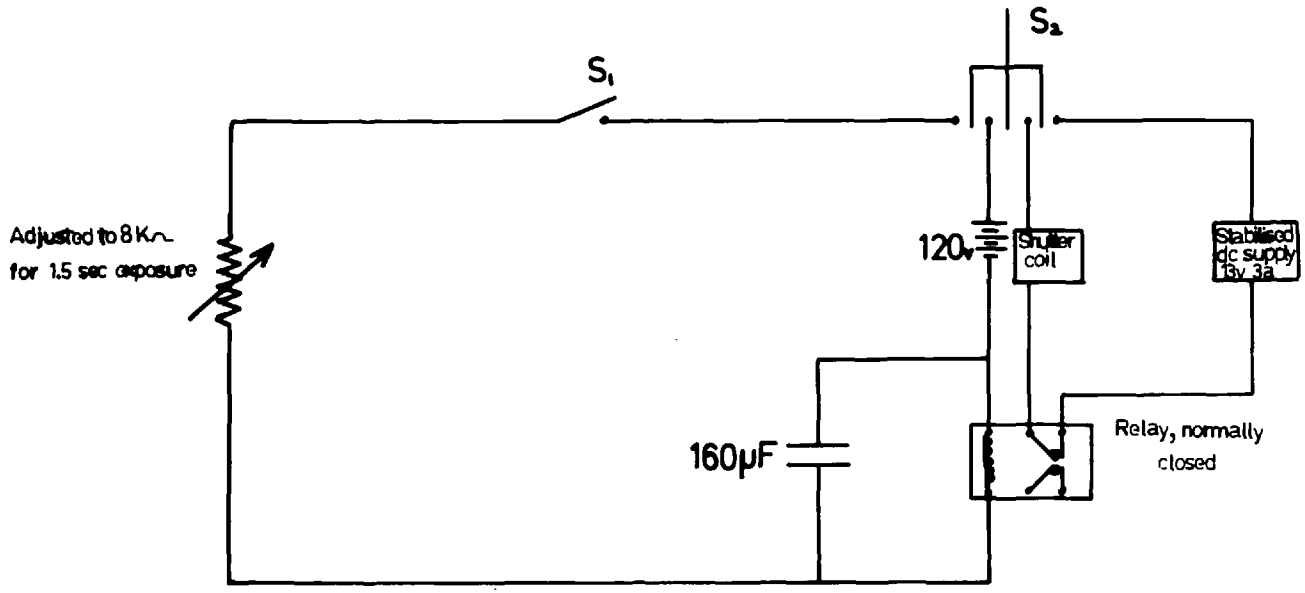


Fig 9

CIRCUIT USED FOR BACKGROUND CALIBRATION

4.8. Procedure for Exposing the Emulsion.

After the cathode had been activated and aged and the pressure had fallen to 5.10^{-7} torr. The high voltage supply was switched on and the voltage raised to the desired value. The H.T. supply used was the Brandenburg MR 50 type and the potential across the tube was measured on a Pye electrostatic voltmeter. This measured up to 40 kV with an accuracy of ½%. The potentials on the annuli and glass walls of the tube were then allowed to stabilise for half an hour. The beam current was monitored and the cathode heater current adjusted until the beam current stabilized at a few x 10^{-11} amps/cm^2 . The phosphor was then moved into position and the appearance of the beam was observed. When the appearance of the phosphor was checked, the phosphor was removed and the beam stability was checked. The deflection coils were switched on and the exposure time was set to the required value. The mechanical shutter was then raised and the beam current was measured on the electrometer. The shutter was then dropped and its relay circuit was switched in. The emulsion was then moved into position across the aperture. The position of each exposure position on the emulsion with respect to the aperture was previously determined and locating marks were made on the flat side-arm of the tube in which the plate holder moves. Each exposure position was then located by aligning the end of the magnetic slug with these marks. With the emulsion positioned the exposure was

made by triggering the flip-flop during the 1.5 secs that the mechanical shutter was raised. The Millisecond Timer reading was noted and then the emulsion was withdrawn from the aperture and the value of beam current was checked and noted. The exposure time was re-set to a new value and the procedure above was repeated.

After the total of eleven exposures had been made dry argon was admitted to the system and was kept continuously passing through the tube until the plate had been removed and replaced by a fresh one.

When the beam was being continuously monitored, it was found that the current slowly dropped at a rate of around 1% per minute. It was considered that this was due to slow poisoning of the sensitive cathode surface by gases emitted by the emulsion, as occurs in Lallemand's electronic camera. The time interval between initial and final beam current measurements was generally less than 1 minute so this did not constitute a serious source of error. It meant that the beam current had to be adjusted two or three times during the course of making eleven exposures to keep all the beam current measurements within a few per cent of each other.

Finally, in this description of the apparatus, some further precautions which were taken to protect the emulsion from fogging by external light should be mentioned :-

(I) Heater tape was used to make and break the black waxed cone and socket join through which the film was introduced into the

tube.

(II) The working end of the tube was painted with a conducting coating of aquadag which was earthed and served as an electrical screen for the beam current and also helped to protect the emulsion from exposure to external light.

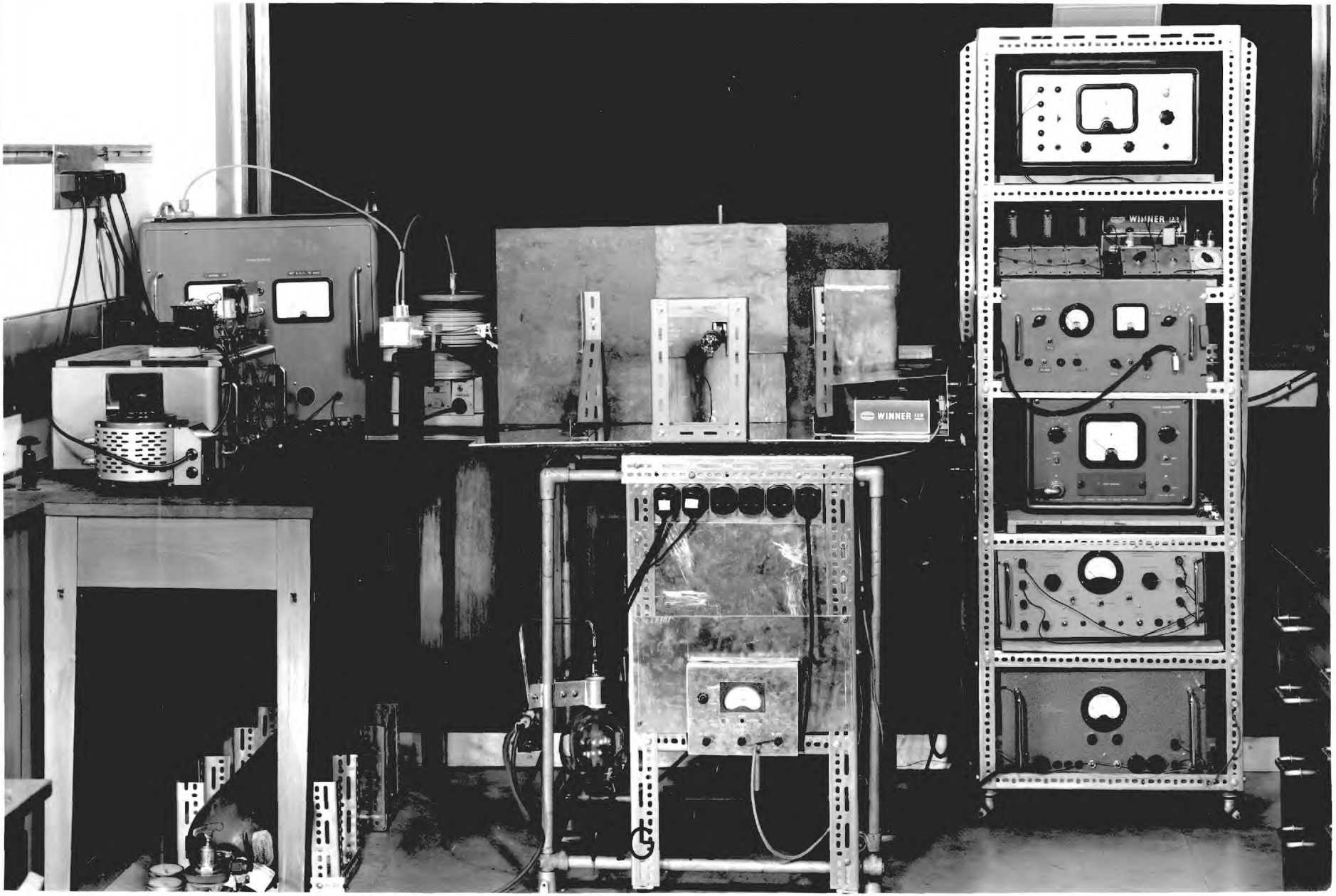
(III) The ionisation guage on the system was wrapped in layers of asbestos paper to absorb the heat developed and also black cloth to absorb the filament light.

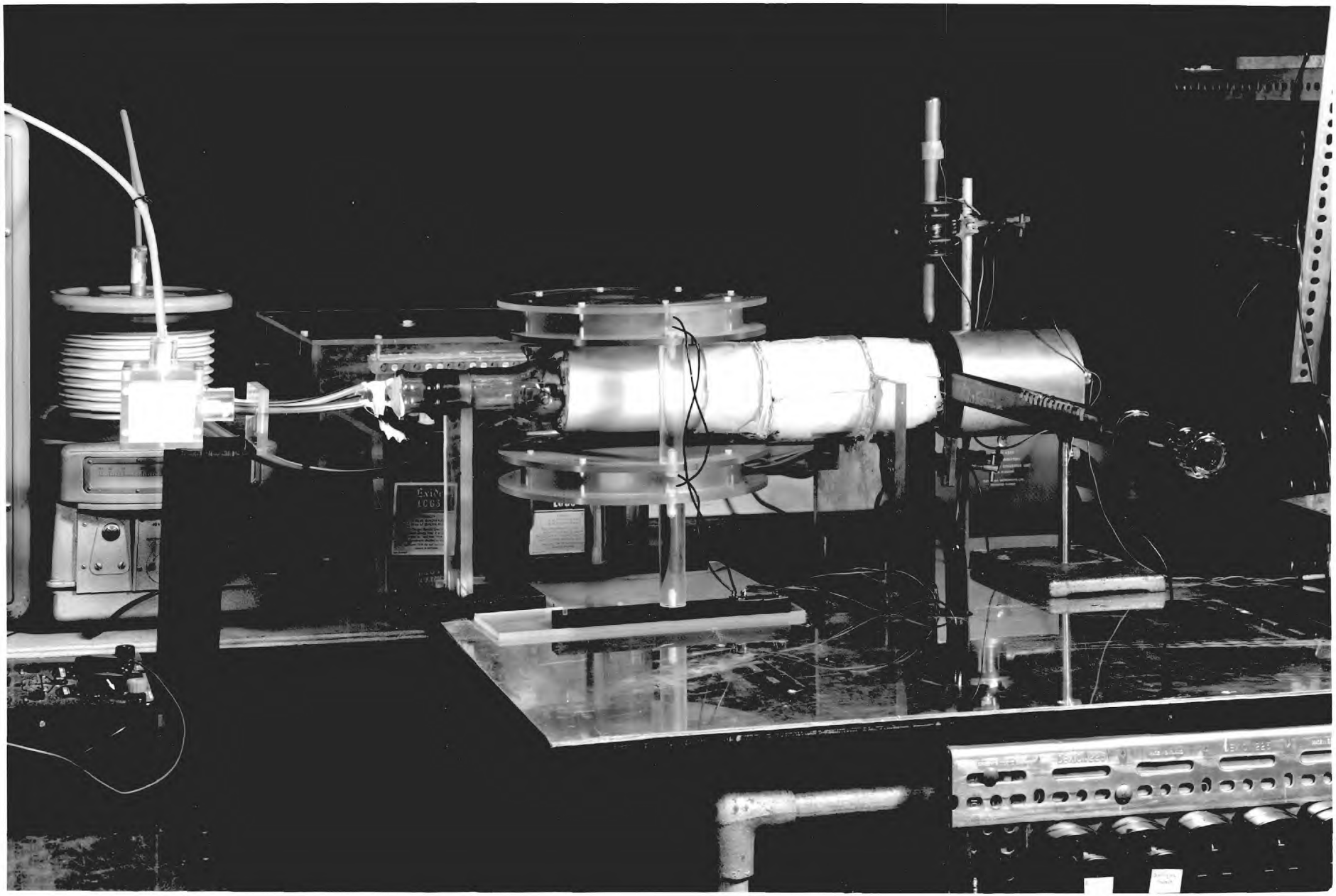
(IV) During the whole time the emulsion was contained in the apparatus, the laboratory was illuminated only by the safelight appropriate to the emulsion.

The complete apparatus is shown in the photographs of Fig.10 and 11. The tube is mounted on the pump table behind the magnetic screen. The Millisecond Timer, timer circuit, pressure guage, electrometer, supply for the timer circuit and supply for the deflecting coils are shown rack mounted on the right. The H.T. supply, electrostatic voltmeter and cathode processing unit can be seen on the left with the argon cylinder. Fig.11. shows a close-up of the tube itself.

4.9. Conclusions :-

An experimental tube has been developed which will allow electron-sensitive emulsions to be exposed to known fluxes of an electron beam of known energy without the film being fogged by


WINNER
WINNER



extraneous effects. The results obtained with this apparatus will now be described and discussed.

Chapter 5

Results Obtained with Nuclear Research Emulsions L4, G5 and XM.

5.1. Procedure for Processing Emulsion

The time interval between exposure of the emulsion and its subsequent development was kept to a minimum in order to avoid latent image fading.[56] Latent image fading is more rapid for emulsions kept at high temperature or humidity. Some data on this effect are available for G5 emulsion. Barron and Wolfendale [57] report a 50% reduction in track density during a period of 520 $\pm$ 50 days with the emulsion stored at 25°C. No difference was observed between storing the emulsion in air or argon. The time interval between exposure and development in the present experiments was of the order of 30 mins and so it is safe to assume that there was negligible latent image fading.

It is well known [4] that the final blackening of the emulsion is dependent on the treatment of the emulsion prior to and during the exposure, the type of developer used, its temperature and the prevailing humidity. The date of manufacture was supplied with each batch of emulsion and the emulsion was generally exposed within two weeks of that date. The emulsions were stored in a refrigerator before use. The developer used was ID19 and it was made up in the laboratory. This developer deteriorates slowly during storage and no developer was used if it was kept for more than one month. Fresh developer was used for each plate and the temperature of the developer

was maintained at 12°C. The plates were developed for 5 mins and the developing dish was slowly rocked during this period. A stop-bath of 200 ccs water plus a few drops of acetic acid was used and the plate was held in this for around 30 secs. The plate was then fixed using 'Hypam' fixer. The fixing time was made twice the emulsion clearing time and this was generally around 5 mins. The plate was then washed for half an hour in tap water and finally rinsed several times in distilled water. The plate was stored in a dessicator to prevent contamination by dust particles. A typical processed plate is shown in Fig. 11(a) This particular plate is L4 emulsion exposed to 25 kV electrons.

Measurements of density were initially made with a Jarrel-Ash microphotometer and later repeated with a recently acquired Joyce-Loebel microdensitometer. The Jarrel-Ash microphotometer had a pen recorder output which gave a measure of the optical transmission of the emulsion. The zero setting was made by placing some black velvet over the microphotometer slit and the 100% setting was made by allowing the light to pass through the glass supporting the emulsion. These settings were frequently checked during the course of measurements. The first exposure on each plate was of the tube background plus emulsion fog and measurements of density on subsequent exposures were corrected for these two effects. The Joyce-Loebel microdensitometer measures density directly and the response of this instrument was

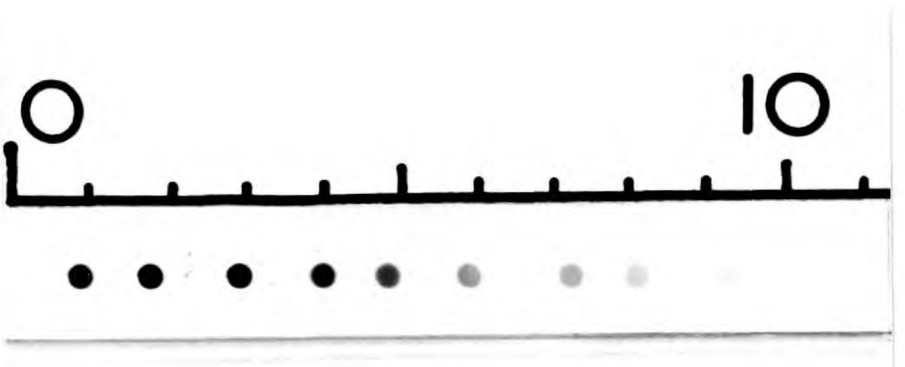


Fig.11 (a).

Typical processed plate-L4 emulsion exposed to 25 kV electron beam.

Scale cms.

checked by Kahan and found to be linear with density over the density range of interest in this investigation. The results presented in this Chapter are those obtained with the Joyce-Loebel microdensitometer. The values of density obtained with both instruments were found to agree to within 10%.

The electron energy range of interest is 0 - 40 kV and results have been obtained on each type of emulsion at 5, 15, 25 and 35 kV. The four plates of each emulsion used were taken from the same batch. Previous investigators in this field,[58, 59, 60] with the exception of Digby et al, [9] have presented their results in the traditional H and D presentation. Whereas this presentation is useful for photographic emulsions, characteristic curves in terms of density versus exposure are more useful for users of electronographic emulsions. The results obtained in this investigation are presented in both forms in Figs. 12 - 17, the H and D plots being useful for comparison with Fig. 1.

The aperture used for exposing the emulsion in these experiments was 3 mm in diameter. It was generally found that the density of the exposed area dropped uniformly by a few per cent in scanning from one side of the exposed area to the other. When exposures were made in the tube, the beam scans in from one direction across the aperture and is subsequently deflected away in the same direction. Consequently one side of the aperture will receive more

exposure than the other and this could explain the effect noted above. If this were the explanation, one would expect longer exposures to be more uniform. This was not observed, all exposures being equally non-uniform and so it was concluded that this non-uniformity was present in the incident electron beam even though it could not be detected on the phosphor screen. This was a small effect amounting to a few per cent and the values of density quoted in the results were averaged over the exposed area. It did mean, however, that reliable granularity measurements could not be made on these plates.

5.2. Reproducibility of Results :-

Since the blackening obtained on these emulsions depends on factors which are not easily controllable e.g. the treatment of the emulsion before exposure, the specific conditions during manufacture and development, etc., the figures given for the exposure producing a certain density are subject to considerable variation. It was found in this investigation that plates of G5 emulsion from the same batch varied in sensitivity by ± 10% . Cranberg and Halpem [7] have found the same variation in sensitivity for Ilford B-2 plates exposed to electrons.

5.3. Results of Speed of Emulsions.

The difficulties associated with defining the speeds of photographic emulsions [61] exposed to light can be avoided in the case of the exposure of electron sensitive emulsions to electrons. For the

linear region of the emulsion characteristic, speed can be simply and conveniently defined as that flux of electrons of a certain energy required to produce a certain density on the emulsion. This definition gives a reciprocal measure of speed, the faster the emulsion, the lower the figure. If we consider an electron energy of 35 kV, for example, the density-exposure characteristics of all three emulsions shown in Figs. 12-14 are found to be linear up to density of 0.9. Under these conditions, speed can be defined as that electron flux of 35 kV energy required to produce a density of 0.9. Thus, the speeds of these emulsions are :-

Beam Energy	Emulsion	Speed, as defined above
35 kV	L4	4.1 electrons / μ^2
35 kV	G5	1.3 " "
35 kV	XM	0.14 " "

The only other published speeds for these emulsions are those given by Valentine and Wrigley.(62) These authors worked only at an electron energy of 60 kV and at this energy found the emulsion characteristic to be linear up to D = 1.0. Thus, their figures of speed refer to that electron flux of 60 kV energy producing a density of 1.0. Valentine and Wrigley's results :-

Beam Energy	Emulsion	Speed
60 kV	L4	1.6 electrons $/\mu^2$
60 kV	G5	0.25 " "
60 kV	XM	0.07 " "

The results found in this investigation at other beam energies are given below together with the density at which the speed measurement was made. The degree of linearity of the emulsion characteristic was found to fall with decreasing electron energy and so the density taken for the speed measurements falls

Beam Energy	Emulsion	Speed	Density
25 kV	L4	3.06 electrons $/\mu^2$	D = 0.5
25 "	G5	0.94 " "	D = 0.5
25 "	XM	0.11 " "	D = 0.5
15 "	L4	2.12 " "	D = 0.2
15 "	G5	0.66 " "	D = 0.2
15 "	XM	0.094 " "	D = 0.2
5 "	L4	2.5 " "	D = 0.05
5 "	G5	0.63 " "	D = 0.05
5 "	XM	0.5 " "	D = 0.05

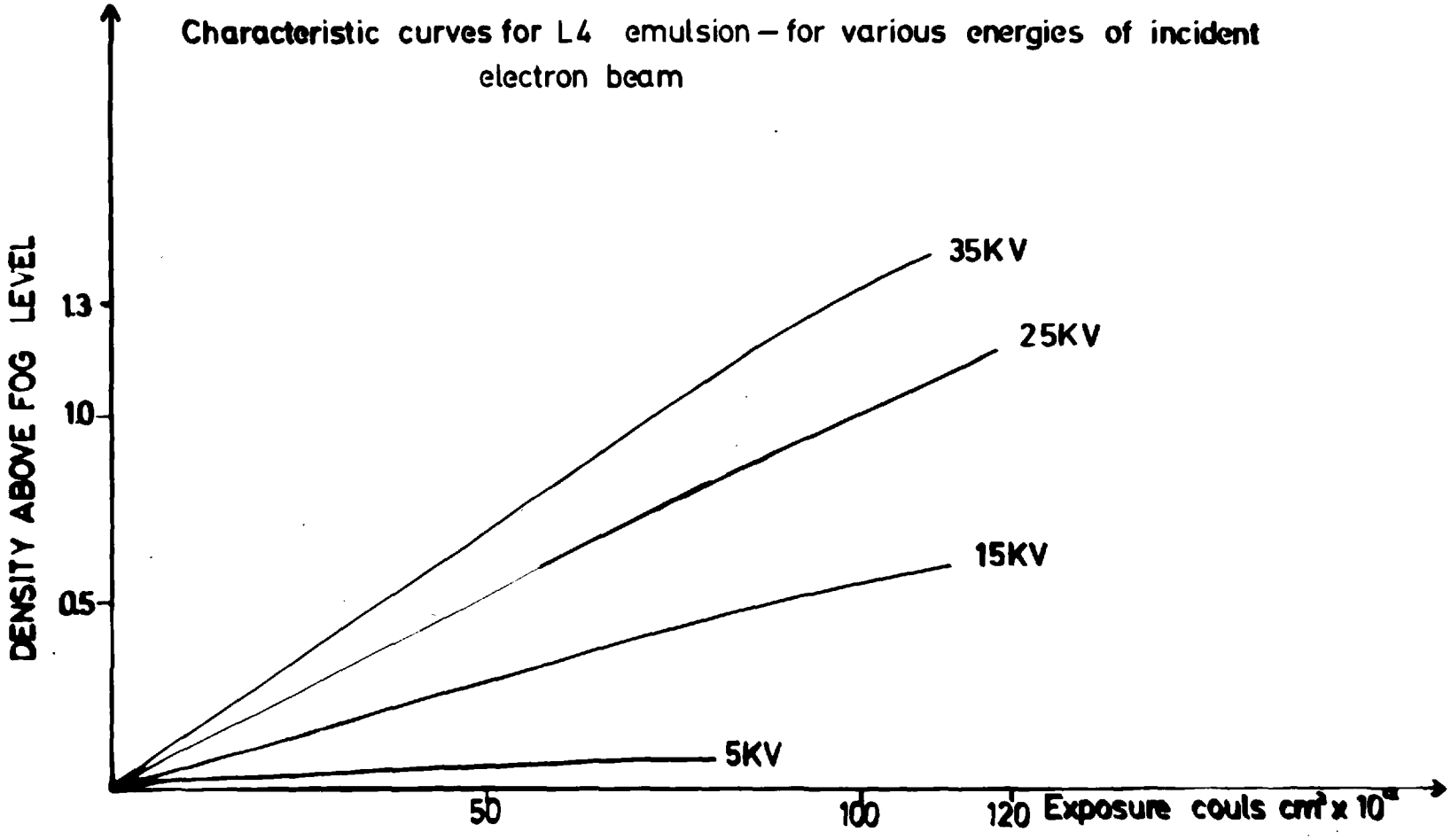

Characteristic curves for L4 emulsion – for various energies of incident electron beam
DENSITY ABOVE FOG LEVEL
1.3
1.0
0.5
35KV
25KV
15KV
5KV
50
100
120
Exposure couls cm² x 10⁻⁶

Fig 12

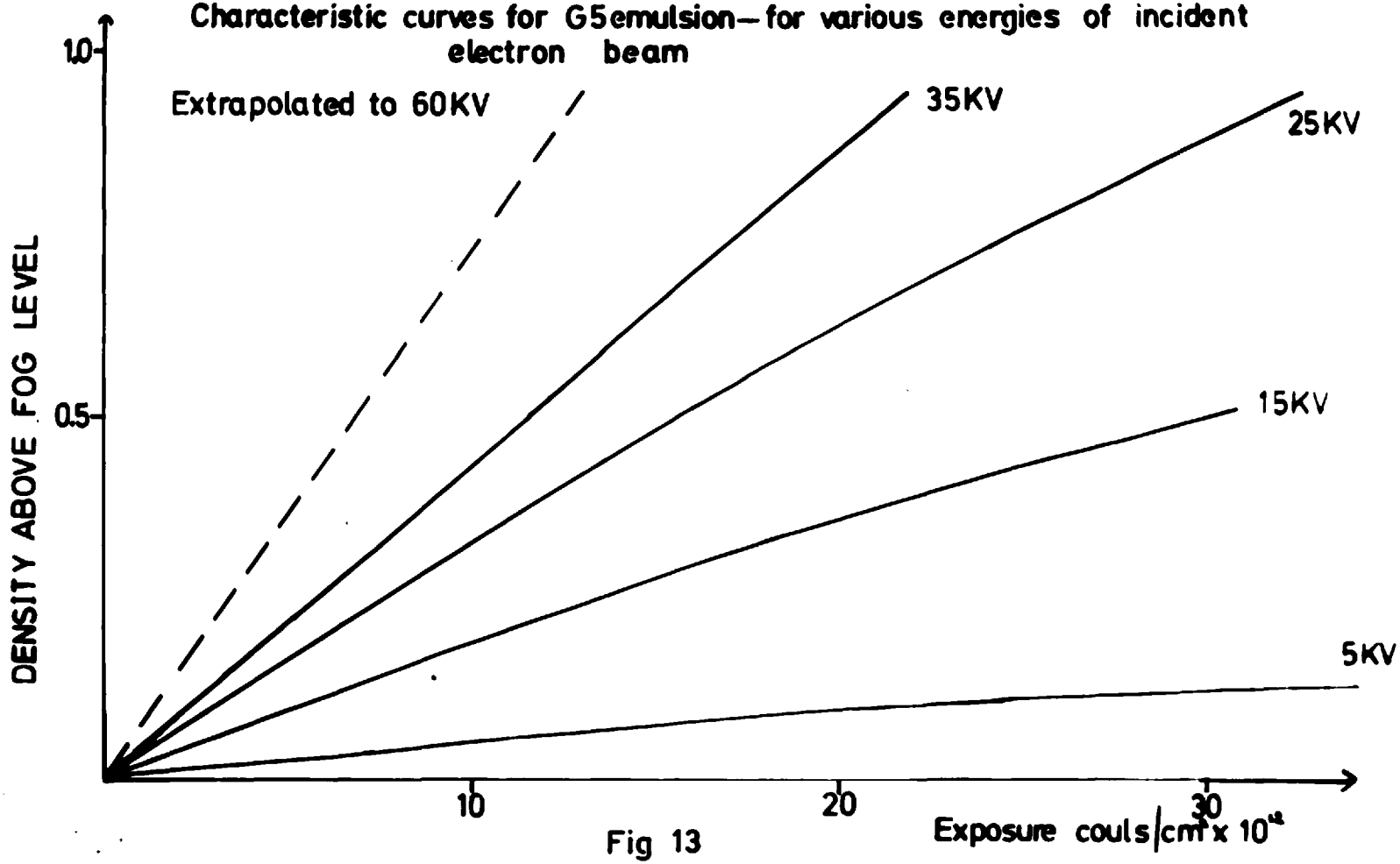

Characteristic curves for G5emulsion—for various energies of incident electron beam
Extrapolated to 60KV
35KV
25KV
15KV
5KV
1.0
0.5
DENSITY ABOVE FOG LEVEL
10
20
30
Exposure couls/cm² x 10⁴

Fig 13

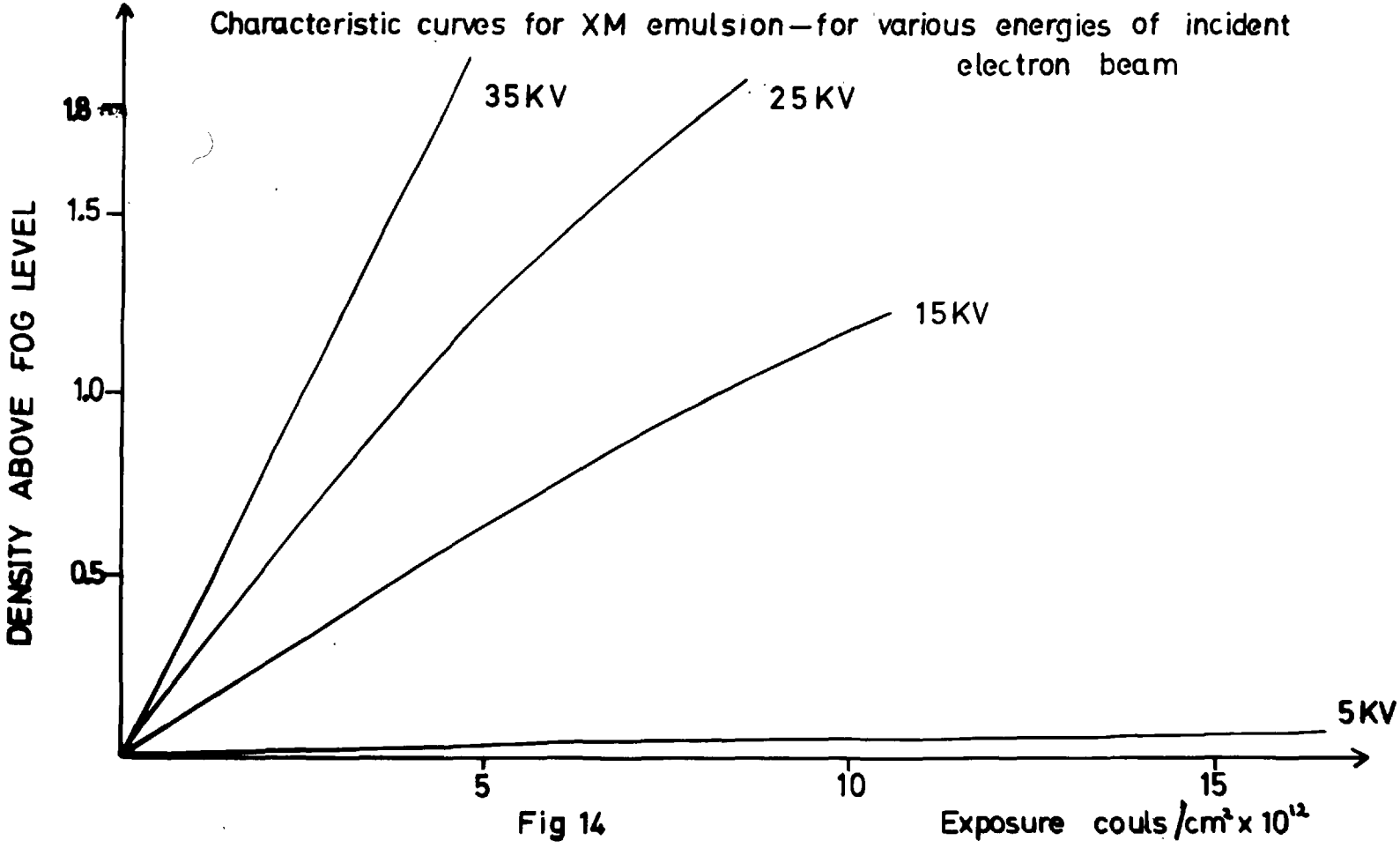

Characteristic curves for XM emulsion—for various energies of incident electron beam
35KV
25KV
15KV
5KV
DENSITY ABOVE FOG LEVEL
1.8
1.5
1.0
0.5
5
10
15
Exposure couls/cm² x 10¹²

Fig 14

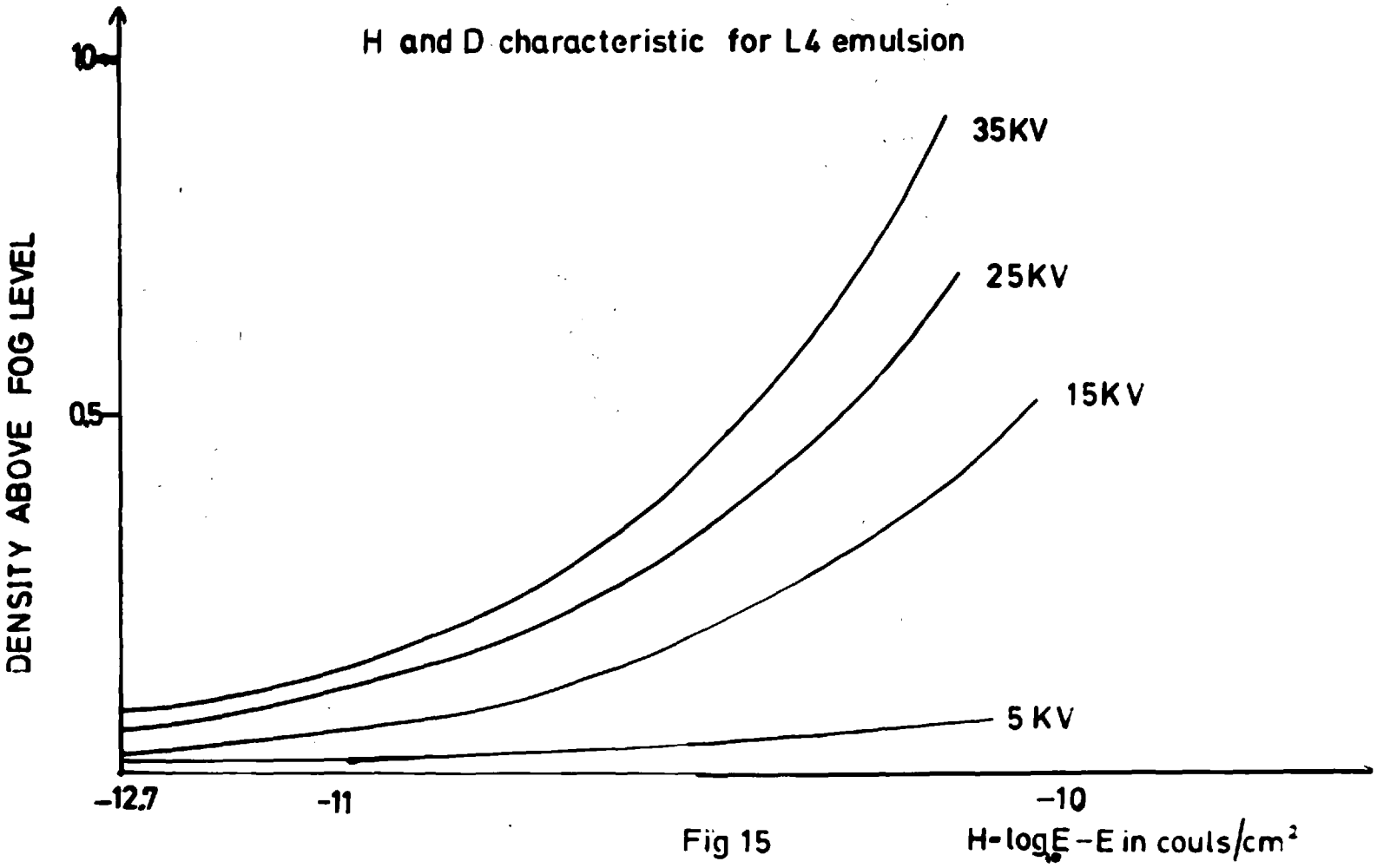

H and D characteristic for L4 emulsion
DENSITY ABOVE FOG LEVEL
1.0
0.5
35KV
25KV
15KV
5 KV
-12.7
-11
-10
H-log E-E in couls/cm²

Fig 15

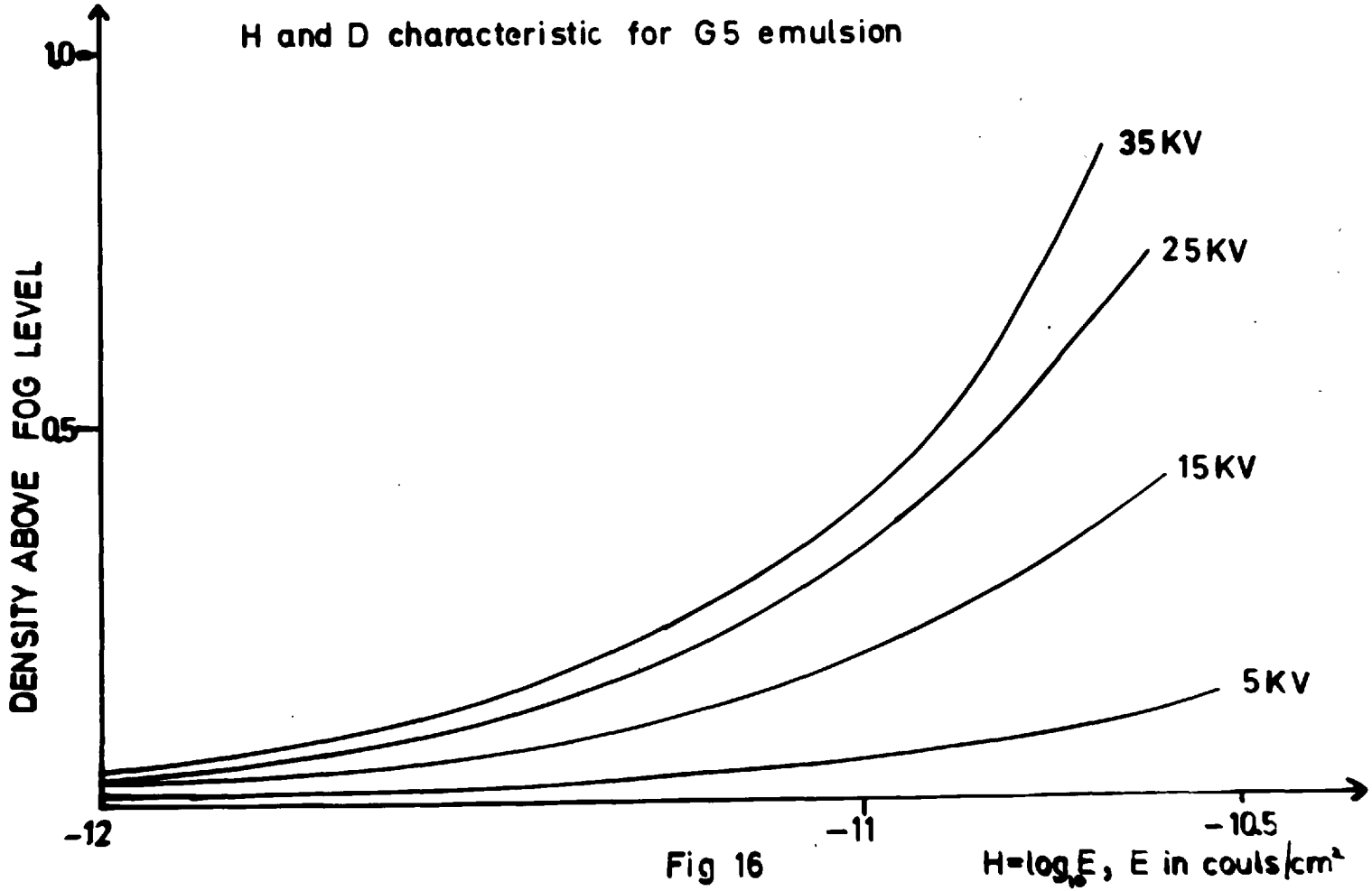

H and D characteristic for G5 emulsion
DENSITY ABOVE FOG LEVEL
1.0
0.5
35KV
25KV
15KV
5KV
-12
-11
-10.5
H=log E, E in couls/cm²

Fig 16

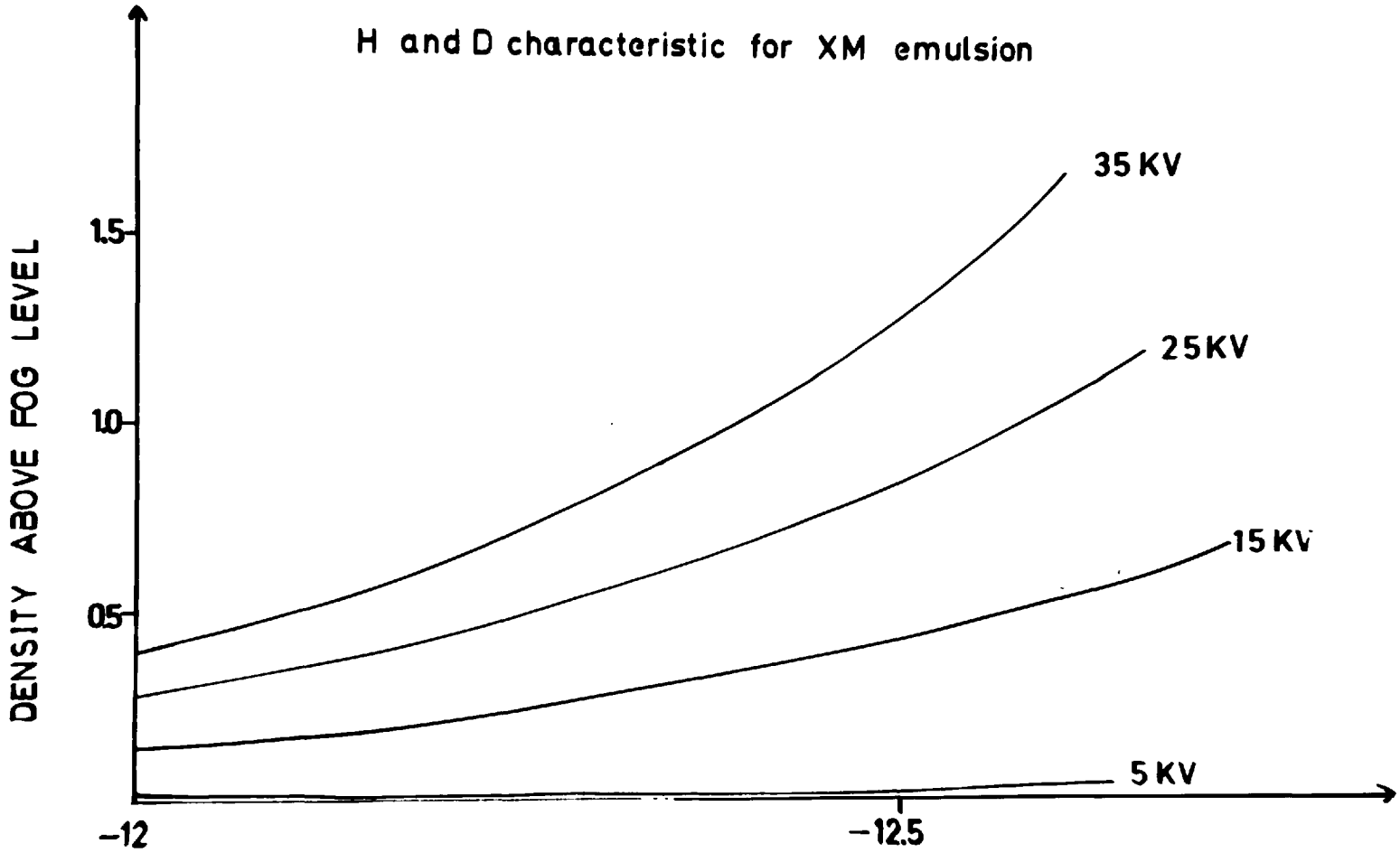

H and D characteristic for XM emulsion
35 KV
25KV
15 KV
5 KV
DENSITY ABOVE FOG LEVEL
1.5
1.0
0.5
-12
-12.5
H=log E-E in coul

Fig 17

The relative exposure times to be given to these emulsions to produce the same density when exposed to the same electron flux is given by the ratio of the reciprocals of the numbers given above. Thus, at 35 kV, the exposure times are in the ratio 1 : 3.2 : 29 for L4 : G5 : XM. At 25 kV and 15 kV, this ratio is found to be 1 : 3.3 : 28.4 and 1 : 3.2 : 22.5 respectively. Taking a variation in emulsion speed of 20% as typical, this is in agreement with the value of 1 : 4 : 24 given by Khogali [49] and 1 : 5 : 25 given by McGee [63] et al.

5.4. Validity of the Single-Hit Law - Results of Contrast.

The theoretical considerations of Chapter 3 are based on the assumption that the process involved in the electron irradiation of nuclear research emulsions is a single-hit process. The H and D curves shown in Figs. 15-17 do show the characteristic slope and long tail of the $\gamma = 1$ curve of Fig. 1 and indicate that the single-hit law may hold. A more sensitive check of the single-hit law is equation (8) of section 3.5 which relates emulsion contrast to optical density. This states that the contrast, γ, is simply given by $\gamma = 2.3.D$, and should be independent of all other factors but the density to which the emulsion has been developed. Values of contrast have been measured from the results of Figs. 15-17 and these are presented in Figs. 18-20. Several values of contrast have been measured for each emulsion at each electron energy. The results for each emulsion at three values of electron energy are shown in each figure. In each case, the dashed

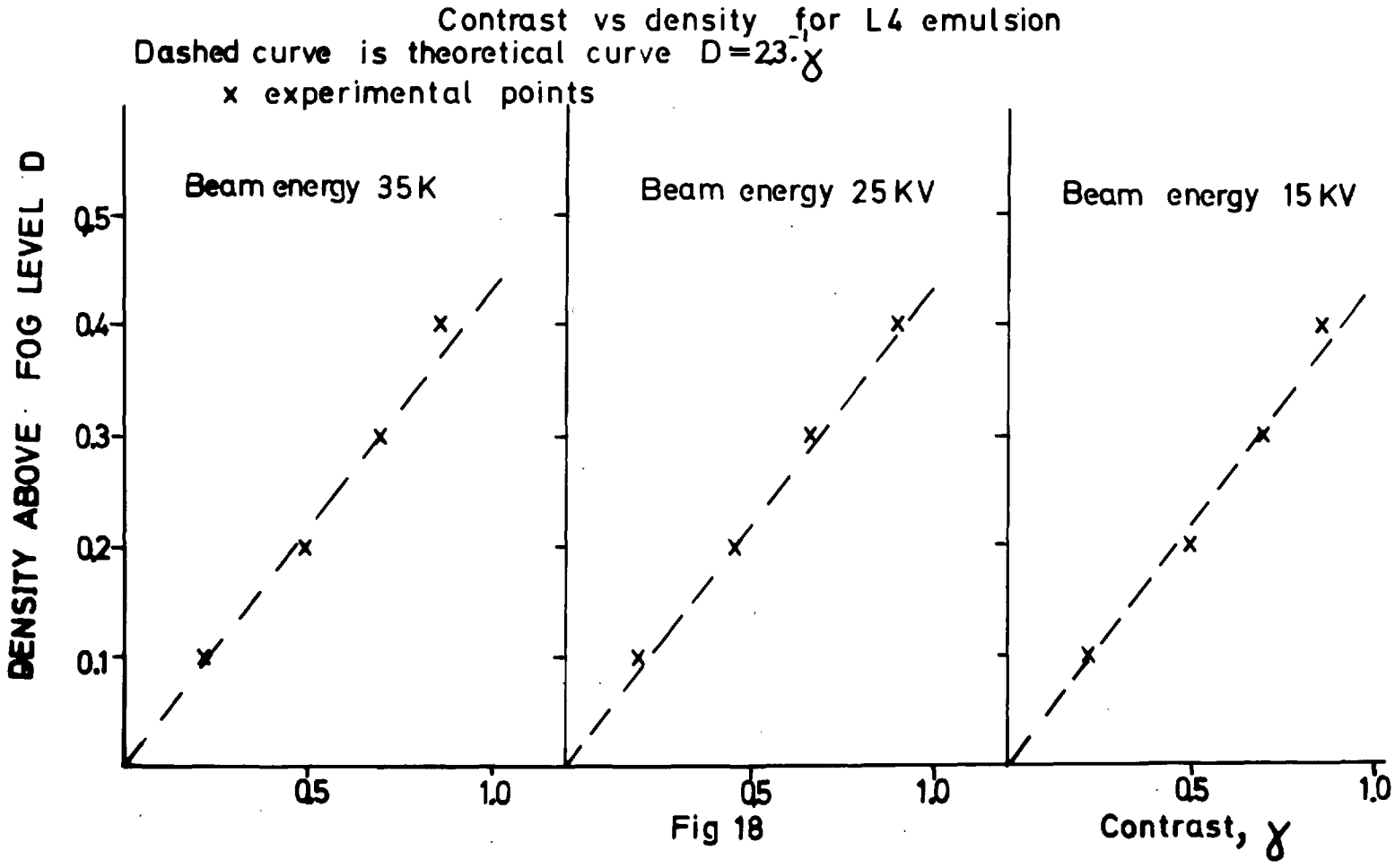

Contrast vs density for L4 emulsion
Dashed curve is theoretical curve D = 2.3 γ
x experimental points
Beam energy 35 K
Beam energy 25 KV
Beam energy 15 KV
DENSITY ABOVE FOG LEVEL D
0.5
0.4
0.3
0.2
0.1
0.5
1.0
0.5
1.0
0.5
1.0
Contrast, γ

Fig 18

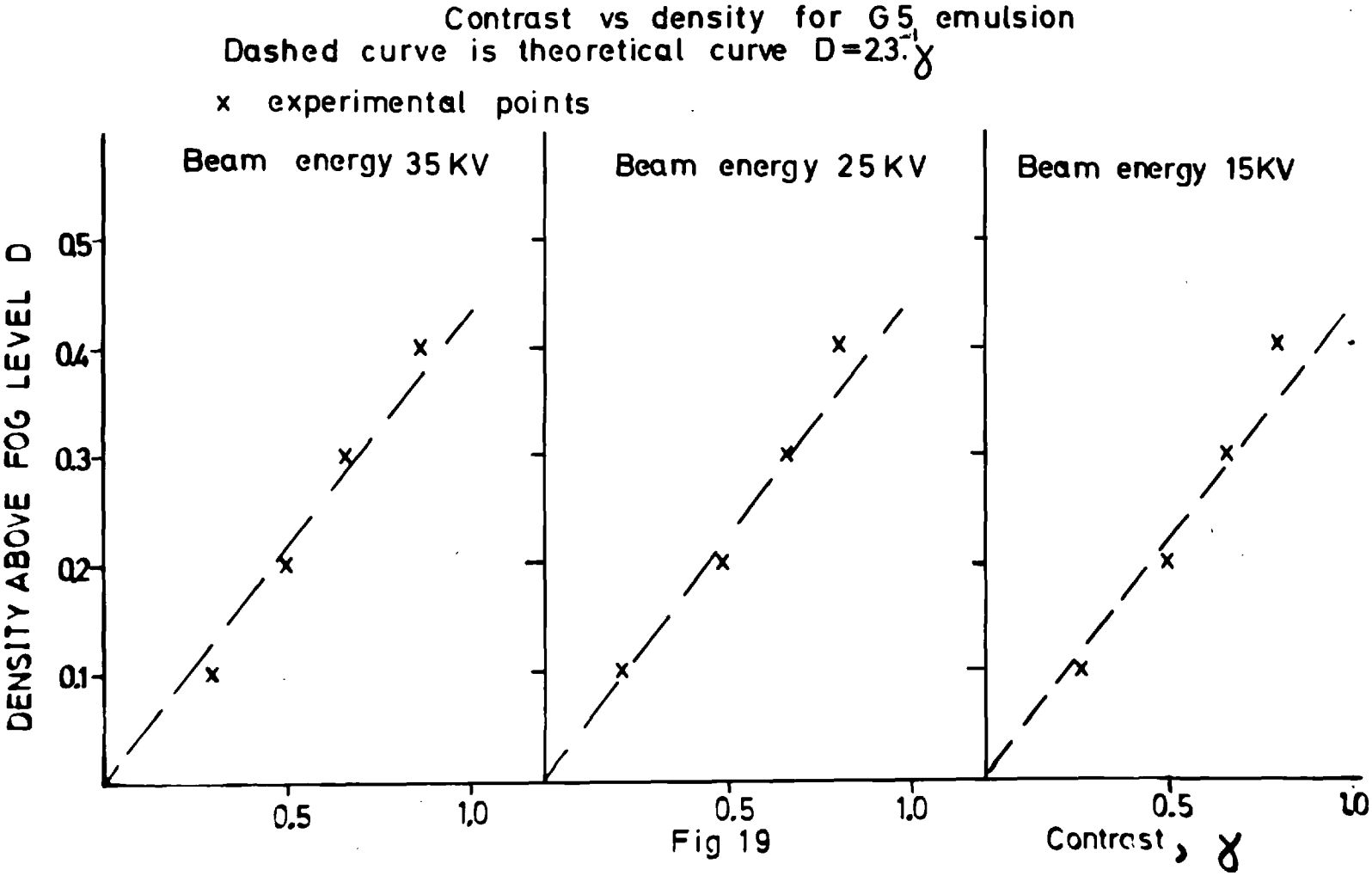

Contrast vs density for G5 emulsion
Dashed curve is theoretical curve D=2.3γ
x experimental points
Beam energy 35 KV
Beam energy 25 KV
Beam energy 15KV
DENSITY ABOVE FOG LEVEL D
0.5
0.4
0.3
0.2
0.1
0.5
1.0
0.5
1.0
0.5
1.0
Contrast, γ

Fig 19

Contrast vs density for XM emulsion
Dashed curve is theoretical curve $D = 2.3\gamma^{-1}$
x experimental points

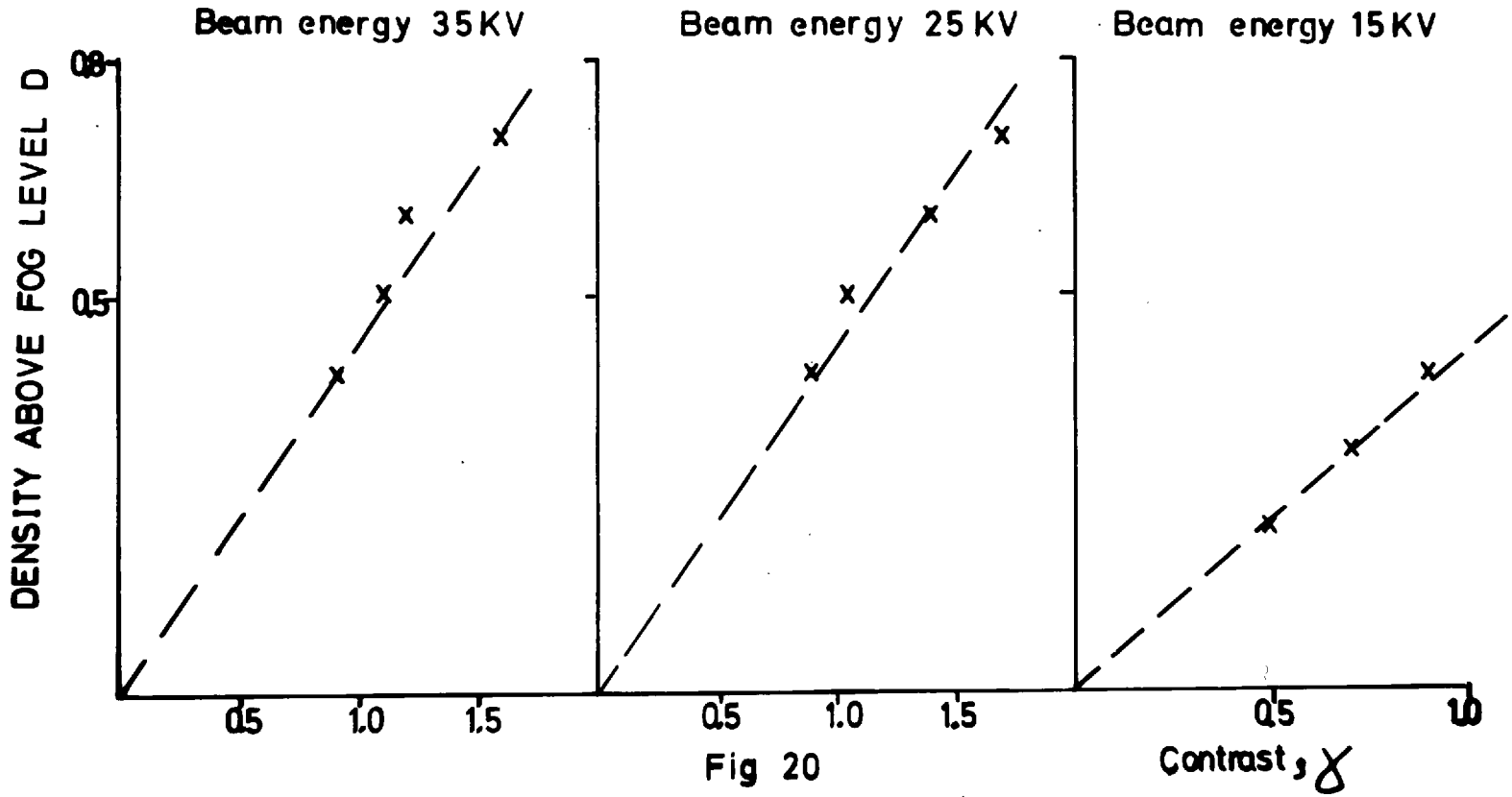


Fig 20

curves are the theoretical curve, $\gamma = 2.3.D$ and the crosses are experimental points. It can be seen that for each emulsion at each energy the values of contrast fall within 10% of the theoretical value, thus providing support for the single hit hypothesis for densities up to at least 0.5. This is in agreement with the findings of other observers.

5.5. Effect of Beam Energy on the Density Produced

One can construct curves of density against beam energy for a constant exposure from the results of density against exposure for a given beam energy shown in Figs. 12-14. These curves are presented in Figs. 21-23.for the three emulsions under investigation.

It can be seen that there is a threshold of between 2 - 4.5 kV for the production of developed grains in these emulsions. For G5, this threshold is 2.1 kV, which agrees with the results of Pniewski.(64) Some emulsions are coated with a thin layer of gelatine in order to protect the surface of the emulsion from abrasions. This is not the case with the emulsions under investigation and so the figure of 2.1 kV may be taken as being the energy required to render a grain of silver halide in G5 emulsion developable (this figure will include energy lost in gelatine). Pniewski investigated G5 emulsion using grain counting techniques and published results of the number of grains produced per electron as a function of electron energy in the range 0 - 150 kV. This function is approximately linear for

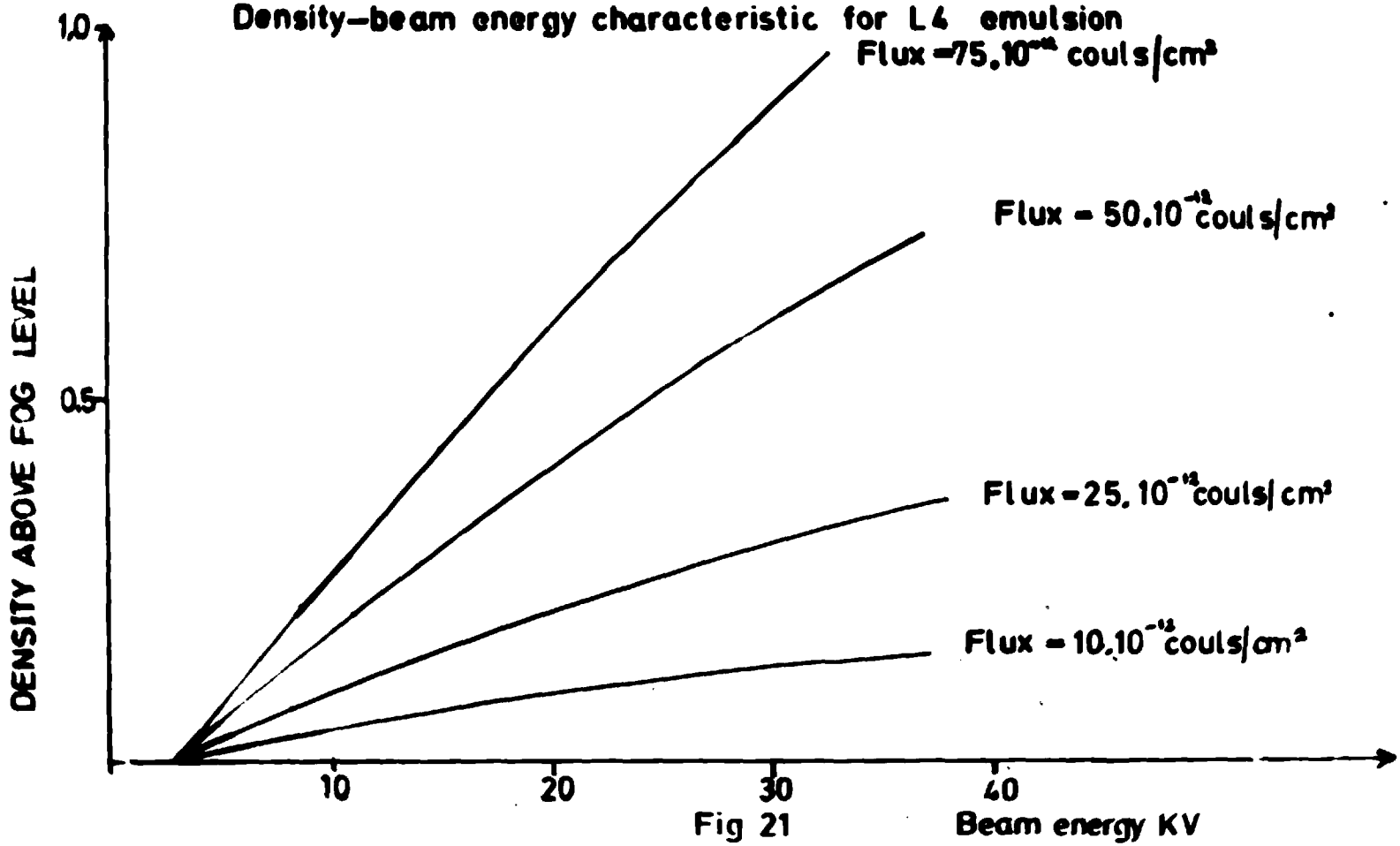

Density–beam energy characteristic for L4 emulsion
Flux = 75.10^-12 coul s/cm²
Flux = 50.10^-12 coul s/cm²
Flux = 25.10^-12 coul s/cm²
Flux = 10.10^-12 coul s/cm²
DENSITY ABOVE FOG LEVEL
1.0
0.5
10
20
30
40
Beam energy KV

Fig 21

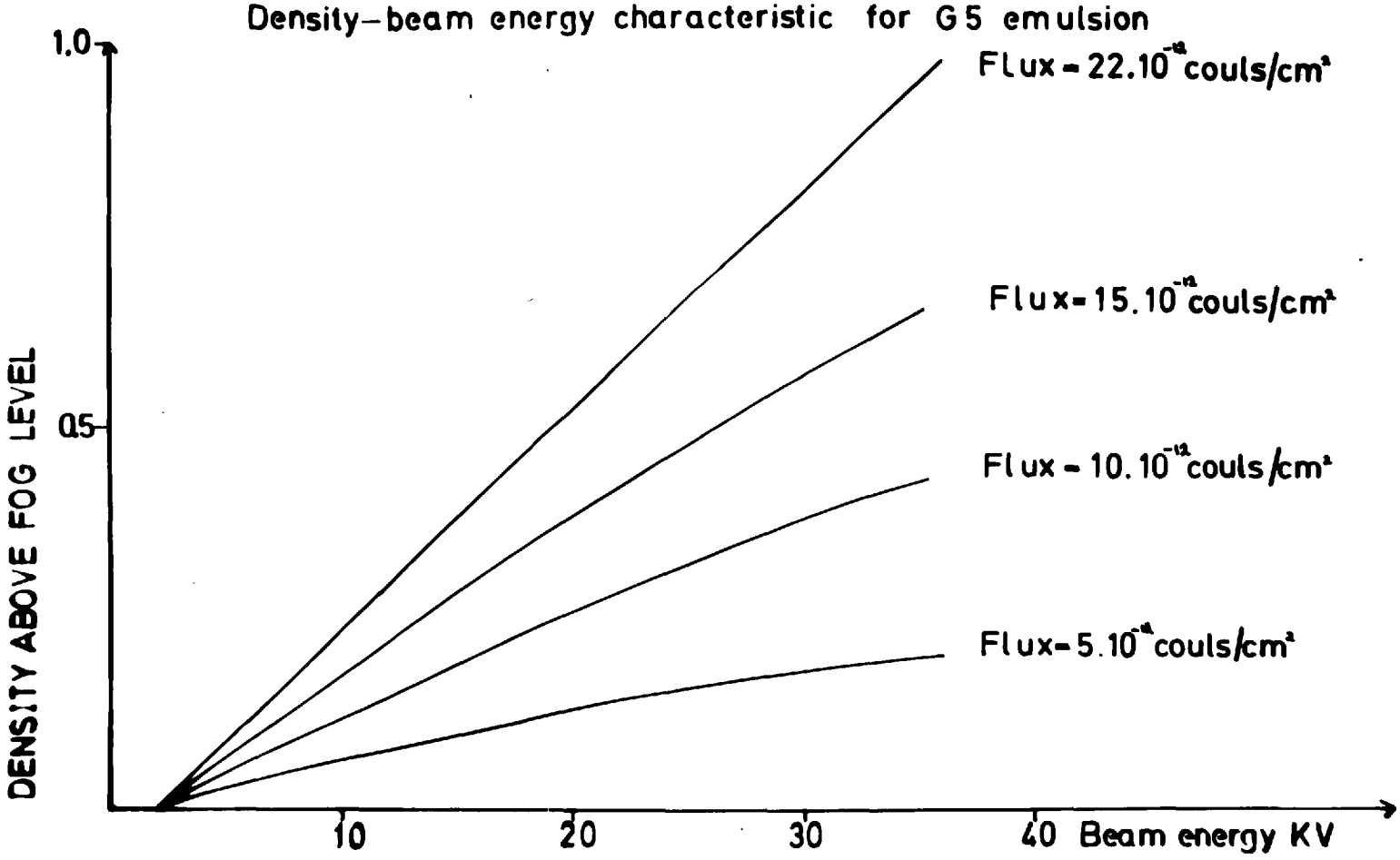

Density–beam energy characteristic for G5 emulsion
1.0
0.5
DENSITY ABOVE FOG LEVEL
Flux = 22.10^-12 couls/cm²
Flux = 15.10^-12 couls/cm²
Flux = 10.10^-12 couls/cm²
Flux = 5.10^-12 couls/cm²
10
20
30
40 Beam energy KV

Fig 22

Density-beam energy characteristic for XM emulsion

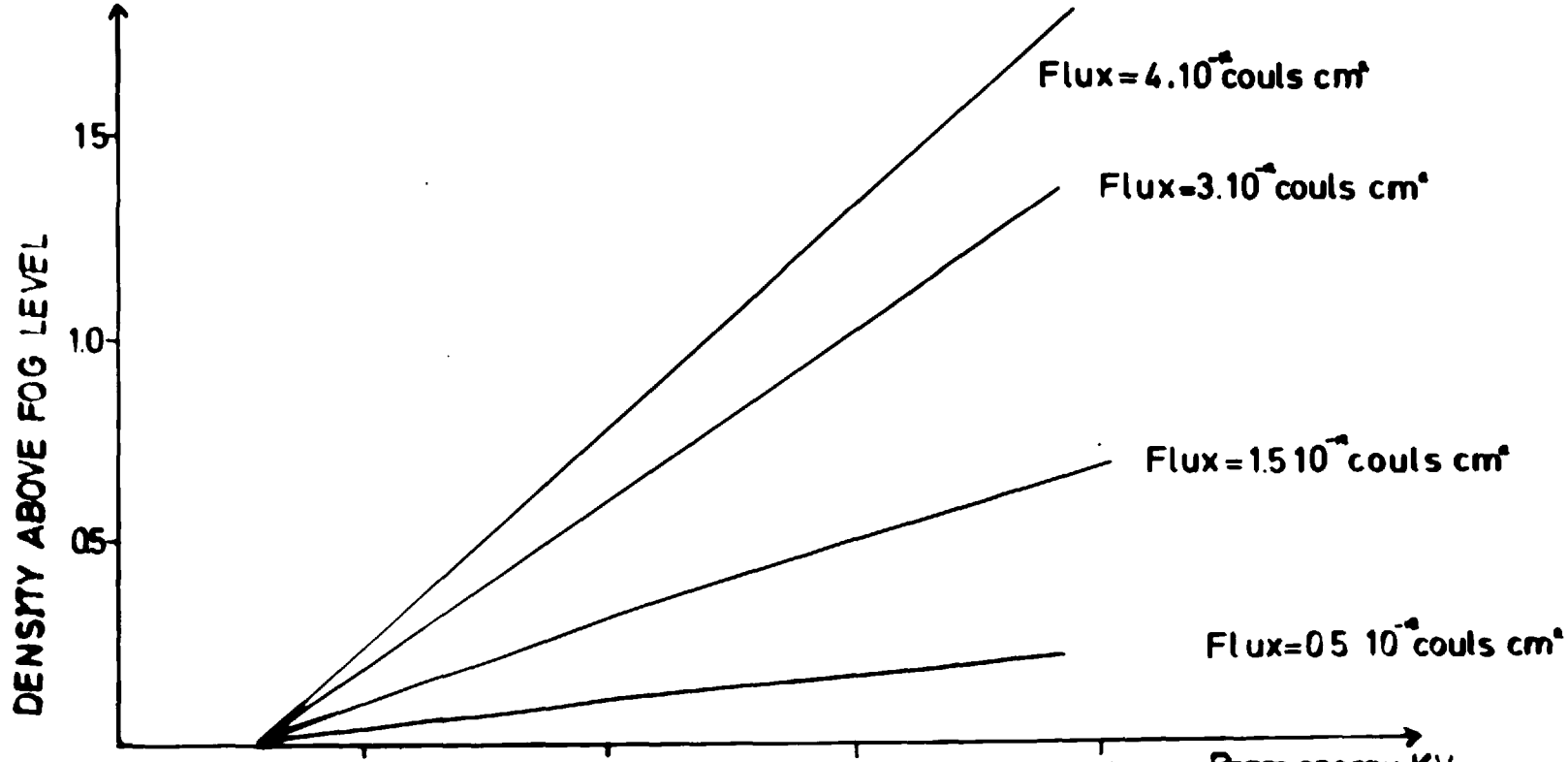


Fig 23

energies less than 50 kV curving slightly towards the 'number of grains' axis. Assuming no overlap of grains, one would expect curves of density versus beam energy to follow the shape of this function. The curves of density against beam energy are linear for XM emulsion and tend to curve towards the beam energy axis for G5 and L4. The results at each energy value were taken from four separate plates of emulsion. Allowing for a 20% variation in sensitivity within these, a straight line could be drawn through the points obtained. Density expressed as a function of beam energy for a constant flux would be more accurately determined by using a single plate and exposing the same flux at various energies.

5.6. Degree of Linearity of Emulsion Characteristic.

The degree of linearity exhibited by these emulsions is of great importance in their application to electronographic image tubes. A low degree of linearity implies a low saturation level which means limited storage capacity and in the detection of low contrast optical images, the highest possible storage capacity is required. One of the difficulties in making accurate measurements in spectroscopy is the non-linear behaviour of ordinary photographic plates. This entails making accurate calibrations for each plate. This difficulty can be avoided if a high degree of linearity of the emulsions used can be insured.

The emulsion that is most commonly used with electronographic

image tubes is G5 emulsion. Data on the degree of linearity exhibited by G5 emulsion have been collected by Kahan [65] from contributors to the Third Symposium on Photoelectronic Imaging Devices and this information together with the results found in the present investigation are presented in Table 1. It is clear that there is considerable lack of agreement amongst the observers listed. Brand [66] has subsequently published characteristic curves for G5 emulsion obtained with a Spectracon image tube which show significant departure from linearity at densities of around 0.3 which is in general agreement with the result found by the author for G5 emulsion exposed to 25 kV electrons (the average transmitted energy of electrons from the Spectracon is of this order).

The analysis of Chapter 3 shows that the degree of linearity of an emulsion is related to the emulsion saturation density which in turn is a function of the incident beam energy. Thus a correlation between the degree of linearity and the incident beam energy may be expected. From the evidence presented in Table 1, it is difficult to correlate the degree of linearity with any of the variables listed with the exception of the last four observations where a correlation with incident beam energy is found. This point is further discussed below.

The discussion of Chapter 3 showed that for a given beam energy the emulsion characteristic should follow the form of :-

Observer	No. of trials	Number found to be linear	Degree of linearity	Input		Range of exposure	DEVELOPMENT				Fixing time	EMULSION		ELECTRON ENERGY
				light const.	exposure const.		Type	Temp	Time	Agit°		Thickness	Temp	
WALKER	4	3	0—3~4	✓		~1 min	D 19	65°F	5 min	yes	5 min	10 μ	−140°C	26 KV
KHOGALI	20	19	0—1.5	✓		~1 min	D 19	68°F	5 min	yes	5 min	5 μ	room temp	30-40 KV
KAHAN	2	0	0—0.25	✓		70 sec	D 19	68°F	5 min	yes	5 min	5 μ	room temp	30-40 KV
KRON	6	6	0—4.0	✓		1 min	D 19	70°F	6 min	yes	5 min	10 μ	room temp	25-30 KV
BECKMAN	3	0	0.5—3.5	✓		1 min	D 19	68°F	5.5 min	yes	10 min	5 μ	20°C	30-40 KV
VERNIER	30	30	0—2~3	✓		1 sec—10 min	D 19	70°F	5 min	no	10 min	10 μ	20°C	15-30 KV
DUCHESNE	5	3	0—1~1.5	✓		5 sec	D 19	68°F	5 min	yes	2 min	10 μ	−140°C	25 KV
BRAND	20 / 10	20 / 10	0-0.8 / 0-1.3	✓ /	/ ✓	2 min / 2 min	D 19	68°F / 68°F	5 / 6	no / yes	5 min	5 μ	20°C	30-40 KV
JEFFERS	1	1	0-0.08	✓		1 sec <	D 19	18°C	5 min	yes	5 min	25 μ	room temp	5 KV
"	1	1	0-0.24	✓		"	"	"	"	"	"	"	"	15 KV
"	1	1	0-0.45	✓		"	"	"	"	"	"	"	"	25 KV
"	1	1	0-0.8	✓		"	"	"	"	"	"	"	"	35 KV

TABLE

INFORMATION ON THE DEGREE OF LINEARITY EXHIBITED BY G5 EMULSION

$$D = Dsat. \ (1 - e^{-\Lambda E})$$

Hamilton [67] has published a characteristic density vs. exposure plot for Kodak Medium Lantern Slide Plate exposed to 50 kV electrons and has found that the equation above can be fitted to the experimental results by suitably adjusting the values of Dsat and Λ. Similarly, for the characteristic of G5 emulsion exposed to 25 kV electrons a fit is found for Dsat = 4.17 and a grain diameter of 0.4 microns, somewhat higher than Ilford's figure of 0.27 microns. This is shown in Fig. 23(a). The value of 0.4 microns for the grain diameter was subsequently used to obtain a fit for the characteristic curves determined at other beam energies. The values of emulsion saturation density found by fitting the above equation are shown in Fig. 23(b) plotted against beam energy. Also shown in this figure is a plot of electron range in emulsion against beam energy. Values of electron range were taken from Barkas.[4] It can be seen that in the range 10 - 35 kV that these two curves follow one another. Thus, in so far as Dsat is linearly related to electron range over this range of beam energy and in so far as the equation above describes the behaviour of these emulsions, then the degree of linearity exhibited by the emulsion will also increase with beam energy.

In the case of the Spectracon tube, the operating potential is limited by the tube background level. Recent Spectracon tubes have shown very low background levels when operated at 40 kV (i.e.

Fit of theoretical characteristic equation to experimental result for G 5 emulsion exposed to 25 kv electrons

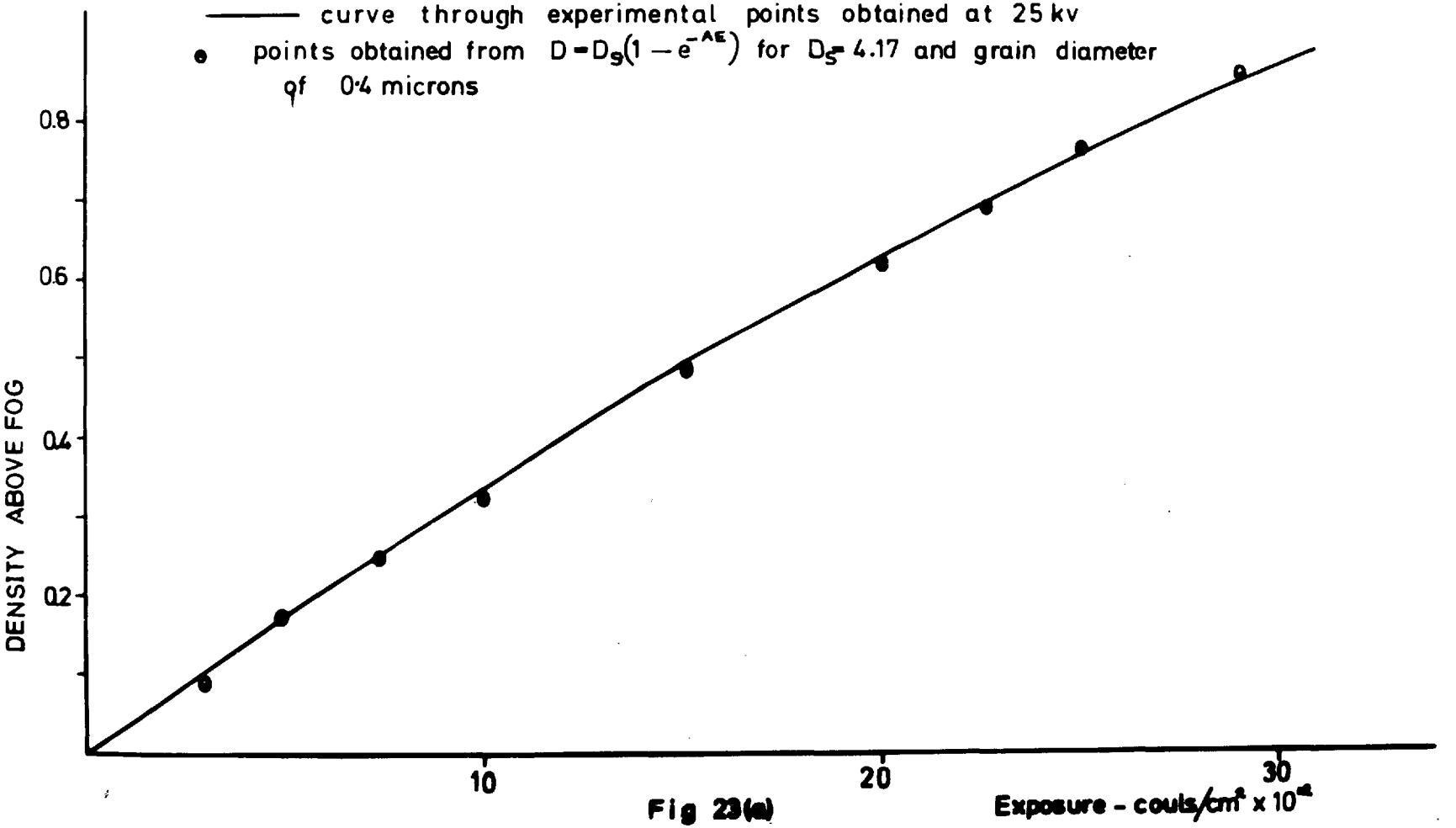


Fig 23(a)

Variation of saturation density and electron range with electron energy for G 5 emulsion

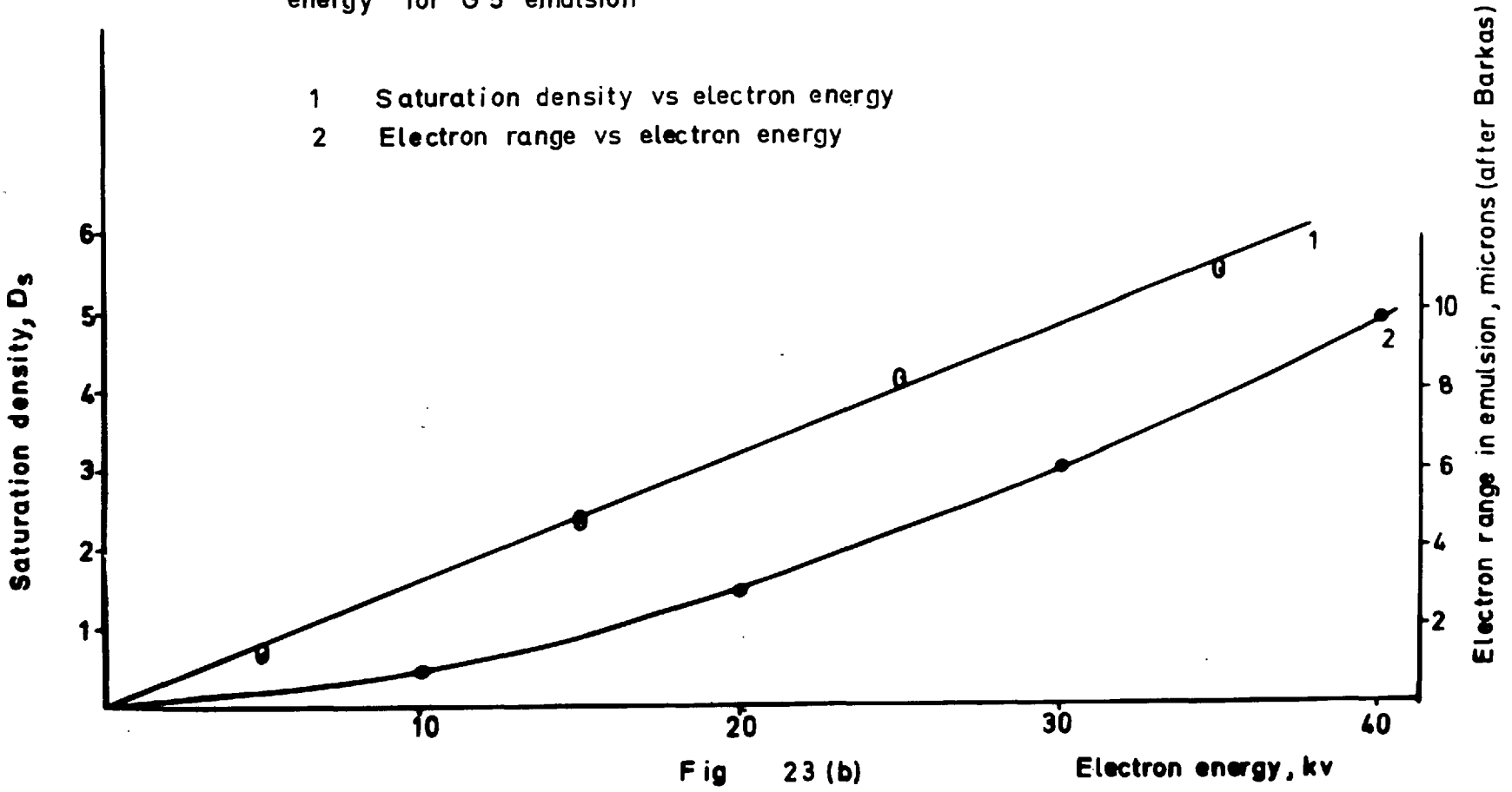


Fig 23 (b)

exposures of 1 hour have been made on XM emulsion with the tube at room temperature without the background density exceeding 0.1). It may be possible to increase the operating potential to 50 kV or more without the background becoming excessive and in so doing the speed and photoelectron recording efficiency of the tube will increase and so may the linear response and granularity of the emulsion.

5.7. Conclusions :-

The response of the nuclear research emulsions G5, L4 and XM to electron irradiation of energy up to 35 kV for densities up to D = 1.0 has been investigated.

The results presented in the form of H and D curves and, in particular, the measurements of the contrast of these emulsions show agreement with the single-hit law for low values of density.

The results presented here and the results of Hamilton can be fitted to the equation for the characteristic curve, $D = Dsat. (1 - e^{-\Lambda E})$. for suitable values of Λ and Dsat, providing some theoretical justification for the low degrees of linearity observed. However, this does not accord with the findings of some other observers and this aspect of the investigation warrants much further consideration, in particular, to determine if emulsion processing conditions and/or the methods used for density measurement have a bearing on the response of the emulsion.

Information has been presented on the speed, contrast and

degree of linearity of the nuclear research emulsions L4, G5 and XM. The other parameter of interest in the application of these emulsions to the recording of electron images is the granularity of these emulsions and this will now be considered.

Chapter 6.

Granularity of Nuclear Research Emulsions.

6.1. Graininess and Granularity.

When a developed photographic image is enlarged, the distribution of the developed silver halide grains over the area of the image is such as to cause a lack of homogeneity which is known as graininess. This effect shows up even though the magnification is such that it is impossible to detect individual grains. Jones and Deisch (68) have defined graininess as 'the sensation or impression of non-uniformity in a photographic deposit produced on the consciousness of the observer when such a deposit is viewed' i.e. graininess is a purely subjective concept. The present investigation is concerned with making a quantitative measurement of this effect and so the definition given above will not suffice. Granularity is the term reserved for definitions of this effect in purely objective terms. Many definitions of granularity have been proposed and many more methods of its measurement have been described.

Much of the early work (69) on this effect was based on the fact that if an image of the uniformly exposed and developed photographic material was moved away from the observer, the sensation of non-uniformity would disappear at a certain distance and the image appear homogeneous. The magnification was fixed and

the relative merging distances for different samples were measured. A variation of this method due to Lowry [70] was to fix the distance and vary the magnification required to produce blending of the image. Dunham [71] suggested that the granularity of a photographic material might be measured from the variations in a microphotometer trace and Goetz and Gould [72] developed a method, based on this idea, for measuring the standard deviation of the relative transmittance $\frac{\Delta T}{Tm}$, where ΔT is the value of the individual transmittance fluctuations measured from the mean and Tm is the mean transmittance. Selwyn [73] developed a theory of graininess based on the statistical distribution of density measured over a large number of small areas on the developed photographic emulsion and defined granularity as the product of the standard deviation of the density from the mean and twice the square root of the scanning area. Jones and Higgins [74-81] in a series of eight papers have made a comprehensive study of graininess and granularity and the relation between them. These authors have used several of the methods described above to measure graininess and granularity of nine samples of photographic material in order to determine any correlation between the methods of measurement and the various definitions. Their results show that none of their granularity - density functions is in agreement with the graininess - density functions and so graininess is not a linear function of granularity as measured by any of the methods studied.

As a result of this work, Jones and Higgins developed a means of measuring granularity, the results of which could be directly related to graininess. They termed their measurement of granularity "syzygetic" granularity. More recently Clark Jones (82) has applied information theory to the question of granularity and points out that both the Selwyn and Jones and Higgins definitions give an imperfect picture of granularity whereas an analysis in terms of noise-power spectrum gives a complete picture. Other authors, notably Zweig, (83) Wall and Steel (84) have developed the application of information theory to photographic granularity and have shown that two equivalent functions may be obtained from a microphotometer trace - a correlogram and a power spectrum - and that both Selwyn's definition of granularity and Jones and Higgins syzygetic granularity are related to these functions under certain conditions. Almost all the published information concerns the granularity of photographic emulsions. From the brief review given above it can be seen that the question of granularity is complex and care has to be taken to specify the definition used and the conditions under which the measurement is made.

A knowledge of the granularity of these emulsions is important in their application to the detection of low contrast optical images by electronographic image tubes since the granularity limits the smallest detail of a given contrast that can be detected.

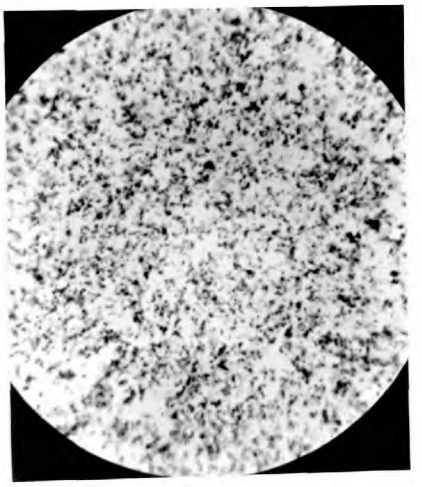
6.2. Definition of Granularity used in the Present Investigation.

The observations made with electronographic image tubes will be subject to analysis by a microphotometer. Thus, the graininess of these emulsions is not of particular interest but what is required is a measurement of the noisiness of the emulsions as seen by a microphotometer. One may get an idea of the relative graininess of the three emulsions by referring to the photomicrographs of Fig. 23(c). The definition of granularity used in this investigation is the root-mean-square variation in density of a uniformly exposed and developed emulsion and this has been measured using a microphotometer as described below.

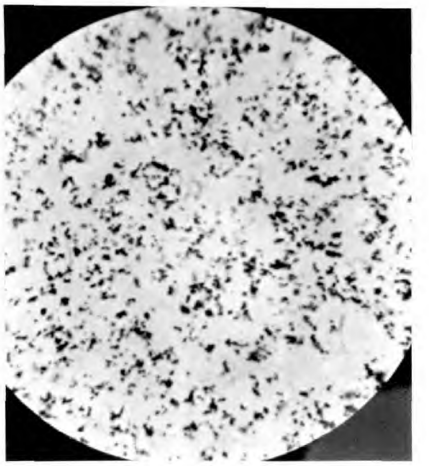
It is very difficult in the case of photographic emulsions exposed to light to give a mathematical analysis of granularity in terms of the emulsion parameters and the incident photon flux because of the complex statistical nature of the photon-silver halide crystal interaction. Such an analysis can be given for nuclear research emulsions exposed to electrons using the definition of granularity given above.

6.3. Theoretical Treatment of the Granularity of Nuclear Research Emulsions Exposed to Electrons.

The following theoretical analysis is strictly valid only over the linear region of the emulsion characteristic. Following Valentine, (55) the density D of a developed image in a nuclear research emulsion, is proportional to the product of n, the mean



L4



G5



XM

Fig. 23(c). Photomicrographs of G5, L4 and XM emulsions exposed to electrons (magnification 750 x).

number of silver grains produced per electron, A, the mean cross-sectional area of the silver halide crystals and E, the exposure. If small areas of the emulsion are considered, each of these three values will be independently subject to random fluctuations from spot to spot and so if σ_D, σ_E, σ_n and σ_A are the root-mean-square fluctuations in D, E, n and A respectively then since E, n and A are independent :-

$$\left(\frac{\sigma_D}{D}\right)^2 = \left(\frac{\sigma_E}{E}\right)^2 + \left(\frac{\sigma_n}{n}\right)^2 + \left(\frac{\sigma_A}{A}\right)^2 \quad \ldots\ldots\ldots (1)$$

If the area of the spot considered is S and a mean of N electrons fall over it, the exposure $E = \frac{N}{S}$. N is subject to a Poissonian distribution and so the fluctuation in N from spot to spot is $\sqrt{N}$ i.e. $\frac{\sigma_E}{E} = \frac{1}{\sqrt{N}}$ Also the fluctuation in n, the number of grains per electron is $\sqrt{n}$. The value for each area S is based on the mean for N tracks and the fluctuation in a mean of r readings is less than that of the individual readings by r and so :-

$$\frac{\sigma_n}{n} = \frac{1}{\sqrt{nN}}$$

Similarly if the root-mean-square fluctuation in the cross-sectional areas of the halide crystals is σ then since the value for the area S is based on nN grains :-

$$\frac{\sigma_A}{A} = \left(\frac{1}{\sqrt{nN}}\right) \times \frac{\sigma}{A}$$

Thus the granularity is given by :-

$$\frac{\sigma_D}{D} = \frac{1}{\sqrt{N}}\left[1 + \frac{1}{n}\left(1 + \frac{\sigma^2}{A^2}\right)\right]^{\frac{1}{2}} \quad \ldots\ldots\ldots\ldots\ldots\ldots (11)$$

Data given by Mees for the scatter in grain sizes of photographic emulsions indicates that the standard deviation of the cross-sectional areas is of the order of the mean areas i.e. $\frac{\sigma}{A} \sim 1$.

So approximately,

$$\frac{\sigma_D}{D} = \frac{1}{\sqrt{N}} \cdot \left(1 + \frac{2}{n}\right)^{\frac{1}{2}} \quad \ldots\ldots\ldots\ldots\ldots\ldots\ldots\ldots (111)$$

In the ordinary photographic process, n is the number of grains produced per photon and will be very small since many photons are required to produce a grain. In the electronographic recording process, however, n will be large (about 6 for 25 kV electrons in G5 emulsion) and so the dominant factor in the granularity will be the electron beam noise, $\frac{1}{\sqrt{N}}$.

In the present investigation σ_D has been measured for several values of D for the emulsions XM and G5. The results presented in the previous chapter give values of N against density for these emulsions and so the validity of equation (111) above may be checked. The method used for the measurement of σ_D will now be described.

6.4. Method of Measurement of Granularity.

None of the exposures made with the apparatus described in Chapter 3 had the required degree of uniformity suitable for making granularity measurements. The exposures used in the present

investigation were made with the Spectracon image tube B 57. This tube had a mica window thickness of 3.9 microns and a cathode sensitivity of 50 μA/lumen. The cathode was uniformly illuminated over an area of 4 mm in diameter and exposures of increasing duration (in order to cover the density range 0.1 - 1.0) were made on XM and G5 emulsions. The emulsions were processed in the normal way using 5 mins. development in ID 19 developer and after fixing were thoroughly washed with distilled water and stored in a dust free atmosphere.

These measurements of granularity were made with the Jarrel-Ash microphotometer. The aperture size of the microphotometer was adjusted to the minimum allowed by the optical arrangement and sensitivity of the instrument. This was 0.1 mm x 30 microns and gave reasonable transmission variations. The exposures were scanned at 0.5 mm per min and five scans gave a sufficiently long trace to enable reliable measurements to be made. The spacing of the scans was greater than 0.2 mm so that the measurements made from each scan were independent of the others. During these measurements frequent checks were made against drift of the zero and 100% settings of the microphotometer.

Zweig (83) reports that for 1000 independent density measurements, the accuracy in the root-mean-square value is $\pm$ 9% for 95% of the time. This degree of accuracy was aimed at in the present

investigation and each measurement of σ_D was based on 900 - 1000 individual density measurements. Four values were determined for each emulsion making a total of nearly 8,000 individual measurements of density. These measurements were made in the following way :-

The output trace of the microphotometer gives the variation in optical transmission across the exposure. Readings of transmission were made at what corresponded to 60 micron intervals on the actual exposure by placing a Perspex sheet over the trace. The Perspex sheet had parallel lines ruled on its surface and these were aligned with the transmission axis on the pen-recorder chart. Values of transmission at the intersection of the trace and the lines on the Perspex sheet were read off. The spacing of lines on the Perspex sheet was chosen so that the spacing of the measurements of transmission on the exposure itself exceeded twice the width of the microphotometer slit. Thus, in this way, about 1000 independent transmission measurements were obtained for each exposure.

The data thus accumulated were processed on the I BM 1401/70 computer installation at Imperial College. A programme (see Appendix 2 was written which firstly calculated the respective density for each transmission measurement. Then the mean density and its root-mean-square value were computed.

The method described above for granularity measurements is not ideal for the following reasons :-

(1) The slit width used, 30 microns, will not detect high frequency variations in density.

(11) The instrument itself measures optical transmission which means that all the readings of transmission have to be converted to density.

(111) The readings of transmission have to be read off from the pen-recorder trace and the data acquired have to be punched up on computer cards. This is a time consuming process.

A system based on a Joyce-Loebel type of microdensitometer with which very small slit widths may be used would be a big improvement, particularly if the density readings obtained could be directly recorded on to punched-tape. A more sophisticated system which can be directly linked to a computer has been described by Dennison. (85)

6.5. Results :- (a) Check on Theory.

The conditions under which equation (111) of section 6.3 apply are :-

(1) it applies to a uniform exposure of monoenergetic electrons.

(11) it applies over the linear region of the emulsion characteristic.

(111) the approximation is made that the scatter in the areas of the silver grains is of the order of the mean grain areas.

In the case of exposures made with the Spectracon tube, the electron beam striking the emulsion has an energy distribution as a result of the passage of the beam through the mica window and thus equation (111) cannot be strictly applied to the results obtained from exposures made with this tube.

In view of this the author obtained some G5 plates that had been exposed in the Lallemand electronic camera. These had been exposed to a uniform flux of 25 kV electrons and three measurements of granularity were made. Curve 1 of Fig. 24 was constructed from the approximate equation (111) of section 6.3 in the following way :-

Values of N were obtained from the results of Fig. 13 for G5 emulsion exposed to 25 kV electrons. The plates in this case were exposed at room temperature whereas plates in the Lallemand camera are exposed at liquid nitrogen temperatures. Duchesne (86) has measured the change in sensitivity of G5 emulsion when it is cooled from room temperature to liquid air temperature and reports a 30% drop in sensitivity. This drop in sensitivity is interpreted not as a drop of 30% in the number of electrons recorded but as a decrease of 30% in the mean number of developed grains produced per electron due to decreased ion mobilities at liquid air temperature. Thus, in order to obtain the same density (i.e. the same total number of developed grains) at liquid air temperature as at room temperature the total number of electrons recorded has to be increased by a factor of $\frac{100}{70}$. The values of N used

Curve 1 — curve obtained from the approximate formula $\frac{\sigma_d}{D} = \frac{1}{\sqrt{N}}\left(1 + \frac{2}{n}\right)^{\frac{1}{2}}$, values of N were obtained from Fig 13 corrected for emulsion temperature difference, values of n were obtained from Pniewski's results.

Curve 2 — curve obtained from $\frac{\sigma_d}{D} = \frac{1}{\sqrt{N}}\left[1 + \frac{1}{n}\left(1 + \frac{\sigma^2}{A^2}\right)\right]^{\frac{1}{2}}$ using values of N and n as above and assuming $\frac{\sigma}{A} \sim 4$.

— experimental results obtained from G 5 plates exposed to 25 KV electrons in Lallemands electronic camera.

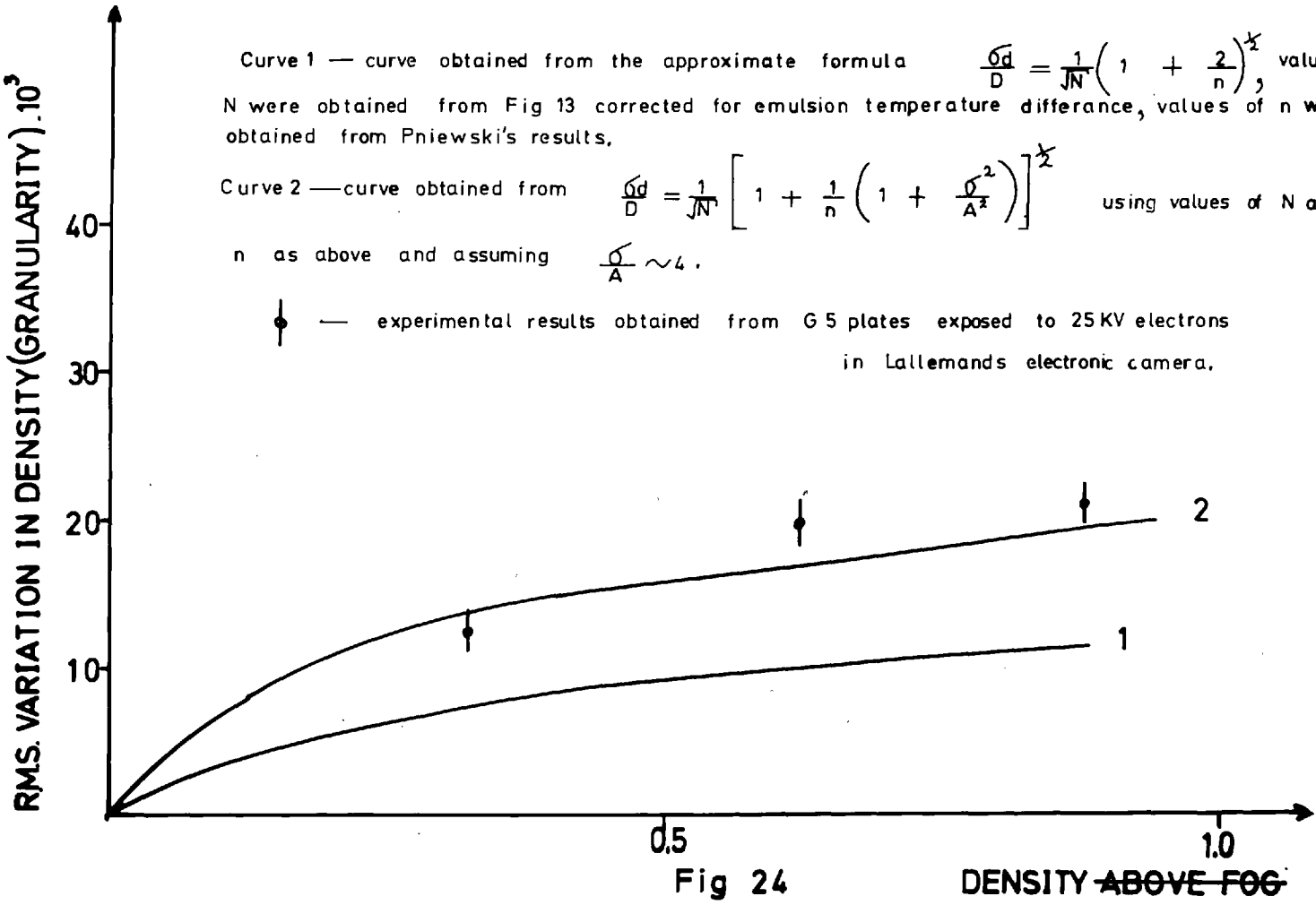


Fig 24

in the equation for granularity were increased accordingly. Pniewski (64) reports a value of around six for the number of grains produced per electron in G5 emulsion for 25 kV electrons recorded at room temperature. Thus, a value of n = 4.2 was used in the equation and in this way corresponding values of σ_D and D were obtained. It can be seen that the three experimental points are not in agreement with this curve, the measured values being of the order of twice the values predicted by equation (111) of section 6.3. It must be stated that a reliable check on this formula could only be made if measurements of N and σ_D were made on the same strip of emulsion since emulsion speeds are subject to variation. To account for the discrepancy above a speed difference of a factor of 4 would be required. Such a variation in speed although very rare is not unknown for G5 emulsion. (87) However, it is possible that the approximation concerning the variation in grain sizes does not hold. The mean area $\bar{a}$ and the spread in grain size distribution has been measured (54) for various photographic films and of the films measured the ratio $\frac{\Delta a}{\bar{a}}$ varies from 0.45 for X-ray film to 1.23 for portrait film. Of the nuclear research emulsions, Barkas (4) has measured the sizes of the silver halide crystals of G5 emulsion and has found a mean diameter of 0.275 microns for which $\sigma^2 = 0.0022 \mu^2$. Using this information the mean area $\bar{A}$ and the scatter in area $\Delta\bar{A}$ may be estimated in the following way :-

For the silver halide crystals of G5 emulsion $\bar{d} = 0.275$ microns and $\overline{\Delta d}^2 = 0.0022\mu^2$ where $\bar{d}$ = mean diameter of crystal, $\overline{\Delta d}$ = variance in $\bar{d}$

The mean area of the crystal

$$\bar{A} = \frac{\pi}{4}\overline{d^2}$$

Now, $$\overline{\Delta d}^2 = \overline{d^2} - \bar{d}^2$$

$$\overline{d^2} = \bar{d}^2 + \overline{\Delta d}^2$$

$$= .0756 + .0022 = .0778.$$

$$\bar{A} = \frac{\pi}{4} .0778 = .0611\mu^2$$

This figure is based on measurements of silver halide crystals. It is the mean area and spread in area of processed silver grains that is of interest. Whereas the silver halide crystal is nearly spherical in shape, the developed silver grain is a fibrous mass of silver generally larger than the silver crystal. No information is available on the distribution in areas of the developed grains of G5 emulsion but assuming the mean grain area is of the order of $.0611\mu^2$ and also that the areas of the grains obey Poissonian statistics then :-

$$\frac{\overline{\Delta A}}{\bar{A}} \sim 4.05$$

Using this figure in equation (11) of section 6.3 :-

$$\frac{\sigma_D}{D} = \frac{1}{\sqrt{N}}\left[1 + \frac{1}{n}\left(1 + 4.05^2\right)\right]^{\frac{1}{2}} \quad \ldots\ldots\ldots\ldots\ldots\ldots (1)$$

Thus, $\frac{\sigma D}{D} = \frac{1}{\sqrt{N}} \cdot \left(1 + \frac{17.4}{n}\right)^{\frac{1}{2}}$ ..... (II)

Using $n = 4.2$:-

$$\sigma D = \frac{D}{\sqrt{N}} \times 2.3 \quad \text{..... (III)}$$

whereas the approximate equation (III) of section 6.3 gives :-

$$\sigma D = \frac{D}{\sqrt{N}} \times 1.22 \quad \text{..... (IV)}$$

Equation (III) above is curve 2 of Fig. 24 and is a much better fit to the experimental points. Although it has been stated that the granularity of electron-sensitive emulsions arises almost entirely from the noise in the incident electron beam, it would appear that there may be a significant contribution from the distribution in the areas of the grains.

(b) Comparative Granularity of XM and G5 Emulsions.

Fig. 25 shows the variation of granularity with density for XM and G5 emulsions as measured from exposures made with the Spectracon. The question of the contribution to granularity from the energy distribution in the incident electron beam is dealt with more fully in the next Chapter. If it is assumed that the contribution to granularity from the distribution in areas of the grains and from the energy distribution in the incident electron beam is the same in both cases then for a given density the ratio of the granularities of these two emulsions is :-

VARIATION OF GRANULARITY WITH DENSITY FOR EXPOSURES MADE WITH SPECTRACON

Data obtained from exposures made with Spectracon tube B 57 which had a mica window thickness of 3,9 microns.

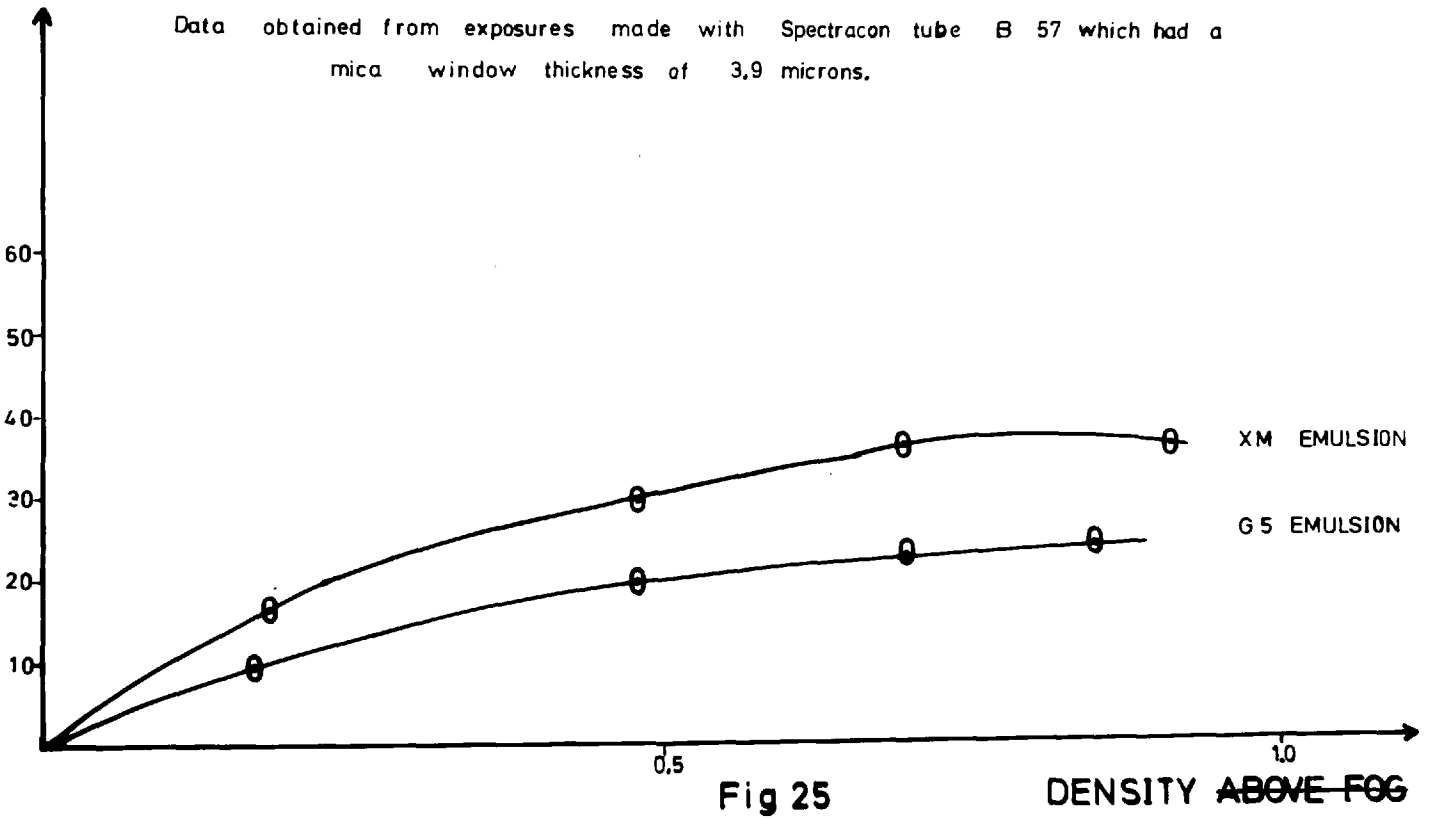


Fig 25

$$\frac{(\sigma D)_{XM}}{(\sigma D)_{G5}} \sim \left(\frac{N_{G5}}{N_{XM}}\right)^{\frac{1}{2}}$$

where N_{XM} and N_{G5} are the electron fluxes producing the same density on each emulsion i.e. the ratio of granularities is of the order of the square root of the speed ratio. Thus; using the more commonly found figure of 5 for the speed ratio of these emulsions :-

$$\frac{(\sigma D)_{XM}}{(\sigma D)_{G5}} \sim (5)^{\frac{1}{2}} \sim 2.2$$

At low densities a value of 1.6 is found. A similar order of magnitude calculation may be made to determine the granularity of L4 emulsion. Thus, at a density of 0.3 :-

$$(\sigma D)_{L4} \sim 0.6 \quad (D)_{G5} \sim 9.10^{-3}$$

(c) Least Detectable Density Variation.

The granularity of the emulsion limits the smallest detail of a given contrast that can be detected. The change in density on the emulsion caused by the signal to be detected must be significantly greater than the random fluctuations in density. In general, the signal-to-noise ratio must be significantly greater than a certain constant (known as the coefficient of certainty) for the signal to be detected with certainty. Assuming a figure of 1.5 for the coefficient of certainty (87) then the minimum change in density that can be detected in the case of the three emulsions under investigation and under the conditions of granularity measurement

outlined above is :-

Emulsion	Minimum Detectable Density Change at D = 0.3
L4	0.014
G5	0.02
XM	0.03

(d) Comparison with Photographic Emulsions.

Kodak [88] have published figures giving the granularity of some of their emulsions. These granularity measurements were made by scanning with a circular aperture of area around 2,000 μ^2 and the figures given refer to a density of 0.8. These figures may be used to give a rough comparison between astronomical plates exposed to light and electronographic emulsions exposed to electrons :

Emulsion	Granularity at Density = 0.8	
103 a - O	0.094	exposed to light
II a - O	0.076	
XM	0.036	exposed to electrons
G5	0.024	by Spectracon tube.

From these figures it can be seen that the granularity of electron-sensitive emulsions is considerably less than that of the most commonly used astronomical plates.

The degradation in the signal-to-noise ration due to the electronographic recording process can be estimated in the following way.

6.6. Degradation in Signal-to-Noise ratio due to Electronographic Recording.

In the case of ordinary photographic emulsions, Fellgett(89) has shown that there is a 100 fold loss of signal-to-noise ratio in the formation of the negative with even the best available emulsions. In the case of electronographic recording, the ratio :-

$$r = \left(\frac{\text{Signal-to-noise in recorded image.}}{\text{Signal-to-noise in incident electron beam}} \right)$$

can be estimated in the following way :-

For the linear region of the emulsion characteristic we may write :-

$$D = k.E$$

where D = density, k = constant, E = exposure.

Thus, the number of electrons, N, incident on an area A of emulsion is :-

$$N = \frac{A.D}{k}$$

The signal-to-noise ratio of the incident electron beam = $\frac{N}{\sqrt{N}} = \sqrt{\frac{A.D}{k}}$

The signal-to-noise ratio of the emulsion = $\frac{D}{\sigma D}$

Thus,

$$r = \frac{D/\sigma D}{\sqrt{\frac{A.D}{k}}} = \frac{1}{\sigma D} \cdot \sqrt{\frac{k.D}{A}}$$

Using the results obtained from the plate of G5 emulsion exposed in Lallemand's electronic camera,

$$D = 0.33, \quad D = 12.5. \ 10^{-3}$$

The value of k was determined from Fig. 13 which gives D vs E for G5 emulsion exposed to 25 kV electrons and the values of E were adjusted for the difference in sensitivity due to the emulsion temperature difference. With E expressed as no. of electrons/micron^2, k = 0.36. The value $A = 3{,}000 \mu^2$ was used in the granularity measurements, so :-

$$r = \frac{1}{12.5\ 10^{-3}} \cdot \sqrt{\frac{0.38 \times 0.33}{3{,}000}}$$

$$= 0.52$$

Thus, the loss in signal-to-noise ratio due to the recording of the electron beam is about 48%. This value of r may be used to calculate the overall loss of signal-to-noise ratio and thus the equivalent quantum efficiency of a single-stage electronographic

image tube.

6.7. Overall Reduction of Signal-to-Noise Ratio in a Single-Stage Electronographic Image Tube.

For a single-stage tube of the Lallemand type, the signal-to-noise ratio of the incident photon flux is degraded firstly by the photon-photoelectron interaction and secondly by the recording of the electron image in the emulsion. If there are N incident photons, the signal-to-noise ratio of the incident photon flux is $\sqrt{N.}$ If the photocathode has a quantum efficiency of q, then Nq photoelectrons leave the cathode and the signal-to-noise ratio in the electron beam is $\sqrt{Nq.}$ As we have seen this is further degraded by a factor of 0.52 in the process of recording the electron beam on G5 emulsion and so the overall reduction of signal-to-noise ratio is $0.52\sqrt{q.}$ For a photocathode of quantum efficiency 35% the overall reduction of signal-to-noise ratio is by a factor of 0.3. This compares with a factor of 0.01 for the best available photographic emulsions.

The equivalent quantum efficiency of such a tube is given by :-

$$q_e = \left(\frac{\text{Signal-to-noise ratio of output events}}{\text{Signal-to-noise ratio of incident photon flux}}\right)^2$$

If N is the incident photon flux on the photocathode and q is the photocathode quantum efficiency then :-

Signal-to-noise ratio of photoelectron beam = $\sqrt{q.N.}$

Signal-to-noise ratio of recorded electron image = $r\sqrt{qN.}$

$$q_e = \left(\frac{r.\sqrt{qN}}{\sqrt{N}}\right)^2 = r^2.\,q$$

For $r = 0.52$,

$$q_e \sim 0.3.q.$$

This compares with previous estimates [49] of the equivalent quantum efficiency of Lallemand's camera of 0.9.q. This estimate was made just taking the distribution in the number of grains produced per electron into account.

The only other measurements of r reported in the literature are those given by Valentine and Wrigley [10]. These authors have measured r for G5 emulsion directly exposed to 60 kV electrons and developed in LD19 developer. In this case, measurements of N and D were made on the same strip of emulsion and measurements of granularity were made using a Joyce-Loebel microdensitometer. A value of r = 1.0 was determined i.e. there was no loss of signal-to-noise ratio in the recording process. Values of r at 60 kV and 25 kV may be compared as follows :-

In this calculation, suffix 1 refers to 25 kV and suffix 2 to 60 kV. For G5 emulsion, we may write :-

$$(\sigma D)_1 = \frac{D_1}{\sqrt{N_1}} \cdot \left(1 + \frac{17.4}{n_1}\right)^{\frac{1}{2}}$$

Also,

$$(\sigma D)_2 = \frac{D_2}{\sqrt{N_2}} \cdot \left(1 + \frac{17.4}{n_2}\right)^{\frac{1}{2}}$$

$$\text{Thus,}\quad \frac{(\sigma D)_1}{(\sigma D)_2} = \frac{D_1}{D_2}\cdot\sqrt{\frac{N_2}{N_1}}\cdot\left[\frac{\left(1+\frac{17.4}{n_1}\right)}{\left(1+\frac{17.4}{n_2}\right)}\right]^{\frac{1}{2}}$$

Pniewski (64) gives $n_2 = 23$ and a value of $n_1 = 4.2$ is used, as before. Also by extrapolating the results of Fig. 13 to 60 kV a value for N_2 can be obtained.

For D = 0.3 :-

$$\frac{(\sigma D)_1}{(\sigma D)_2} = \sqrt{\frac{4.05 \times \frac{100}{70}}{8.8}}\cdot\left[\frac{\left(1+\frac{17.4}{4.2}\right)}{\left(1+\frac{17.4}{23}\right)}\right]^{\frac{1}{2}}$$

$$= 1.38$$

What is of interest is the relative loss of signal-to-noise ratio in recording the electron beam at these energies. Now :-

$$r_1 = \frac{D_1/\sigma D1}{N_1/\sqrt{N_1}}\quad,\qquad r_2 = \frac{D_2/\sigma D2}{N_2/\sqrt{N_2}}$$

$$\frac{r_1}{r_2} = \frac{D_1}{D_2}\,\frac{\sigma D_2}{\sigma D_1}\cdot\sqrt{\frac{N_2}{N_1}}$$

For same density :-

$$\frac{r_1}{r_2} = \frac{1}{1.38}\cdot\sqrt{\frac{5.78}{8.8}} = 0.58$$

A value of $r_1 = 0.52$ is found by the author and a value of $r_2 \sim 1.0$ is found by Valentine and Wrigley and these figures are in agreement with the calculation above.

On this basis, it may be concluded that previous figures quoted for the equivalent quantum efficiency of electronographic devices may be overestimates due to the fact that the contribution to granularity from the distribution in areas of the grains was overlooked. It is worth noting that this particular source of noise becomes less significant as n, the number of grains produced per electron, increases. Thus, increasing the operating potential of direct recording electronographic devices will lead to an improvement in equivalent quantum efficiency and also improve the linear response of the emulsions. This may not be a practical proposition with the existing Lallemand technique since increasing the operating potential may lead to excessive background. One way in which the contribution to noise from the distribution in grain areas can be completely eliminated is to use grain counting techniques and this method will be discussed below.

6.8. Variation of Equivalent Quantum Efficiency with Exposure.

For low values of density the relationship between granularity and density may be expressed as :-

$$\sigma_D \propto \frac{D}{\sqrt{N}}$$

where N is the number of electrons integrated over area A of the emulsion, where A is the area of the microphotometer scanning slit used for the measurement of granularity.

Also, $D \propto N$

and $q_e = r^2 . q. = \frac{kD}{A\sigma_D^2} = \text{CONSTANT}.$

i.e. the equivalent quantum efficiency is constant with exposure over this range of density. Results of q_e corresponding to values of D are given below, calculated from the results derived in Chapter 5 and 6 and are applicable to Lallemand's camera :-

Equivalent Quantum Efficiency vs. Density for G5 emulsion exposed to 25 kV Electrons in Lallemand's Camera.

Density	Equivalent Quantum Efficiency, q_e.
0.1	0.25. q
0.3	0.23. q
0.6	0.25 q
0.8	0.24. q

q = photocathode quantum efficiency.

These results show that the equivalent quantum efficiency of G5 emulsion is fairly constant with density for low values of density, unlike photographic emulsions whose quantum efficiency - density characteristics generally peak for low values of density. This behaviour has been observed for G5 emulsion in some preliminary results given by Brand. (90)

6.9. Use of Grain Counting Techniques for Image Evaluation.

The evaluation of the blackening of an emulsion exposed to

electron irradiation is essentially a process whereby output events (developed silver grains) are counted. In the case of evaluation by a microdensitometer grain counting is done by averaging the effect of the stopping power of grains to light over the area of the microdensitometer slit. As we have seen there may be a significant contribution to the noise in the output of this system due to the distribution in area of the developed grains. This effect can be completely eliminated by observing the grains through a high power microscope and actually counting them. By comparison, this is a very laborious technique but it may lead to a big improvement in equivalent quantum efficiency.

Discounting the contribution to granularity from the grain area distribution, the theory of 6.3 gives :-

$$\frac{\sigma_D}{D} = \frac{1}{\sqrt{N}} \left(1 + \frac{1}{n}\right)^{\frac{1}{2}}$$

$$\text{i.e.} \quad r = \frac{D/\sigma_D}{\sqrt{N}} = \frac{1}{\left(1 + \frac{1}{n}\right)^{\frac{1}{2}}}$$

For 25 kV electrons recorded in G5 emulsion then :-

$$r = \frac{1}{\left(1 + \frac{1}{4.2}\right)^{\frac{1}{2}}} = 0.82$$

Thus, $q_e = r^2 . q \sim 0.7 . q$

Thus, the use of grain counting techniques can lead to an equivalent quantum efficiency approaching the photocathode quantum efficiency.

6.10. Conclusions:-

The granularity of electron sensitive emulsions exposed to electrons has been investigated from a theoretical and experimental point of view. Agreement between the two is reached by assuming a wide distribution in the areas of developed silver grains. The results of granularity and the measured values of electron flux producing a certain density have been combined to evaluate the equivalent quantum efficiency of a single-stage electronographic tube using G5 emulsion to record 25 kV electrons. This may be around 0.3.q for evaluation with a microdensitometer, where q is the photocathode quantum efficiency and may rise to 0.7.q if grain counting techniques are employed.

Besides the quantitative investigation of the electronographic effect, the apparatus described in Chapter 4 has been used to evaluate the comparative rates of blackening of the Spectracon and Lallemand's electronic camera and these experiments are described in the next Chapter.

Chapter 7.

Comparative Speed and Granularity of the Spectracon and Lallemand's Electronic Camera.

7.1. Introduction :-

The speeds (i.e. rate of emulsion blackening) of electronographic image tubes are generally quoted by referring to a comparison with unaided photography. Thus, Lallemand et al [31] quote a blue (4,000A°) light gain in speed over Kodak 103a - O of 50 - 100 times. Walker [91] using a Lallemand camera and G5 emulsion has shown that the gain over Kodak 103a - O varies from about 20 times at short exposures to about 120 times at long exposures of 100 minutes when the best antimony caesium photocathodes are used. The increase in gain with time of exposure is due to the reciprocity failure effect experienced with photographic emulsions. Similar measurements have been made with type - A Spectracon tubes [49] resulting in speed gains of around seven times over Kodak II a - O for a Spectracon tube of photocathode sensitivity 40 μA/lumen employing G5 recording emulsion. These measurements were made in the blue region of the spectrum. Accurate comparison of the speeds of these electronographic tubes on the basis of such published information is not possible because (a) the conditions during exposure and processing of the various films can vary considerably and so affect the final blackening.

(b) Corrections would have to be made for different responses of the photocathodes that are inserted into these tubes and these are rarely published.

The considerations of section 7.2 suggest that the speeds of these two devices should be of the same order. To investigate this McGee suggested that the experimental tube described in Chapter 4 could be used to partially simulate the conditions that exist in the Spectracon and Lallemand camera. These conditions, in so far as they affect the blackening of the emulsion are as follows :-

(a) Spectracon - the emulsion is exposed at room temperature in air by pressing it against the mica window. The electron beam from the photocathode is accelerated to 40 kV and arrives at the mica window with unit magnification. Thus, the electron beam striking the emulsion has a significant energy distribution.

(b) Lallemand's electronic camera - here the emulsion is exposed at approximately liquid air temperature in a vacuum. The electron beam from the photocathode is accelerated to 25 kV and is generally linearly demagnified by a factor of 0.7. In this case, the beam striking the emulsion is effectively monoenergetic.

The rate of blackening of the emulsion depends on the flux and energy of the electrons striking the emulsion, the temperature

of the emulsion, the pressure on the emulsion and the emulsion processing conditions. It can be seen from the above that the conditions that exist in the two devices as they affect the rate of blackening of the emulsion are markedly different. It was only possible to simulate some of these conditions, suitable corrections bing applied for the rest.

7.2. Calculation of Comparative Speeds.

In the experiments described below, the same electron flux was :-

(1) Directly recorded on to G5 emulsion with an energy of 25 kV.

(11) Indirectly recorded (i.e. by passing the beam through a thin mica foil) with a primary energy of 40 kV.

It is required to calculate the comparative blackening produced on the emulsion under these conditions. The optical density produced on the emulsion is proportional to the total number of grains produced times the cross-sectional area of a grain. If the electron flux is No, g(E) is the average number of grains produced by an electron of energy E and A is the mean cross-sectional area of a grain, then for conditions (1) above :-

Density produced = $D_1 \propto$ No. $g(E_L).A$ ..... (1)

where E_L = energy of the electron beam in Lallemand's camera

To calculate the density D_2, produced by the same electron flux, No, under conditions (11) above is more complicated. In this case, in order to calculate the total number of grains produced, one needs to know how the energies of the electrons in the beam transmitted through the mica foil are distributed. As far as the author is aware, no comprehensive retardation potential measurements have been made on the electron beams transmitted through thin mica foils. Such an analysis of the electron beams transmitted through thin aluminium oxide films has been made by Young (92) and the results are presented as normalised transmitted current against reduced energy $\frac{E_T}{E_C}$, where E_T = energy of transmitted electrons, E_C = critical energy i.e. the energy of the primary beam corresponding to the onset of transmission. Results are presented for various values of $\frac{Ep}{Ec}$ where E_p = beam primary energy. A curve is presented for $\frac{Ep}{Ec}$ = 1.75. In the case of the Spectracon, Ep = 40 kV and so Ec = 22.9 kV and this value of Ec corresponds to a mica foil 4.5 microns thick. Thus, a curve of normalised transmitted current against residual electron energy for this mica thickness can be constructed. By making the area under this curve unity, a curve of P(E) versus E can be constructed where P(E) = probability of finding an electron in the transmitted beam of energy, E. This curve is shown in Fig. 26. Now, the mean number

P(E) = Probability of an electron in the beam transmitted by a 4.5 micron mica foil having energy E. Energy of incident beam = 40 kv.

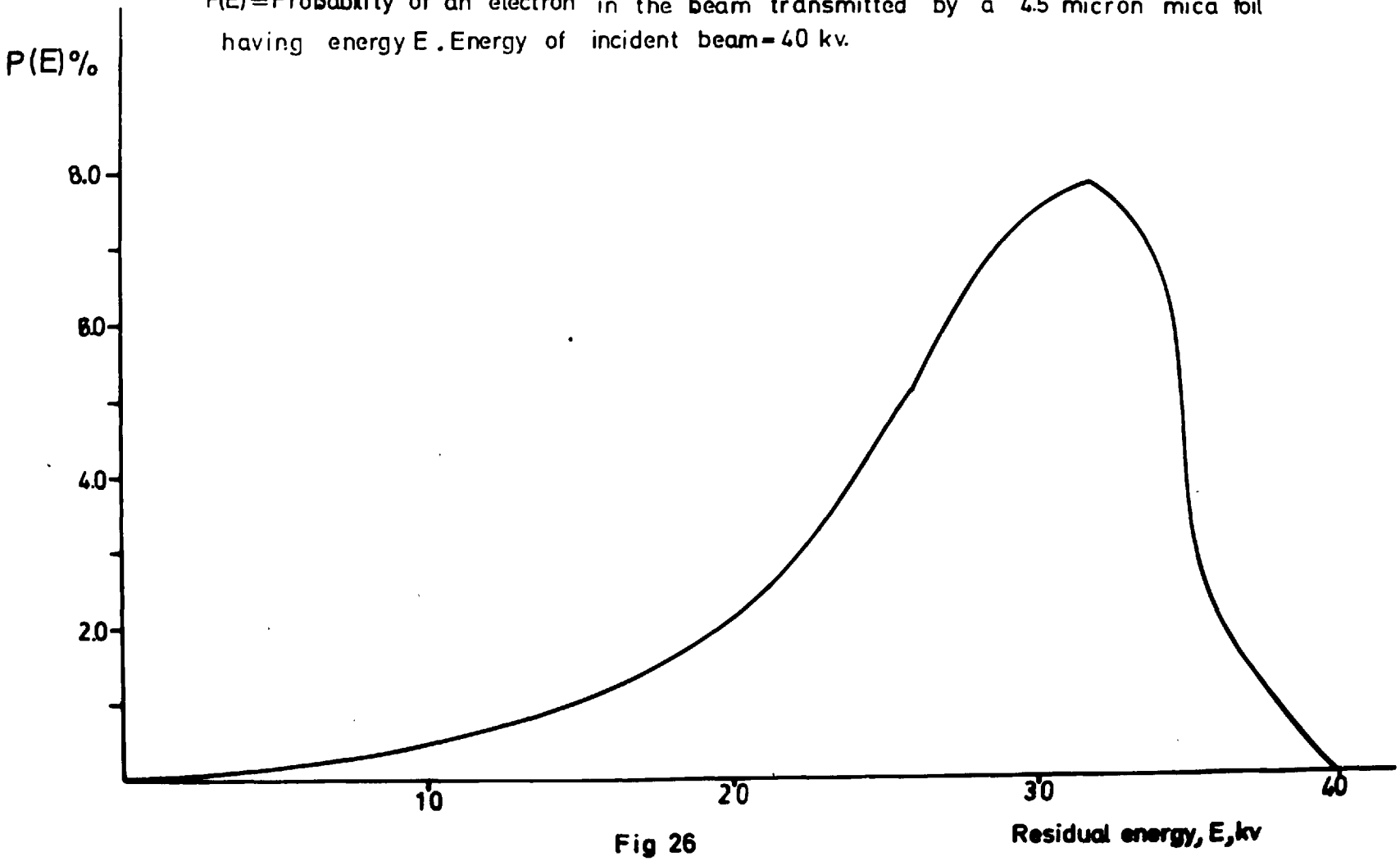


Fig 26

of grains produced per electron in this case is $\int_{o}^{Es} p(E).\ g(E).\ dE$, where Es = Spectracon's operating potential. $g(E)$ as a function of E is given by Pniewski [64] and the curve of $p(E).\ g(E)$ against E has been constructed and is shown in Fig. 27. The mean number of grains produced per electron is calculated to be 4.54 which is in reasonable agreement with a value of 4.3 measured by Khogali. [49] Now, the ratio of densities produced by the same exposure under conditions (1) and (11) above is given by :-

$$\frac{D_2}{D_1} = \frac{No.P_2}{No.P_1} \frac{\int_{o}^{Es} p(E).\ g(E).\ dE.\ A.}{g(E_L)\ A.}$$

where P_1 = photoelectron recording efficiency of Lallemand's camera, P_2 = photoelectron recording efficiency of Spectracon.

P_1 may be 0.95, allowing for a few per cent reflected electrons from the emulsion and P_2 has been measured [49] as being 0.75 for a Spectracon with a mica window of thickness 4.5 microns. Under these conditions the speed ratio is :-

$$\frac{D_2}{D_1} = \frac{0.75 \times 4.54}{0.95 \times 6} \sim 0.6$$

This calculation has been done for a mica foil 4.5 microns thick. Higher values will be obtained for thinner mica foils since both the transmission and the average energy of a transmitted electron will increase. Thus, there will be more electrons of a higher energy striking the emulsion. For a mica foil 3.0 microns thick, the

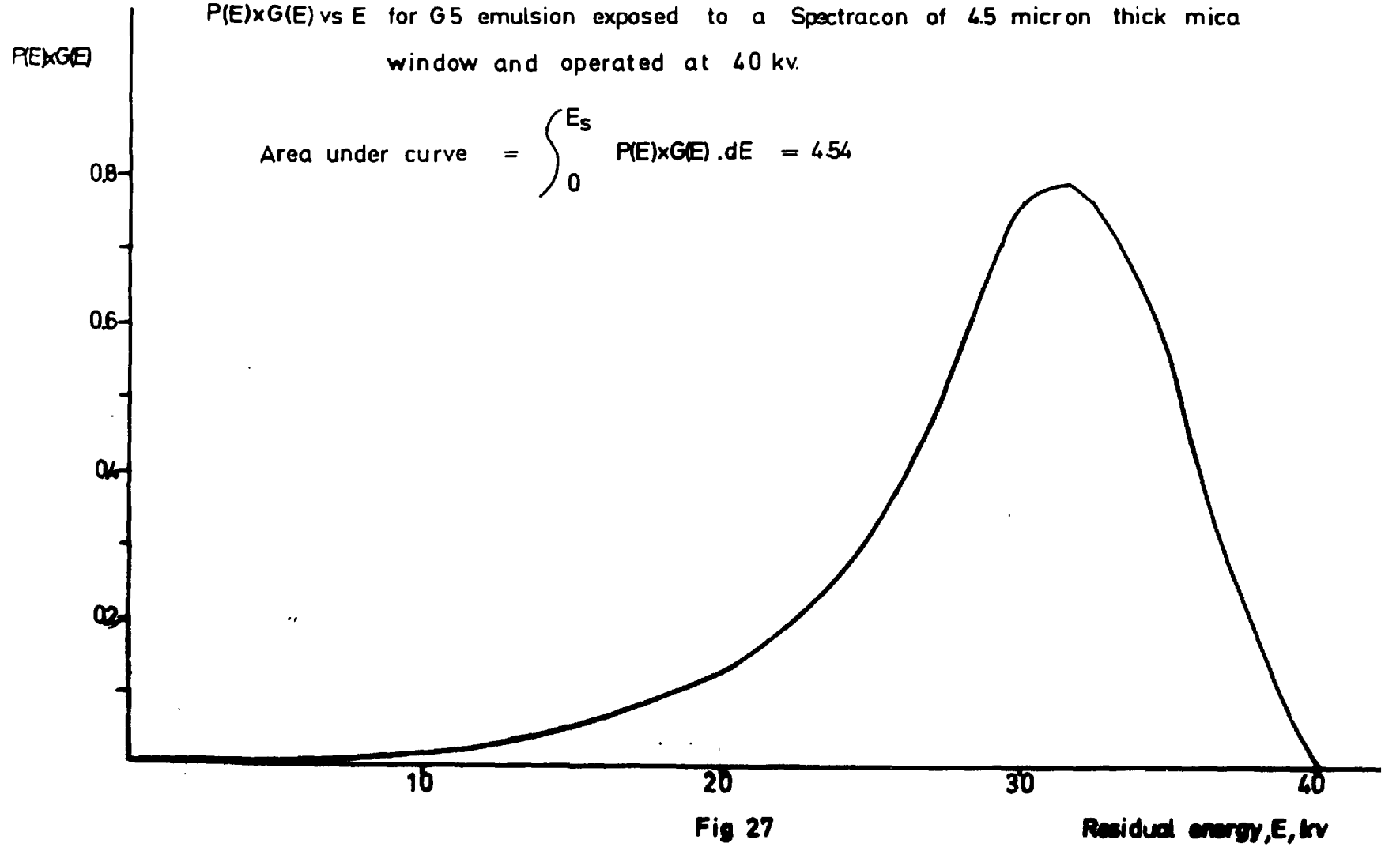

P(E)xG(E) vs E for G5 emulsion exposed to a Spectracon of 4.5 micron thick mica window and operated at 40 kv.
Area under curve = $\int_0^{E_s} P(E)xG(E)\,.dE = 4.54$
P(E)xG(E)
0.8
0.6
0.4
0.2
10
20
30
40
Residual energy, E, kv

Fig 27

transmission may be 0.85 and the average transmitted energy may be 31 kV compared with 25 kV for a mica foil 4.5 microns thick. This will give a corresponding increase in the speed ratio $\frac{D_2}{D_1}$

7.3. Experimental Procedure.

Spectracon tubes are currently made with mica windows having a thickness between 3.5 - 4.0 microns. In these experiments mica foils in the range 3.1 - 4.1 microns were used. The thicknesses of the foils were determined both by weighing the foil and by measurements with a Zeiss interference microscope. Pieces of mica $\frac{3}{4}$" x $\frac{1}{2}$" were cut to size and mounted using Araldite on to a stainless steel framework. This framework could be clipped on to the emulsion plate and loaded into the plate holder. Five mica foils of varying thicknesses were mounted on to the framework leaving five spaces on the emulsion for direct recording at 25 kV. With the stainless steel framework clipped on to the emulsion plate, the mica foils were held $\frac{1}{2}$ - 1 mm away from the emulsion surface. The mica window of the Spectracon is aluminised on its inner surface in order to stabilise the potential of the window. The thickness of the aluminium layer is guaged by observing the white hot tungsten filament of the aluminium evaporator through the mica foil and evaporation is stopped when the filament just disappears. The mica foils used in the present experiment were aluminised in this way. A new cathode gun was mounted

in the experimental tube while the framework and mica foils were being pumped in an evaporation plant. The foils were aluminised in the manner described above. Air was admitted to the evaporation plant, the framework recovered and immediately mounted on to a G5 emulsion plate which was then loaded into the experimental tube which was then pumped. This process was completed as quickly as possible in order to prevent excessive oxidation of the aluminium layer.

The tube was prepared for making exposures in the manner previously described. Five exposures were made at 25 kV with the electron beam falling directly on to the emulsion. The exposure time was varied to give a range of densities up to 1.4. The accelerating potential was then increased to 40 kV and the beam current was adjusted to be the same as was used at 25 kV. Approximately the same exposure was made through each mica foil. This experiment was repeated for low and moderate values of density recorded through mica and the results are presented in Tables 2 and 3. Also, five foils of the same thickness of mica (3.44 microns) were mounted on the framework and two sets of varying exposures were made with direct recording at 25 kV and through mica at 40 kV. These results are shown in Fig. 28.

These results show a speed ratio of 0.9 for mica thickness of 4.15 microns increasing to 1.1 for mica thickness of 3.1 microns. Thus, as far as the rate of emulsion blackening is concerned, the loss of electrons due to absorption in the mica foil is compensated by the

Results on Comparative Speeds

Beam Current A x 10^{-11}	Exposure no of electrons x 10^6	Mica thickness (microns)	Mica surface density (mg/cm^2)	Density produced	Corresponding density for same exposure at 25kv	Speed ratio
3.25	4.16	3.1	0.67	0.274	0.25	1.1
3.25	4.37	3.75	0.81	0.261	0.26	1.005
3.25	2.95	4.15	0.91	0.172	0.185	0.93

TABLE 2

Beam Current A x 10^{-11}	Exposure no of electrons x 10^6	Mica thickness (microns)	Density produced	Corresponding density for same exposure at 25kv	Speed ratio
4.9	16.5	4.15	1.19	1.24	0.96
5.1	17.2	3.97	1.19	1.27	0.94
4.8	16.5	3.65	1.27	1.24	1.02
4.9	17.2	3.50	1.28	1.27	1.01
4.9	16.7	3.12	1.43	1.25	1.14

TABLE 3

Direct and indirect recording on G5 emulsion

o — Direct recording of 25 kv beam

θ — Result obtained by recording 40 kv beam after penetrating mica foils 3.44 microns thick

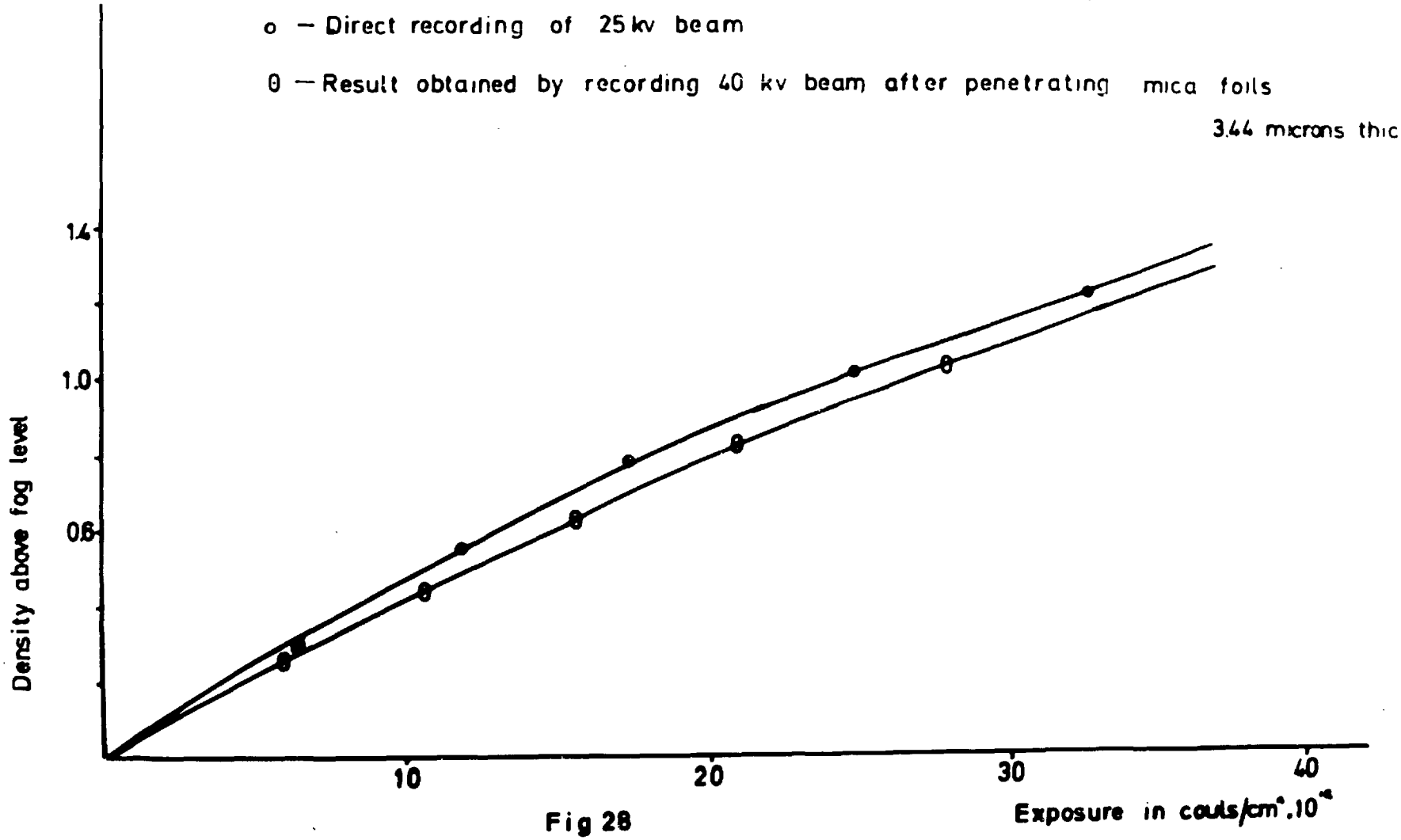


Fig 28

greater average residual energy of the transmitted electrons, resulting in a rate of blackening comparable with the direct recording of 25 kV electrons. These results are in general agreement with the considerations of 7.2.

7.4. Comparative Speeds of Spectracon and Lallemand's Electronic Camera.

The results obtained above have to be corrected in order to determine the comparative speeds of the Spectracon and Lallemand's camera. Consider a Spectracon tube with a mica window of 4.15 microns and operating at 40 kV and a Lallemand camera operating at 25 kV. The results above have to be corrected for the different emulsion temperature. Reducing the temperature of G5 emulsion from room temperature to liquid air temperature reduces its sensitivity by 30%[86], thus :-

$$\frac{\text{Speed of Spectracon}}{\text{Speed of Lallemand's Camera}} = \frac{0.9}{0.7} = 1.28$$

Thus, for these two tubes with identical photocathodes, exposed under the same conditions and with the same magnification, the speed gain of the Spectracon may be around 30% greater than Lallemand's camera. The speed of the electronic camera may be enhanced by electron optical demagnification which is not used with the Spectracon system.

7.5. Comparative Granularity of the Spectracon and Lallemand's Electronic Camera.

Also of interest is the comparative granularity of the

Spectracon and Lallemand's electronic camera. The granularity of a nuclear research emulsion exposed to electrons is essentially a function of N, the incident electron flux, $\frac{\Delta n}{n}$, the spread in the number of grains produced per electron and $\frac{\Delta A}{A}$, the spread in the areas of the developed grains. In the case of Lallemand's camera, where the incident electron beam is monoenergetic, $\frac{\Delta n}{n}$ is given by Pniewski's results and $(\overline{\sigma D})_L$ as shown in Chapter 6. In the case of the Spectracon $\frac{\Delta n}{n}$ will be greater than in the case of the electronic camera due to the spread in energies of the electrons striking the emulsion. In order to calculate the comparative granularities of the recorded images produced by these two devices, it is required to calculate $\frac{\Delta n}{n}$ for the Spectracon.

7.6. Calculation of the Spread in the Number of Developed Grains produced per Electron by the Spectracon.

As above, the results of Young [92] are used in this calculation and it is assumed that they may be applied to a Spectracon tube operated at 40 kV and having a mica window of 4.5 microns thickness. From these results, we know the probability distribution, p(E) of finding an electron of energy E in the electron beam transmitted by the mica window. Also, for an electron of given energy E striking the emulsion, the probability p(n) of it producing

n developed grains is known from the results of Pniewski. Those show that p(n) is Gaussian in form and if we write g(E) = mean value of n, then p(n) may be written as :-

$$p(n) = \frac{1}{\sqrt{2\pi . g(E)}} \cdot e^{-\frac{(n - g(E))^2}{2.g(E)}} \quad \ldots\ldots\ldots (1)$$

The probability distribution of interest is p(n,E) - the total probability of electrons in the electron beam transmitted by the mica window producing n developed grains and this is given by :-

$$p(n,E) = p(E) \quad p(n) \quad \ldots\ldots\ldots\ldots\ldots\ldots\ldots\ldots\ldots\ldots (11)$$

Now $(\Delta n)^2$ is given by the difference between the mean of the squares of the number of grains produced per electron $\overline{n^2}$ and the square of the mean number of grains produced per electron $\overline{n}^2$ $\overline{n^2}$ and $\overline{n}^2$ for the probability distribution p(n, E) can be calculated in the following way :-

$$\overline{n} = \int_0^{\infty} \int_0^{Es} n.\ p(E)\ \frac{1}{\sqrt{2\pi . g(E)}} \cdot e^{-\frac{(n-g(E))^2}{2.g(E)}}\ dn.dE$$

This integration is done in Appendix 1, where it is shown that :-

$$\overline{n} = \int_0^{Es} f_a(E).dE. \quad + \quad 2\int_0^{Es} f_b(E).dE$$

$$- \int_0^{Es} f_c(E).dE$$

where $f_a(E) = \frac{1}{\sqrt{2\pi}} \; p(E).g(E).^{\frac{1}{2}} \; e^{-\frac{g(E)}{2}}$

$f_c(E) = \frac{p(E).\,g(E)}{2} \; \text{erf}\,(y)$, $f_b(E) = \frac{P(E).q(E)}{2}$

Using the known values of p(E) and g(E), these functions have been calculated and plotted and the areas beneath the curves between the limits 0 and Es have been measured. Thus :-

$$\bar{n} = 0.013 + 4.54 - 0.00012 = 4.55$$

Similarly :-

$$\overline{n^2} = \int_0^{\infty} \int_0^{Es} n^2 \, \frac{p(E)}{\sqrt{2\pi.g(E)}} \, e^{-\frac{(n-g(E))^2}{2.g(E)}} \, dn.dE$$

and this is shown in Appendix 1 to be :-

$$\overline{n^2} = \int_0^{Es} f_d(E).dE. - \int_0^{Es} f_e(E).dE.$$

$$+ \int_0^{Es} f_f(E).dE. + \int_0^{Es} f_g(E).dE.$$

$$- \int_0^{Es} f_h(E).dE.$$

where $f_d(E) = p(E).\,g(E).$

$f_e(E) = \frac{p(E).g(E).}{2} \; \text{erf}\,(y).$

$$\int_1(E) = p(E).\ g(E)^2$$

$$\int_h(E) = \frac{p(E).\ g(E)^2}{2} \quad \text{erf}\ (y)$$

Evaluation of these integrals gives :-

$$\overline{n^2} = 4.54 - 0.00012 + 0.066 + 37 - 0.0005$$
$$= 41.61$$

Thus,

$$\left(\frac{\Delta n}{n}\right)^2 = \frac{\overline{n^2}}{\overline{n}^2} - 1 = 1.01$$

This compares with a figure of $\left(\frac{\Delta n}{n}\right)^2 = 0.24$ for direct recording of monoenergetic 25 kV electrons.

From the analysis of Chapter 6, we may write for the granularity of the recorded image produced by Lallemand's camera :-

$$\left(\frac{\sigma_D}{D}\right)_L = \frac{1}{\sqrt{N_L}} \cdot \left[1 + \frac{1}{n_L} \cdot \left(1 + \left(\frac{\sigma}{A}\right)^2\right)\right]^{\frac{1}{2}}$$

where N_L = electron flux incident on the emulsion, n_L = means number of grains produced per electron, $\frac{\sigma}{A}$ = spread in areas of developed grains.

For the granularity of the recorded image produced by the Spectracon, we may write :-

$$\left(\frac{\sigma D}{D}\right)_s^2 = \left(\frac{1}{\sqrt{Ns}}\right)^2 + \left[\frac{1}{\sqrt{Ns}} \cdot \left(\frac{\Delta n}{n_s}\right)^2 + \left[\frac{1}{\sqrt{ns\ Ns}} \quad \frac{\sigma}{A}\right]^2\right]$$

$$\text{i.e.} \left(\frac{\sigma D}{D}\right)_s = \frac{1}{\sqrt{Ns}} \cdot \left[1 + \left(\frac{\Delta n}{ns}\right)^2 + \frac{1}{n_s}\left(\frac{\sigma}{A}\right)^2\right]^{\frac{1}{2}}$$

Thus, for the same density, the ratio of the granularities produced on G5 emulsion is given by :-

$$\frac{(\sigma D)s}{(\sigma D)L} = \sqrt{\frac{N_L}{Ns}} \cdot \left[\frac{1 + \left(\frac{\Delta n}{ns}\right)^2 + \frac{1}{ns}\left(\frac{\sigma}{A}\right)^2}{1 + \frac{1}{n_L}\left(1 + \left(\frac{\sigma}{A}\right)^2\right)}\right]^{\frac{1}{2}}$$

$$= \sqrt{\frac{N_L}{Ns}} \cdot \left[\frac{1 + 1.01 + \frac{16.4}{4.54}}{1 + \frac{17.4}{4.2}}\right]$$

$$= \sqrt{\frac{N_L}{Ns}} \quad 1.05$$

$\frac{N_L}{Ns}$ is the ratio of the electron fluxes actually striking the emulsion in Lallemand's camera and the Spectracon in order to produce the same density. For the linear part of the emulsion characteristic curve, the speed ratio measurements previously described in this Chapter give a figure which is either the ratio of densities produced by the same exposure (for direct recording at 25 kV or through mica at 40 kV) or the ratio of the reciprocals of the exposures which produce the same density in each case. Thus, if S = speed ratio, D_s, D_L are the densities produced by the same exposure in each case and Es and E_L are the exposures required to

produce the same density, then :-

$$S = \frac{Ds}{D_L} = \frac{1/Es}{1/E_L} = \frac{E_L}{Es}$$

Extrapolating the results of speed measurement to a mica thickness of 4.5 microns, a figure of S 0.8 is found. Now, Es = exposure in terms of the electron flux incident upon the mica foil mounted in front of the emulsion. If Ns = corresponding electron flux incident upon the emulsion then Ns = T.Es where T = transmission of this thickness of mica foil and so :-

$$0.8 = \frac{E_L . T}{Ns}$$

Now E_L = electron flux of 25 kV energy incident upon the emulsion at room temperature. Correcting for the drop in emulsion sensitivity in Lallemand's camera :-

$$E_L = 0.7 . N_L$$

Thus,

$$\frac{N_L}{Ns} = \frac{0.8}{0.7 \times 0.75} = 1.52$$

Substituting in the formula derived for the relative granularities :-

$$\frac{(\sigma D)s}{(\sigma D)_L} = \sqrt{1.52} \times 1.05 = 1.29$$

i.e. for this thickness of mica window the granularity of the recorded image of the Spectracon will be $\sim$ 30% greater than the same recorded image produced by Lallemand's camera. For thinner

mica windows, more electrons will be transmitted with a higher average residual energy and so Ns, the electron flux producing a given density will fall. This means that the contribution to $\frac{(\sigma D)s}{(\sigma D)_L}$ from the factor $\frac{N_L}{Ns}$ will increase. The other factor in the expression for $\frac{(\sigma D)s}{(\sigma D)_L}$ will decrease, however, since $\frac{\Delta n}{\bar{n}}$ will decrease and $\bar{n}$ will increase as the thickness of the mica window decreases. It is difficult to estimate at what rate this factor will decrease with decreasing mica thickness without a knowledge of the distribution of the energies of the electrons transmitted through thinner mica windows.

7.7. Experimental Results.

The results of Figs. 24 and 25 may be used to check the above calculation. One of the curves of Fig. 25 shows the variation of granularity with density for G5 emulsion which had been exposed with a Spectracon tube having a mica window of 3.9 microns thickness. The experimental points of Fig. 24 were obtained from a plate of G5 emulsion which had been exposed to 25 kV electrons in Lallemand's camera. Comparing the results at D = 0.33, $\frac{(\sigma D)s}{(\sigma D)_L} = 1.28$ for the experimental point and $\frac{(\sigma D)s}{(\sigma D)_L} = 1.11$ when the comparison is made with the curve drawn through the points of Fig. 24. This is in reasonable agreement with the above calculation.

7.8. Comparative Equivalent Quantum Efficiencies.

As we have seen the equivalent quantum efficiency, q_e of an electronographic device may be written as :-

$q_e = \Gamma^2 . q$, where q is the photocathode quantum efficiency and Γ is a factor giving the reduction in signal-to-noise ratio for the electronographic process.

Now, $\Gamma = \frac{1}{\sqrt{D}} \cdot \sqrt{\frac{kD}{A}} = \frac{D}{\sigma D} \cdot \sqrt{\frac{1}{E.A}}$

substituting, $k = \frac{D}{E}$, where E = exposure.

Thus, comparing equivalent quantum efficiencies,

$$\frac{qeL}{qes} = \frac{(\sigma D)s^2}{(\sigma D)_L^2} \times \frac{Es}{E_L}$$

For a Spectracon tube of mica window thickness 3.9 microns $\frac{(\sigma D)s}{(\sigma D)_L}$ may be 1.29. From the relative speed measurements, we may write for this thickness of mica window :- $\frac{Es}{E_L} = \frac{0.7.\ 0.8}{0.94}$

Thus, $\frac{qeL}{qes} = (1.29)^2 \times \frac{0.7.\ 0.8}{0.94} \sim 1.0$

Thus, although the granularity of the Spectracon's recorded image is greater than that of the equivalent image produced by Lallemand's camera, this is compensated by the fact that a smaller number of electrons have to be integrated in order to produce the same density. This is due to the average residual energy of the electrons

being greater than 25 KV (for mica windows < 4.5 microns) and to the lowered sensitivity of the emulsion in Lallemand's camera due to cooling.

7.9. Conclusions :-

It has been shown that for the typical operating conditions of the Spectracon and Lallemand's camera and for identical photocathodes and magnification in each case, the speed gain of the Spectracon may be $\sim 30\%$ greater than that of Lallemand's camera. Also, the granularity of the Spectracon's recorded image may be $\sim 30\%$ greater than that of the equivalent image recorded by Lallemand's camera. The equivalent quantum efficiencies of these two devices may be of the same order, however, since the increased granularity of the Spectracon is offset by the fact that comparatively fewer electrons have to be integrated in order to produce the same density.

Chapter 8

Conclusions

Some of the properties of the electron sensitive emulsions XM, G5 and L4 have been investigated for exposure to medium energy electrons. The results in terms of optical density produced on the emulsion as a function of exposure all show a low degree of linearity. For low values of density, the results obtained provide further confirmation that the silver halide crystals of these emulsions require a single hit by an electron in order to be rendered developable.

The shape of the characteristic curves may be fitted to an equation derived on the basis of a single-hit hypothesis. There is, however, some disagreement between observers as to the extent of the linear region of the characteristic curves, other observers reporting a higher degree of linearity than has been found in this investigation for G5 emulsion. This aspect of the investigation merits more attention with particular reference to the emulsion processing conditions and the methods used for density measurement. A series of experiments could be made to determine any correlation between these factors and the shape of the emulsion characteristic curve. These experiments could be most conveniently made using a Spectracon image tube. The results presented in this

thesis show a correlation between the extent of the linear region of the emulsion characteristic curve and the energy of the incident electron beam, the degree of linearity of the emulsion increasing with increasing beam energy.

Some measurements have been made on the granularity of XM and G5 emulsions and the results obtained agree with the theoretical predictions of Valentine's analysis when the assumption is made that there is a wide distribution in the areas of developed silver grains. This assumption needs to be investigated by an electron microscope study of developed silver grains.

The results of granularity measurement and the measurements of the electron flux producing a certain density on the emulsion have been combined to evaluate the reduction in signa to-noise ratio in the electronographic recording process and consequently the equivalent quantum efficiency of a single-stage electronographic image tube. This gives a figure of $(25 \pm 6)\%$ of the photocathode quantum efficiency for the equivalent quantum efficiency of a Lallemand type system operated at 25kV and using G5 emulsion. The error in this figure includes a 10% error in granularity and an error of 20% in the value of the electron flux producing a given density. This value of equivalent quantum efficiency may also be appropriate to a Spectracon tube with a mica window of around

4.0 microns thickness operated at 40kV and using G5 emulsion. However, the equivalent quantum efficiency may approach the photocathode quantum efficiency if the operating potential of the system could be considerably increased.

The main practical conclusion arising from the work described in this thesis is the desirability of increasing the operating potential of electronographic image tube systems to improve the linear response of the emulsion and the speed and equivalent quantum efficiency of the system. In the application of such a system for the detection and recording of weak, low-contrast optical images, these gains will have to be balanced against a consequent lowering of emulsion storage capacity since higher energy electrons will produce more grains.

ACKNOWLEDGEMENTS

The author would like to acknowledge the constant interest shown by Professor J. D. McGee throughout this work. He acknowledges useful discussions with Dr. M. E. Barnett and some technical assistance given by Mr. J. Westlake.

The author wishes to acknowledge the receipt of a maintenance grant from the Science Research Council.

REFERENCES

1. Kinoshita, S., Proc. Roy. Soc. A(83)(1910) 432.
2. Powell, C.F. and Fertel, G.E.F., Nature, Lond., 144 (1939) 115.
3. Powell, C.F., Proc. Roy. Soc. A 181 (1943) 344.
4. Barkas, W.H. 'Nuclear Research Emulsions' Academic Press 1963.
5. Ilford Technical Information Sheet Y 44.1.
6. McGee, J.D. Reports on Progress in Physics, XXIV, 167, (1961).
7. Ganberg and Halpern, J., Rev. Sci. Instrum. 20, 641, (1949).
8. Premsela, H.F., Nieuwenhuizen, J.M. and Schotanus, B. (1961) 'Photographic Techniques for Electron Microscopy' Phillips Scientific Equipment Department, Eindhoven, Holland.
9. Digby, N., Firth, K. and Hercock, R.J., J. Photogr. Sci. 1, 194, (1953).
10. Valentine, R.C. and Wrigley, N.G., Nature, 203, 713, (1964).
11. Rose, A., Advances in Electronics and Electron Physics, 1, 131, (1948),
12. Fellgett, P.B., Mon. Not. R. Astr. Soc. 118, 223, (1958).
13. Jones, R.C., Photogr. Sci. and Eng. 2, 57, (1958).
14. Sommer, A.H., Rev. Sci. Inst. 26, 725, (1955).
15. Sommer, A.H., I.R.E. Trans. Nucl. Sci. NS3, 8, (1956).
16. Spicer, W.E., Phys. Rev. 112, 114, (1958).
17. Spicer, W.E., J. Appl. Phys. 31, 2077,(1960).
18. Sommer, A.H., Appl. Phys. Letters 3, 62, (1963).

19. McGee, J.D., 'The Present and Future of the Telescope of Moderate Size'. ed. Wood, F.B., Philadelphia University Press, p.35. (1956).

20. Mandel, L., J. Sci. Instrum. 32, 405 (1955).

21. Wilcock, W.L., Emberson, D.L. and Weekley, B., Trans. I.R.E. NS7, 126, (1960).

22. Wachtel, M.M., Doughty, D.D., Anderson, A.E. and Sternglass, E.J., Rev. Sci. Instrum. 3, 576, (1960).

23. Groo, H.R., Proceedings of Image Intensifier Symposium, U.S.A. E.R.D.L. Fort Belvoir, Va., p.55. (1961).

24. Zavoisky, E.T., Butslov, M.M. and Smolkin, G.E., Dokl. Akad. Nauk. S.S.S.R. 100, 241 (1955) and III, 996 (1956).

25. Stoudenheimer, R.G., Advances in Electronics and Electron Physics, XII, 41, (1960).

26. Davis, E.J., M.Sc. Thesis, London (1959).

27. Davis, G.P., Advances in Electronics and Electron Physics XVI, 119 (1962).

28. Catchpole, G.E., Ph.D. Thesis, London, (1963).

29. Powell, J.R., Ph.D. Thesis, London, (1967).

30. Lallemand, A., C.R. Acad. Sci., Paris, 203, 243, (1936).

31. Lallemand, A., et al., Advances in Electronics and Electron Physics, 12, 5, (1960).

32. Lallemand, A., Advances in Electronics and Electron Physics 16, 1, (1962).

33. Duchesne, M., Advances in Electronics and Electron Physics, 16, 27, (1962).

34. Lallemand, A. et al., C.R. Acad. Sci. 248, 2191, (1959).

35. Lallemand, A., Advances in Electronics and Electron Physics, 22, 1, (1966).

36. Alpern, M., Bijaoui and Duchesne, M., Advances in Electronic and Electron Physics, 22, 5, (1966).

37. Walker, M.F., Private Communication.

38. Kron, G.E., Advances in Electronics and Electron Physics, 16, 25, (1962).

39. Kron, G.E., and Papiashvili, I.I., Advances in Electronics and Electron Physics, 22, 59, (1966).

40. Kron, G.E., Private Communication.

41. Hiltner, W.A., 'The Present and Future of the Telescope of Moderate Size', ed. Wood, F.B., Philadelphia University Press, p.11. (1958).

42. Hiltner, W.A. and Niklas, W.F. Advances in Electronics and Electron Physics, XVI, 37, (1962).

43. McGee, J.D. and Wheeler, B.E., J. Phot. Sci., 9, 106, (1961).

44. McGee, J.D. and Wheeler, B.E., Advances in Electronics and Electron Physics, 16, 47, (1962).

45. McGee, J.D. et al. Advances in Electronics and Electron Physics, 22, 11, (1966).

46. McGee, J.D., et al. Advances in Electronics and Electron Physics, 22, 31, (1966).

47. Wheeler, B.E., Ph.D. Thesis, London, (1962).

48. Zacharov, B. and Douxlen, S., Advances in Electronics and Electron Physics, XII, 31, (1960).

49. Khogali, A., Ph.D. Thesis, London, 1964.

50. Bacik, H. Private Communication.

51. Wheeler, B.E., and Emberson, C.J., Advances in Electronics and Electron Physics, 22, 51, (1966).

52. Fellgett, P.B. 'The Present and Future of the Telescope of Moderate Size' ed. Wood, F.B., University of Pennsylvani Press, p.51. (1958).

53. Valentine, R.C., 'Advances in Optical and Electron Microscopy', 1, 180, (1966).

54. Mees, C.E.K., 'The Theory of the Photographic Process', Macmillan, New York, (1948).

55. Valentine, R.C., Advances in Optical and Electron Microscopy, 1, p.180, Academic Press, (1966)

56. Leide, G., Arkiv Fysik 11, 329, (1956).

57. Barron, W.C., and Wolfendale, A.W., Brit. J. Appl. Phys. 8, 297, (1957).

58. Baker, R.F., Ramberg, E.G. and Hillier, J., (1942). J. Appl. Phys. 13, 450.

59. Crook, E.M., Sheffield, F.M.L. and Chilton, L.V. (1945) Photogr. J. 85B, 6.

60. von Borries, 13, (1942). Phys. 2. 43, 190.

61. Mees, C.E.K., and James, T.H. 'The Theory of the Photographic Process'. Third Edition, Macmillan, New York, (1966).

62. Valentine, R.C., and Wrigley, N.G. Nature, 203, 713, (1964).

63. McGee, J.D., Khogali, A., Ganson, A. Advances in Electronics and Electron Physics, 22A, (1966), Academic Press.

64. Pniewski, J. Acta. Phys. Polon. 11, 230, (1951-52)

65. Kahan, E. Private Communication.

66. Brand, P.W.J.L., Ph.D. Thesis, Edinburgh, (1967).

67. Hamilton, J.F., Technique of Inorganic Chemistry, Vol. 3, p. 81, (1963) Interscience Publishers, New York.

68. Jones, L.A. and Deisch, N. J. Frank Inst., 190, 657, (1920).

69. Hardy, R.A.C. and Jones, L.A. Trans. Soc. Mot. Pict. Eng. No. 14, 107, (1922).

70. Lowry, R.E.M. J. Op. Soc. Am. 26, 65, (1936).

71. Dunham, R.T., Ber. VIII Internat. Kongr. Phot. Dresden, 287, (1931).

72. Goetzy, A. and Gould, W.O. J. Soc. Mot. Pic. Eng. 29, 510, (1937).

73. Selwyn, E.W.H., Phot. J. 75, 571, (1935).

74. Jones, L.A. and Higgins, G.C. J. Op. Soc. Am. 35 435 (1945)

75. " 36 203 (1946)

76. " 37 217 (1947)

77. " 38 398 (1948)

78. " 41 41 (1951)

79. " 41 64 (1951)

80. " 41 192 (1951)

81. Jones, L.A., Higgins, E.C. and Stultz. J. Op. Soc. Am. 45, 107, (1955).

82. Jones, R.C. J. Op. Soc. Am. 45, 799, (1955).

83. Zweig, H.J. J. Op. Soc. Am. 46, 805, (1956)

84. Wall, F.J.B. and Steel, B.G. J. Phot. Sci. 12, 34, (1964).

85. Dennison, E.W. Advances in Electronics and Electron Physics. 22A, 435, (1966).

86. Duchesne, M. Private Communication.

87. McGee, J.D. Private Communication.

88. Eastman Kodak Company. 'Kodak Plates and Films for Science and Industry'. (1962).

89. Fellgett, P.B. J. Phot. Sci. 11, 31, (1963).

90. Brand, P.W.J.L. Advances in Electronics and Electron Physics. 22A, (1966).

91. Walker, M.F. Private Communication. See ref. 49.

92. Young, J.R. J. Appl. Phys. 28, 524, (1957).

Appendix I

Evaluation of Integrals Used in the Calculation of $\frac{\Delta n}{\bar{n}}$ for Spectracon

1. Evaluation of $\bar{n}$

$$\bar{n} = \int_0^{\infty}\int_0^{E_s} n.\ \frac{p(E).}{\sqrt{2\pi\, g(E)}}\ .\ e^{-\frac{(n-g(E))^2}{2g(E)}}\ .dn.dE$$

Put $y = n - g(E)$, then $n = y + g(E)$, $dn = dy$
Then $n = I_1 + I_2$
where

$$I_1 = \int_{-g(E)}^{\infty}\int_0^{E_s} y.\ \frac{p(E)}{2\ g(E)}\ .\ e^{\frac{-y^2}{2g(E)}}\ .\ dy.dE.$$

$$= \int_0^{E_s} \frac{p(E)}{\sqrt{2\pi\, g(E)}} \cdot \left[-\frac{1}{2 \times \frac{1}{2g(E)}}\ .\ e^{\frac{-y^2}{2g(E)}} \right]_{-g(E)}^{\infty} .\ dE.$$

$$= \int_0^{E_s} \frac{p(E).\ g(E)^{\frac{1}{2}}.\ e^{-\frac{g(E)}{2}}}{\sqrt{2\pi}}\ .\ dE.$$

$$= \int_0^{E_s} fa(E).\ dE.$$

$$I_2 = \int_{-g(E)}^{\infty}\int_0^{E_s} \frac{p(E).g(E)}{\sqrt{2\pi\, g(E)}}\ .\ e^{\frac{-y^2}{2g(E)}}\ dy.dE.$$

$$= \int_0^{\infty}\int_0^{E_s} \frac{p(E).g(E)}{\sqrt{2\pi\, g(E)}}\ .\ e^{\frac{-y^2}{2g(E)}}\ .dy.dE.$$

$$+ \int_{-q(E)}^{0} \int_{0}^{E_s} \frac{p(E).g(E)}{\sqrt{2\pi\, g(E)}} \cdot e^{\frac{-y^2}{2g(E)}} dy.dE.$$

Now:-

$$\int_{-q(E)}^{\infty} \int_{0}^{E_s} \frac{p(E).g(E)}{\sqrt{2\pi\, g(E)}} \cdot e^{\frac{-y^2}{2g(E)}} dy.dE.$$

$$= \int_{0}^{q(E)} \int_{0}^{E_s} \frac{p(E).g(E)}{\sqrt{2\pi\, g(E)}} \cdot e^{\frac{-y^2}{2g(E)}} dy.dE.$$

$$= \int_{0}^{\infty} \int_{0}^{E_s} \frac{p(E).g(E)}{\sqrt{2\pi\, g(E)}} \cdot e^{\frac{-y^2}{2g(E)}} dy.dE. - \int_{q(E)}^{\infty} \int_{0}^{E_s} \frac{p(E).g(E)}{\sqrt{2\pi\, g(E)}} \cdot e^{\frac{-y^2}{2g(E)}} dy.dE.$$

$$I_2 = 2 \int_{0}^{\infty} \int_{0}^{E_s} \frac{p(E).g(E)}{\sqrt{2\pi\, g(E)}} \cdot e^{\frac{-y^2}{2g(E)}} dy.dE - \int_{q(E)}^{\infty} \int_{0}^{E_s} \frac{p(E).g(E)}{\sqrt{2\pi\, g(E)}} \cdot e^{\frac{y^2}{2g(E)}} dy.dE.$$

$$= 2.\, I_3 - I_4$$

Now, $I_3 = \int_{0}^{\infty} \int_{0}^{E_s} \frac{p(E).g(E)}{\sqrt{2\pi\, g(E)}} \cdot e^{\frac{-y^2}{2g(E)}} dy.dE.$

This can be evaluated precisely since:-

$$\int_{0}^{\infty} e^{-bx^2} \cdot dx = \frac{1}{b^{\frac{1}{2}}} \cdot \frac{\sqrt{\pi}}{2}$$

$$I_3 = \int_{0}^{E_s} \frac{p(E).g(E)}{2} \cdot dE. \quad {}_2 = \int_{0}^{E_s} f_b(E).dE.$$

$$I_4 = \int_{q(E)}^{\infty} \int_{0}^{E_s} \frac{p(E).g(E)}{\sqrt{2\pi\, g(E)}} \cdot e^{\frac{-y^2}{2g(E)}} \cdot dy.dE.$$

The function, $\text{erf}(x) = \sqrt{\frac{2}{\pi}} \int_{\infty}^{\infty} e^{\frac{-x^2}{2}}.dx.$

is tabulated.

Thus, $I_4 = \int_0^{E_s} \frac{p(E).g(E)}{2} . \text{erf}(y).dE.$

$= \int_0^{E_s} f_c(E).dE.$

Thus, $\overline{n} = \int_0^{E_s} f_a(E).dE. + 2\int_0^{E_s} f_b(E).dE. - \int_0^{E_s} f_c(E).dE.$

2. Evaluation of $\overline{n^2}$

$$\overline{n^2} = \int_0^{\infty}\int_0^{E_s} n^2 . \frac{p(E)}{\sqrt{2\pi g(E)}} . e^{\frac{-(n-g(E))}{2g(E)}} .dn.dE.$$

As before put $y = n - g(E)$
Then:-

$$\overline{n^2} = I_6 + I_7 + I_8$$

where

$$I_6 = \int_{-g(E)}^{\infty}\int_0^{E_s} \frac{p(E)}{\sqrt{2\pi g(E)}} y^2 . e^{\frac{-y^2}{2g(E)}} dy.dE.$$

$$I_7 = \int_{-g(E)}^{\infty}\int_0^{E_s} \frac{p(E).2g(E)}{\sqrt{2\pi g(E)}} . y . e^{\frac{-y^2}{2g(E)}} . dy.dE.$$

$$I_8 = \int_{-g(E)}^{\infty}\int_{0}^{E_s} \frac{p(E).g(E)^2}{\sqrt{2\pi\, g(E)}} \cdot e^{\frac{-y^2}{2g(E)}}\, dy.dE.$$

Using similar methods as for the previous integration, it can be shown that:-

$$I_6 = \int_0^{E_s} p(E).g(E).dE. - \int_0^{E_s} \frac{p(E).g(E)^{3/2} e^{\frac{-g(E)}{2}}}{\sqrt{2\pi}}\, dE.$$

$$- \int_0^{E_s} \frac{p(E).g(E)}{2} \cdot \mathrm{erf}(y).dE.$$

$$I_7 = 2 \int_0^{E_s} \frac{p(E).g(E).^{3/2} e^{\frac{-g(E)}{2}}}{\sqrt{2\pi}}.dE.$$

$$I_8 = \int_0^{E_s} p(E).g(E)^2.\, dE$$

$$- \int_0^{E_s} \frac{p(E).g(E)^2.}{2} \mathrm{erf}(y).dE.$$

Thus:-

$$\overline{n^2} = I_6 + I_7 + I_8$$

$$= \int_0^{E_s} f_d(E).dE. - \int_0^{E_s} f_e(E).dE$$

$$+ \int_0^{E_s} f_f(E).dE. + \int_0^{E_s} f_g(E).dE.$$

$$- \int_0^{E_s} f_h(E).\, dE.$$

where $f_d(E) = p(E).g(E)$

$f_e(E) = \frac{p(E).g(E).\,\mathrm{erf}(y)}{2}$

$f_f(E) = p(E).\, g(E)^2$

$f_h(E) = \frac{p(E).g(E)^2.\,\mathrm{erf}(y)}{2}$, $f_g(E) = \frac{p(E).\,q(E)^{3/2}\, e^{\frac{-q(E)}{2}}}{\sqrt{2\pi}}$

The programme below was written to compute the root-mean-square variation in density (granularity) from measurements made of optical transmission.

The language used is Fortran IV and the calculations were made on the I.B.M. I40ϕ/7090 installation at Imperial College.

E03013 10050062 DATE

```
$IBFTC DECK 1
DECK 1    -  EFN   SOURCE STATEMENT  -  IFN(S)  -
      REAL A(1100),DENS(1100),AN,SUMSQ,GRAN,AVERAG,D
      INTEGER N,I
      DO 301 K=1,5
      D=0.
      SUMSQ=0.
      READ(5,20)N
   20 FORMAT (I4)
      READ(5,10)(A(I),I=1,N)
   10 FORMAT(20F4.3)
C  N=NUMBER OF A
      DO 101 I=1,N
      DENS(I)=-ALOG10(A(I))
  101 D=D+DENS(I)
      AN=N
      AVERAG=D/AN
      DO 201 I=1,N
  201 SUMSQ=SUMSQ+(DENS(I)-AVERAG)*(DENS(I)-AVERAG)
      GRAN=SQRT(SUMSQ/AN)
      WRITE(6,30)AVERAG,N,SUMSQ,GRAN
   30 FORMAT(9H0AVERAGE=,F5.3,3H N=,I4,12H SUM SQUARE=,F11.6,6H GRAN=,
     1F8.6)
  301 CONTINUE
      STOP
      END
```